Comparative Analysis of Localization Techniques and Security Mechanisms in WSN

Publisher: IEEE

Sudhakar Avareddy ; Rajashree V. Biradar **All Authors**

Abstract: Wireless sensor network (WSN) contains spatially distributed independent sensor nodes to cooperatively monitor physical or environmental conditions. There are several res... **View more**

Metadata

Abstract:

Wireless sensor network (WSN) contains spatially distributed independent sensor nodes to cooperatively monitor physical or environmental conditions. There are several research challenges in WSN, among them Localization and Security are more prominent. To spot location of the sensor node, each node can make the installation of GPS, but GPS is costlier and cannot provide exact location of node in an indoor environment. Manually fixing position reference on each sensor node is additionally difficult within the case of deep network. To beat the above drawbacks, in recent years most of the localization techniques make use of beacon nodes (anchor nodes) where only the present position of the beacon nodes must be known. While transformation of knowledge from one node to a different node, we would like our data to be secured from unauthorized person. So for this issue we would like to think about security aspects like encryption and decryption by using several trust key management techniques where each node is trusted by providing the safety keys. In our proposed research work, by considering localization and securing aspects, we develop location-based energy efficient trust aware localized key management protocol and hence during this paper we discuss about the localization techniques and security solutions utilized in wireless sensor networks.

Published in: 2021 IEEE International Conference on Mobile Networks and Wireless Communications (ICMNWC)

Date of Conference: 03-04 December 2021

INSPEC Accession Number: 21593016

Date Added to IEEE *Xplore*: 26 January 2022

DOI: 10.1109/ICMNWC52512.2021.9688549

Publisher: IEEE

ISBN Information:

Electronic ISBN:978-1-6654-3883-4

Print on Demand(PoD) ISBN:978-1-6654-4607-5

Conference Location: Tumkur, Karnataka, India

Contents

Wireless sensor network (WSNs) is an emerging technology which consists of several numbers of sensors nodes by having its own battery, sensing and memory units in each node (Fig. 1). There are several challenges in WSN based applications like environment monitoring, habitat monitoring, structural monitoring, healthcare, disaster management, object tracking, surveillance etc. In these applications source node sense the data, process it and transfer to the destination node through intermediate nodes. Once the information reach the destination node server can access the information through the web [1].

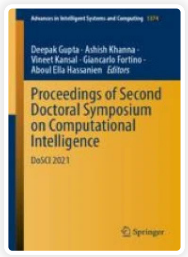

Proceedings of Second Doctoral Symposium on Computational Intelligence pp 279–289

An Intelligent Flood Forecasting System Using Artificial Neural Network in WSN

K. S. Raghu Kumar & Rajashree V. Biradar

Conference paper | First Online: 20 September 2021

Part of the Advances in Intelligent Systems and Computing book series (AISC,volume 1374)

Abstract

The flood forecasting system is widely used in the hydrological research, and neural network has provided considerable assistance in the prediction of the flood. The flood alert system enhances by mitigating the damage and public safety. The proposed model is an intelligent flood alerting system using the neural network for a wireless sensor network (WSN). The neural network model is composed of past rainfall measurements with rainfall in diverse duration and flow of water. Various environmental factors are considered, while training the proposed model and the significant insights are framed. This paper incorporates the

fuzzy and sigmoid function for the identification runoff rainfall process. The proposed model is investigated by comparing the parameters end to end delay, packet loss, and throughput. From the observation and comparison of results, the proposed model has the best outcome. The simulation analysis is compared with the existing approach and obtained an effective prediction.

Keywords

Neural network **Flood forecasting**

Water level **Packet loss** **And throughput**

References

1. Ragnoli, M., Barile, G., Leoni, A., Ferri, G., & Stornelli, V. (2020). An autonomous low-power LoRa-based flood-monitoring system. *Journal of Low Power Electronics and Applications, 10*(2), 15.

2. Shamsi, S. (2019). Flood forecasting review using wireless sensor network. *Global Sci-Tech, 11*(1), 13–22.

3. Patil, P. S., & Jain, S. S. Survey on flood monitoring & alerting systems.

4. Dwivedi, R. K., Kumari, N., & Kumar, R. (2020). Integration of wireless sensor networks with cloud towards efficient management in IoT: A review. In *Advances in data and information sciences* (pp. 97–107). Springer.

5. Ullah, T. F., Gnana Prakasi O. S., & Kanmani, P. (2020). A review on flood prediction algorithms and a deep neural network model for estimation of flood occurrence. *International Research Journal of Multidisciplinary Technovation*, *2*(5), 8–14.

6. Sakib, S. N., Ane, T., Matin, N., & Kaiser, M. S. (2016). An intelligent flood monitoring system for Bangladesh using wireless sensor network. In *2016 5th International Conference on*

Informatics, Electronics and Vision (ICIEV) (pp. 979–984). IEEE.

7. Aziz, N. A. A., & Aziz, K. A. (2011, February). Managing disaster with wireless sensor networks. In *13th International Conference on Advanced Communication Technology (ICACT2011)* (pp. 202–207). IEEE.

8. Pant, D., Verma, S., & Dhuliya, P. (2017, September). A study on disaster detection and management using WSN in Himalayan region of Uttarakhand. In *2017 3rd International Conference on Advances in Computing, Communication and Automation (ICACCA)(Fall)* (pp. 1–6). IEEE.

9. Singh, V. P., Jain, S., & Singhai, J. (2010). Hello flood attack and its countermeasures in wireless sensor networks. *International Journal of Computer Science Issues (IJCSI), 7*(3), 23.

10. Lee, J. U., Kim, J. E., Kim, D., Chong, P. K., Kim, J., & Jang, P. (2008, September). RFMS: Real-time flood monitoring system with wireless sensor networks. In *2008 5th IEEE International Conference on Mobile Ad Hoc and Sensor Systems* (pp. 527–528). IEEE.

11. Hughes, D., Greenwood, P., Blair, G., Coulson,

G., Grace, P., Pappenberger, F., … Beven, K. (2008). An experiment with reflective middleware to support grid-based flood monitoring. *Concurrency and Computation: Practice and Experience*, *20*(11), 1303–1316.

12. Roy, J. K., Gupta, D., & Goswami, S. (2012, December). An improved flood warning system using WSN and Artificial Neural Network. In *2012 Annual IEEE India Conference (INDICON)* (pp. 770–774). IEEE.

13. Castillo-Effer, M., Quintela, D. H., Moreno, W., Jordan, R., & Westhoff, W. (2004, November). Wireless sensor networks for flash-flood alerting. In *Proceedings of the Fifth IEEE International Caracas Conference on Devices, Circuits and Systems, 2004* (Vol. 1, pp. 142–146). IEEE.

14. Merkuryeva, G., Merkuryev, Y., Sokolov, B. V., Potryasaev, S., Zelentsov, V. A., & Lektauers, A. (2015). Advanced river flood monitoring, modelling and forecasting. *Journal of Computational Science, 10*, 77–85.

15. Ahamed, A., & Bolten, J. D. (2017). A MODIS-based automated flood monitoring system for southeast Asia. *International Journal of Applied Earth Observation and Geoinformation, 61*, 104–117.

16. Alfieri, L., Cohen, S., Galantowicz, J., Schumann, G. J., Trigg, M. A., Zsoter, E., ..., Rudari, R. (2018). A global network for operational flood risk reduction. *Environmental Science and policy*, *84*, 149–158.

17. Seal, V., Raha, A., Maity, S., Mitra, S. K., Mukherjee, A., & Naskar, M. K. (2012). A simple flood forecasting scheme using wireless sensor networks. *arXiv preprint* arXiv:1203.2511.

18. Panganiban, E. B., & Cruz, J. C. D. (2017, November). Rain water level information with flood warning system using flat clustering predictive technique. In *TENCON 2017–2017 IEEE Region 10 Conference* (pp. 727–732). IEEE.

19. Udo, E. N., & Isong, E. B. (2013). Flood monitoring and detection system using wireless sensor network. *Asian Journal of Computer and Information Systems*, *1*(04).

20. Jegadeesan, S., Dhamodaran, M., & Sri Shanmugapriya, S. (2018). Wireless sensor network based flood and water quality monitoring system using IoT. *Taga Journal of Graphic Technology,* Online ISSN (1748-0345).

21. Yoon, S., Ye, W., Heidemann, J., Littlefield, B., & Shahabi, C. (2011). SWATS: Wireless sensor

networks for steamflood and waterflood pipeline monitoring. *IEEE Network, 25*(1), 50–56.

Author information

Authors and Affiliations

Department of CSE, RYM EC, Ballari, Karnataka, India

K. S. Raghu Kumar

Department of CSE, BITM, Ballari, Karnataka, India

Rajashree V. Biradar

Editor information

Editors and Affiliations

Department of Computer Science Engineering, Maharaja Agrasen Institute of Technology, Rohini, Delhi, India

Dr. Deepak Gupta

Maharaja Agrasen Institute of Technology, Rohini, Delhi, India

Dr. Ashish Khanna

Institute of Engineering and Technology, Lucknow, Uttar Pradesh, India

Prof. Vineet Kansal

University of Calabria, Rende, Cosenza, Italy

Prof. Giancarlo Fortino

Department of Information Technology, Cairo University, Giza, Egypt

Prof. Aboul Ella Hassanien

Rights and permissions

Copyright information

About this paper

Cite this paper

Kumar, K.S.R., Biradar, R.V. (2022). An Intelligent Flood Forecasting System Using Artificial Neural Network in WSN. In: Gupta, D., Khanna, A., Kansal, V., Fortino, G., Hassanien, A.E. (eds) Proceedings of Second Doctoral Symposium on Computational Intelligence . Advances in Intelligent Systems and Computing, vol 1374. Springer, Singapore. https://doi.org/10.1007/978-981-16-3346-1_23

.RIS .ENW .BIB

DOI
https://doi.org/10.1007/978-981-16-3346-1_23

Published	Publisher Name	Print ISBN
20 September 2021	Springer, Singapore	978-981-16-3345-4

Online ISBN	eBook Packages
978-981-16-3346-1	Intelligent Technologies and Robotics

Intelligent Technologies and Robotics (R0)

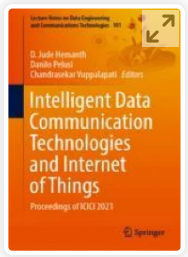

Intelligent Data Communication Technologies and Internet of Things pp 453–461

A Survey on Image Emotion Analysis for Online Reviews

G. N. Ambika & Yeresime Suresh

Conference paper | First Online: 28 February 2022

Part of the Lecture Notes on Data Engineering and Communications Technologies book series (LNDECT,volume 101)

Abstract

Emotions are sentiments, opinions, and feelings which are expressed by the public through text, images, and videos. Opinion analysis for the Internet data is now attracting a growing research people provide feedback on the Internet through the reviews and images in different platforms like Instagram, Facebook, Twitter, and other online Websites on the products. Major work was implemented for processing the sentences. Finite amount of the research that focuses on analyzing opinions of image information. Image emotion topics will be ANPs, i.e., adjective noun pairs manually concealed tags for Internet imagery those

helpful of predicting opinions, or else emotions convey by the people in terms of pictures. The main aim is to predict emotions of the images which are not label. To raise this issue, deep learning methods are utilized for opinion analysis of images, since the deep learning techniques have the capabilities for successfully understanding the behavior of images.

Keywords

Convolutional neural network

Image processing **Deep learning techniques**

Image classification

References

1. Doshi U, Barot V, Gavhane S (2020) Classification of images for social networks. In: 2020 IEEE international conference on convergence to digital world—quo vadis. ICCDW

2. Maas A, Daly RE, Pham PT, Huang D, Ng AY, Potts C (2011) Learning word vectors for sentiment analysis. In: ACL

3. You Q, Cao L, Jin H, Luo J (2016) Robust visual-textual sentiment analysis: when attention meets tree-structured recursive neural networks. In ACM MM

4. Zhao Z, Zhu H, Xue Z, Liu Z, Tian J, Chua MCH, Liu M (2019) An image-text consistency driven multimodal sentiment analysis method for social media. Inf Process Manag 56(6):102097

5. Huang F, Zhang X, Zhao Z, Xu J, Li Z (2019) Image–text sentiment analysis via deep multimodal attentive fusion. Knowl-Based Syst 167:26–37

6. Xu J, Huang F, Zhang X, Wang S, Li C, Li Z, He Y (2019) Visual-textual sentiment classification with bi-directional multi-level attention networks. Knowl-Based Syst 178:61–73

7. Ortis A, Farinella GM, Torrisi G, Battiato S (2020)

Exploiting objective text description of images for visual sentiment analysis. Multimedia Tools and Appl 1–24

8. Ye J, Peng X, Qiao Y, Xing H, Li J, Ji R (2019) Visual-textual sentiment analysis in product reviews. In: 2019 IEEE International conference on image processing (ICIP). IEEE, pp 869–873

9. Yang L, Li Y, Wang J, Sherratt RS (2020) Sentiment analysis for e-commerce product reviews in Chinese based on sentiment lexicon and deep learning. IEEE Access 8:23522–23530

10. Kausar S, Huahu X, Shabir MY, Ahmad W (2019) A sentiment polarity categorization technique for online product reviews. IEEE Access

11. Pang B, Lee L et al (2008) Opinion mining and sentiment analysis. Found Trends R Inf Retrieval 2(1–2):1–135

12. Bollen J, Mao H, Pepe A (2011) Modeling public mood and emotion: twitter sentiment and socio-economic phenomena.” In: ICWSM

13. Hu X, Tang J, Gao H, Liu H (2013) Unsupervised sentiment analysis with emotional signals. In: WWW

14. Ren Y, Zhang Y, Zhang M, Ji D (2016) Context—sensitive twitter sentiment classification using neural network. In: AAAI

15. D'Avanzo E, Pilato G (2015) Mining social network users' opinions' to aid buyers' shopping decisions. Comput Hum Behav 51:1284–1294

Author information

Authors and Affiliations

Department of CSE, BMSIT & M, Yelahanka, 560064, India

G. N. Ambika

Department of CSE, BITM, Ballari, 583104, India

Yeresime Suresh

Corresponding author

Correspondence to G. N. Ambika .

Editor information

Editors and Affiliations

Department of Electronics and Communication Engineering, Karunya Institute of Technology and Sciences, Coimbatore, India

Dr. D. Jude Hemanth

Faculty of Communication Sciences, University of Teramo, Teramo, Italy

Dr. Danilo Pelusi

Department of Computer Engineering, San Jose State University, San Jose, CA, USA

Dr. Chandrasekar Vuppalapati

Rights and permissions

Copyright information

About this paper

Cite this paper

Ambika, G.N., Suresh, Y. (2022). A Survey on Image Emotion Analysis for Online Reviews. In: Hemanth, D.J., Pelusi, D., Vuppalapati, C. (eds) Intelligent Data Communication Technologies and Internet of Things. Lecture Notes on Data Engineering and Communications Technologies, vol 101. Springer, Singapore. https://doi.org/10.1007/978-981-16-7610-9_33

.RIS .ENW .BIB

DOI
https://doi.org/10.1007/978-981-16-7610-9_33

Published	Publisher Name	Print ISBN
28 February 2022	Springer, Singapore	978-981-16-7609-3

Online ISBN	eBook Packages

978-981-16-7610-9

Intelligent Technologies and Robotics

Intelligent Technologies and Robotics (R0)

A Binary Cross Entropy U-net based Lesion Segmentation of Granular Parakeratosis

Sheetal Janthakal ; Girisha Hosalli **All Authors**

Abstract: The segmentation of skin lesion plays a vital role in the automated diagnosis of skin diseases like Granular parakeratosis that grows into the malignant stage, if not tre... **View more**

Metadata

Abstract:

The segmentation of skin lesion plays a vital role in the automated diagnosis of skin diseases like Granular parakeratosis that grows into the malignant stage, if not treated properly. However, the automatic segmentation of the dermoscopic images is considered to be a challenging task in computer vision applications due to the presence of several difficulties like artifacts, varying shape, size, and irregular boundaries. In this paper, U-net with the binary cross entropy method is proposed and compared with fully convolutional network (FCN) and state-of-the-art techniques, on the lesions of granular parakeratosis. Most of the neural networks require graphics processing unit (GPU) for segmenting the lesion, but, here, we perform the segmentation using only central processing unit (CPU). The images are trained end-to-end and the performance is evaluated using accuracy, sensitivity, precision and dice co-efficient metrics. The implementation results show that the U-net with binary cross entropy provides the best performance in terms of all metrics compared to FCN and state-of-the-art methods.

Published in: 2021 International Conference on Advancements in Electrical, Electronics, Communication, Computing and Automation (ICAECA)

Date of Conference: 08-09 October 2021

INSPEC Accession Number: 21552478

Date Added to IEEE *Xplore*: 18 January 2022

DOI: 10.1109/ICAECA52838.2021.9675661

ISBN Information:

Publisher: IEEE

Conference Location: Coimbatore, India

Contents

I. Introduction

A sensory organ in a human body is Skin that covers the muscles and other parts of the body [1]. The functioning of skin is very important because any changes in the skin may affect other parts of the body. So, it is better to diagnose these changes or diseases at the earlier stage so that it will not have adverse effects in the future. Any change in the skin or abnormal growth or appearance of cells is known as skin lesion. One such type of skin lesion or disease is granular parakeratosis. Granular parakeratosis is a skin disease that appears as brownish-red hyperkeratotic papules that can combine to form plaques . Granular parakeratosis (GP) or also known as “Axillary granular parakeratosis” or “Intertriginous granular parakeratosis” is a disorder of keratinization. Several cases of the disease are reported in last few years in middle-aged persons as well as in infants . The main causes of the disease are frequent application of zinc oxide or change of deodorant. These diseases are to be treated at an earlier stage otherwise it may lead to the malignant stage. Hence, an imaging diagnosis system is required that can diagnose the disease and give an accurate treatment.

Materials Today: Proceedings xxx (xxxx) xxx

Contents lists available at ScienceDirect

Materials Today: Proceedings

journal homepage: www.elsevier.com/locate/matpr

Analysis of strength and durability properties of ternary blended geopolymer concrete

S. Khalid [a], T.V. Reshma [b,*], M.S. Shobha [c], G. Priyanka [a], Vineetha Satyanarayana Siriki [a]

[a] Department of Civil Engineering, BITM, Ballari 583104, India
[b] Department of Civil Engineering, GITAM University, Bengaluru 562163, India
[c] Department of Civil Engineering, RYMEC, Ballari 583104, India

ARTICLE INFO

Article history:
Available online xxxx

Keywords:
Fly ash (FA)
Ground granulated blast furnace slag (GGBS)
Geopolymer concrete (GPC)
Molarity (M)
Metakaolin (MK)

ABSTRACT

Cement is the primary raw material in any construction works, being an indispensable binding material. The production associate degreed consumption of cement is an index of its industrial development. However, excess production of cement pollutes the setting by emotional CO2 gas. So, it is necessary to exchange cement with alternative binding materials. In this study, one such trial is attempted using mineral admixtures like Fly ash, GGBS which are industrial waste byproducts. The concrete specimens are cast using, Fly ash, GGBS, and Metakaolin, with Alkaline liquid like Sodium silicate, and Sodium Hydroxide solution with 10 M, in the ratio of 1:1.5 and 1:2. Fibers such as steel fibers and polypropylene fibers are added with a 0–1.5% percentage to enhance the concrete properties. The moulds are cured under sunlight. The mechanical properties such as flexural strength, compressive strength, and split-tensile strength are performed along with durability tests to evaluate the optimized ratio of using mineral admixtures and fibers. The test results indicate that the combination of Metakaolin and GGBS can be used to develop environmentally friendly geopolymer concrete.

Selection and peer-review under responsibility of the scientific committee of the 5th International Conference on Advanced Research in Mechanical, Materials and Manufacturing Engineering-2021

1. Introduction

Infrastructure development in the modern era has made use of cement concrete in huge quantities. Concrete construction has made to deplete natural resources and causing pollution in the environment. The binding material used in manufacturing concrete is cement, leading to CO2 emission in its manufacturing process, causing environmental pollution. Moreover, the extraction of limestone for cement manufacturing will cause in the reduction of renewable resources like limestone [1]. Hence, it is essential to use environmentally friendly alternative binding cementitious material [2].

This study focuses on the experimental investigation using ternary blended GPC reinforced with steel fibers [34]. The development of ternary GPC consisting of ground granulated blast furnace slag, flyash, and metakaolin as mineral admixture activated with sodium hydroxide & sodium silicate solution [5–7]. To improve the split-tensile strength property of concrete, Steel fibres are also added to this concrete. The minor research studies are done on fiber reinforced ternary blend GPC under sunlight curing. Strength and durability characteristics were also studied. Finally, the test results are analyzed to know the suitability of using this concrete [3].

Past Literatures available on geo-polymer concrete shows that this type of concrete is a good alternative for conventional concrete. Therefore, although very little research study is there on ternary blended geopolymer concrete using fibers [8]. Therefore, this study has been carried out with the gaps present on geopolymer concrete.

Joseph Davidovits [9,10] developed the idea of using polymer concrete as an alternative cement concrete. It can be manufactured by using alumina-silicate materials using alkali activators. It has very good strength & durability properties.

T Bakharev [11] conducted experimental study on durability characteristics of geopolymer concrete such as acid resistance and sulphate resistance. It was found that ternary blended geopolymer concrete showed good performance under these attacks [12–14].

* Corresponding author.
E-mail address: rvishwes@gitam.edu (T.V. Reshma).

https://doi.org/10.1016/j.matpr.2021.08.307

Selection and peer-review under responsibility of the scientific committee of the 5th International Conference on Advanced Research in Mechanical, Materials and Manufacturing Engineering-2021

Sathia and Ganesh Babu [15] investigated durability characteristics of geopolymer concrete. They observed superior durability characteristics under acid attack & absorption characteristics. Raja Mane [16] et al. conducted rapid chloride ion penetration test & concluded that geopolymer concrete has chloride ion penetration with a low permeability. Satish Kumar et al. conducted experimental investigation on ternary blended GPC with different molarities of sodium hydroxide. It was noticed that higher the molarity of sodium hydroxide, higher is the strength of concrete [17–18].

2. Materials and methodology

The materials used in this experimental investigation are ground granulated blast furnace slag, flyash, metakaolin, M-sand, natural 20 mm size aggregate, steel fibers, sodium hydroxide & sodium silicate solution [19]. Fig. 1 exhibits the research methodology for this investigation.

In this study, Low calcium Flyash used was collected from BTPS, Ballari. It is a base binding material, consisting of SiO2 and Al2O3, ground granulated blast furnace slag was collected JSW Steels, Ballari mainly consists of Cao, MgO, and SiO2. Size of particle is less than 30microns.

Metakaolin [7] is used, which is having significant components are SiO2, Al2O3, and Fe2O3. The Filler material used was M−sand. Sieve analysis is conducted, and the fineness modulus of M sand is 2.90 and specific gravity of M sand 2.40.

Coarse aggregate used is natural 20 mm size aggregate and specific gravity 2.78.

Alkali activator solution was prepared using Na2SiO3 and NaOH with 12 M.Fosroc superplasticizer is used to improve the workability of concrete [20].

Crimped steel fibers with aspect-ratio 60 were used in varying volume forming this concrete [20].

3. Mix design

GPC Mix design code yet not specified and formulated. Hence, mix design was done by trial-and-error method. The mix design for the M50 grade of concrete is performed. The trial-and-error method was adopted for various mineral admixture. fibres were used in 0, 0.5, 1, and 1.5% by volume of concrete and named M1, M2, M3, and M4, respectively [21].

The mix proportion adopted in this experimental investigation consisting of GGBS, flyash, and metakaolin [1422]. Some authors have performed evaluation on self-compacting GPC under ambient temperature [23]. Table 1 represents the details of mixed proportions.

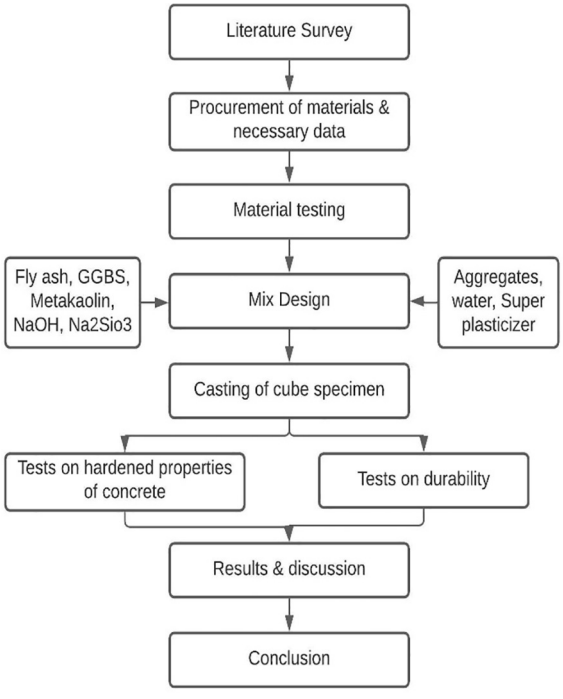

Fig. 1. Methodology.

3.1. Casting of test samples

All the ingredients are mixed in dry condition. Fibers are added uniformly. The alkaline solution with 12 M is used along with Superplasticizer. This Mixture is mix till homogeneity is obtained [24].

Cubes of size 150 mm is used for testing the compressive strength & durability tests. Concrete cylinder moulds of 150 mm diameter and height 300 mm is used for testing of split tensile strength and Beam specimens of size 150 mm* 150 mm* 700 mm for testing the flexural strength. Curing of the samples is carried out under sunlight for 28 days. Fig. 2 shows the casted specimens of GPC.

3.2. Tests conducted

The casted samples after curing are tested for mechanical, and durability properties. Mechanical properties include determining compressive strength, splitting tensile strength, and flexural strength. Also, durability properties include testing for acid Resistance, chloride attack, sulphate attack [25].

4. Result and discussions

4.1. Compressive strength

Cubes of 150 mm*150 mm size were tested for compression to find out the concrete's compressive strength. The test is performed

Table 1
Mix proportion.

Constituent used	Quantity used (kg/m^3)
Flyash	120.35
Ground granulated blast furnace slag	283.25
Metakaolin	72.46
M−sand	676.26
Natural Coarse aggregate	1396.25
NaOH solution	42.06
Na_2SiO_3 solution	108.64
Superplasticizer	6.00
Water	92.36

Fig. 2. Casted Specimen.

Table 2
Mechanical properties test results after 28, and 90 days of curing.

Mix ID	Compressive strength (MPa)		Split-tensile strength (MPa)		Flexural strength (MPa)	
	28 days	90 days	28 days	90 days	28 days	90 days
M1	50.43	53.68	3.72	3.86	4.72	4.96
M2	52.62	55.42	3.89	4.08	5.26	5.42
M3	54.30	58.57	3.98	4.18	6.22	6.45
M4	58.65	61.34	4.24	4.35	7.40	7.62

as per IS:516–1959 at 28 and 90 days of curing. Table 2 shows compressive strength at different curing days. From results it was observed that increase in fiber volume increases the compressive strength of concrete. An increase in strength is noticed with an increase in fibres at both the curing ages. Fig. 3 represents the graphical variation of compressive strength of concrete at both curing ages. Maximum strength is noticed at M4 mix comprising 1.5% of steel fibres. [14]

4.2. Splitting tensile strength

Cylinder of 150 mm*300 mm size casted & after curing it is tested for split tensile strength. The maximum load is noted when the specimens breaks or splits into two halves. The test is performed as per IS:516–1959 at 28 and 90 days of curing. Table 2 shows split tensile strength at different curing days. From results it was observed that enhancement in fiber volume enhances the split tensile strength of concrete. An increase in strength is noticed with an increase in fibres at both the curing ages. Fig. 4 represents the graphical representation of concrete's split-tensile strength at twain curing ages. Maximum strength is noticed at M4 mix comprising of higher volume fraction of fibers.

4.3. Flexural strength

Beam of 150 mm*150 mm*700 mm size casted & after curing it is tested for flexural strength under two-point loading. The test is performed as per IS:516–1959 at 28 and 90 days of curing. Table 2 shows flexural strength at different curing days. From results it was observed that rise in fiber volume increases the flexural strength of concrete Fig. 5 represents the graphical representation of concrete's flexural strength at twain curing ages. Maximum strength is noticed at M4 mix comprising 1.5% of steel fibres [3].

Durability properties are analyzed by considering weight loss on the concrete specimens immersed in sulphuric acid, Magnesium sulphate and hydrochloric acid. This test helps determine the long-term variation in the weight of concrete and, thereby, the strength of concrete.

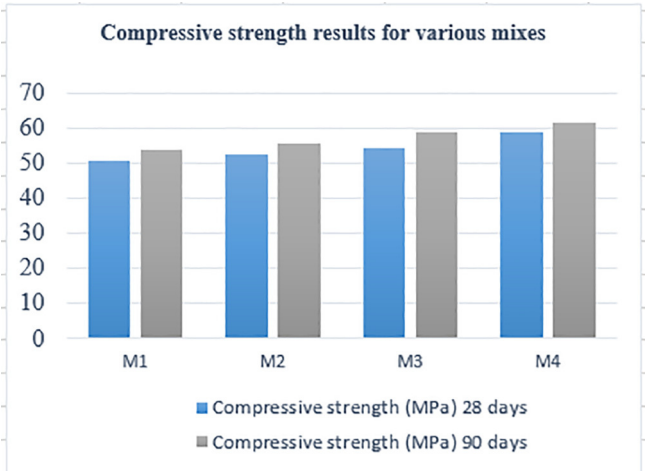

Fig. 3. Compressive strength at 28 and 90 days of curing.

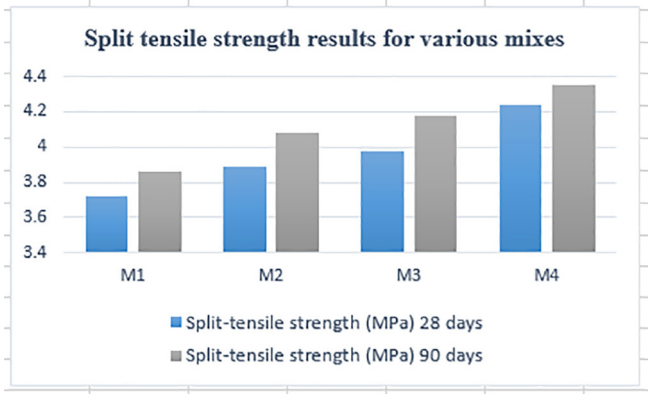

Fig. 4. Split-tensile strength at 28, and 90 days of curing.

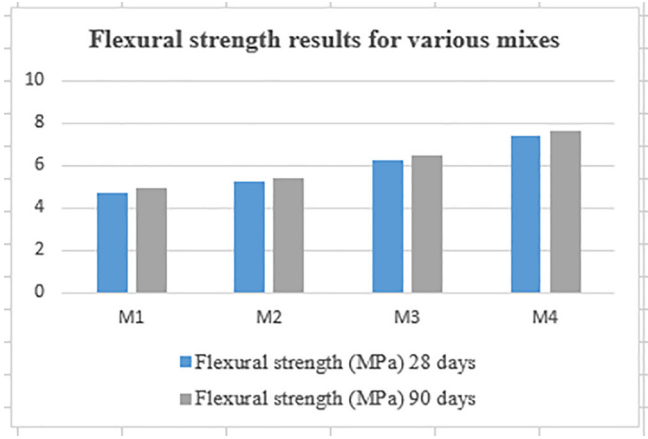

Fig. 5. Flexural strength at 28, and 90 days of curing.

4.4. Sulphuric acid resistance

Cubes after 28 days of curing period were kept in 5% concentrated sulphuric acid solution. To prepare, 5% concentration sulphuric acid, 95 g of water and 5 g (by weight) of H2So4 are mixed. Loss in weight of specimens when it is subjected to sulphuric acid is tabulated below in Table 3. Percentage loss in weight is found to be declining with an increase in fibres. Hence, we can say that using GPC we can achieve better strength and durability even after 90 days.

4.5. Chloride attack

Chloride especially in groundwater contact with concrete causing deterioration. Cubes after 28 days of curing period were kept in

Table 3
% Loss in weight after 90 days in when immersed in H_2SO_4.

Mix	Initial Weight (kg)	Final Weight (kg)	% Loss in weight (90 days)
M1	7.56	6.79	10.18
M2	7.68	6.89	10.28
M3	7.65	6.92	9.28
M4	7.58	6.88	9.23

Table 4
% Loss in weight after 90 days in when immersed in HCL.

Mix	Initial weight (kg)	Final Weight (kg)	% Loss in weight (90 days)
M1	7.80	7.62	2.30
M2	7.74	7.60	1.80
M3	7.78	7.62	2.05
M4	7.75	7.60	1.93

Table 5
% Loss in weight after 90 days in when immersed in $MgSo_4$.

Mix	Initial weight (kg)	Final Weight (kg)	% Loss in weight (90 days)
M1	7.74	7.60	1.80
M2	7.79	7.69	1.28
M3	7.72	7.64	1.03
M4	7.80	7.69	1.41

5% concentrated HCL solution. To prepare, 5% solution of concentrated hydrochloric acid, 95 g of water, and 5 g (by weight) of Hydrochloric acid is added. Loss in weight of specimens when it is subjected to HCL is tabulated below in Table 4. Percentage loss in weight is found to be fluctuating with an increase in fibres, and we can notice maximum resistance to chloride attack is noticed. Also, minimum weight loss is at 0.5% of fibres. Hence, we can say that using GPC, we can achieve better strength and durability even after 90 days.

4.6. Sulphate resistance

Some soil containing sulphate or groundwater containing sulphate contact with concrete causing deterioration. Cubes after 28 days of curing period were kept in 5% concentrated magnesium sulphate solution. To prepare, 5% solution of concentrated magnesium sulphate, 95 g of water, and 5 g (by weight) of Magnesium sulphate is added. Loss in weight of specimens when it is subjected to magnesium sulphate solution. is tabulated below in Table 5. Percentage loss in weight is found to be fluctuating with an increase in fibres, and we can notice that maximum resistance to sulphate attack is observed. Also, minimum weight loss is at 0.5 and 1% of fibres. Hence, we can say that using GPC, we can achieve better strength and durability even after 90 days.

5. Conclusion

Ternary blended geopolymer concrete with the incorporation of steel fibres shows superior strength & durability properties both 28 and 90 days of curing. Concrete mix with higher volume fraction of steel fibres has shown the maximum increase in the mechanical properties of GPC. 14.27% increase in compressive strength at 90 days of curing. Similarly, 12.69% increase in flexural strength and 53.63% increase in split tensile strength is observed at 90 days of curing. It also gives good results when it is subjected to chemical attacks. GPC performed well against chloride and sulphate attack with minimum reduction in its weight even after 90 days of exposure. It also reduces the wastage of thermal power plant production and is found to be environment friendly.

The scope of this study on GPC can be explored to determine the microstructural properties and cement binding using SEM, XRD tests. Moreover, additional tests on durability, such as water absorption, reduced compressive strength after 90 days of exposure to chemicals. Also, modulus of elasticity [26] can be determined by considering various admixtures along with life cycle assessment [27] of GPC.

CRediT authorship contribution statement

S Khalid: Investigation, Methodology. **Reshma T V:** Writing review & editing. **M S Shobha:** Supervision, Validation. **G Priyanka:** Investigation, Writing original draft. **Vineetha Satyanarayana Sirki:** Investigation, Writing original draft.

Declaration of Competing Interest

The authors declare that they have no known competing financial interests or personal relationships that could have appeared to influence the work reported in this paper.

References

[1] T.V. Reshma, M. Manjunatha, S. Sankalpasri, H.M. Tanu, Effect of waste foundry sand and fly ash on mechanical and fresh properties of concrete, Mater. Today Proc. (2021), https://doi.org/10.1016/j.matpr.2020.12.821.
[2] L.N. Assi, K. Carter, E. Deaver, P. Ziehl, Review of availability of source materials for geopolymer/sustainable concrete, J. Clean. Prod. 263 (2020) 121477, https://doi.org/10.1016/j.jclepro.2020.121477.
[3] D. Leela, S. Manjula, Mechanical strength characteristics of ternary blend geopolymer concrete with steel fibres under ambient curing, Int. J. Recent Technol. Eng. 8 (2020) 3013–3016, https://doi.org/10.35940/ijrte.e6103.018520.
[4] N. Ganesan, R. Abraham, S. Deepa Raj, Durability characteristics of steel fibre reinforced geopolymer concrete, Constr. Build. Mater. 93 (2015) 471–476, https://doi.org/10.1016/j.conbuildmat.2015.06.014.
[5] K. Singh, Experimental study on metakolin and baggashe ash based geopolymer concrete, Mater. Today Proc. 37 (2020) 3289–3295, https://doi.org/10.1016/j.matpr.2020.09.116.
[6] F.-Z. Refaie, R. Abbas, F.H. Fouad, Sustainable construction system with Egyptian metakaolin based geopolymer concrete sandwich panels, Case Stud. Constr. Mater. 13 (2020) e00436, https://doi.org/10.1016/j.cscm.2020.e00436.
[7] H.Y. Zhang, G.H. Qiu, V. Kodur, Z.S. Yuan, Spalling behavior of metakaolin-flyash based geopolymer concrete under elevated temperature exposure, Cem. Concr. Compos. 106 (2020) 103483, https://doi.org/10.1016/j.cemconcomp.2019.103483.
[8] Y.H.M. Amran, R. Alyousef, H. Alabduljabbar, M. El-Zeadani, Clean production and properties of geopolymer concrete; a review, J. Clean. Prod. 251 (2020) 119679, https://doi.org/10.1016/j.jclepro.2019.119679.
[9] J. Davidovits, S. France, Geopolymer chemistry and sustainable development. "The Poly (s ialate) term inology : a very useful and simp le model for th e p rom otion and understanding of green-chemistry", Conf. Pap. (2019).
[10] J. Davidovits, Geopolymer Chemistry and Applications. 5-th edition, 2020.
[11] T. Bakharev, Resistance of geopolymer materials to acid attack, Cem. Concr. Res. 35 (2005) 658–670, https://doi.org/10.1016/j.cemconres.2004.06.005.
[12] N. Lloyd, V. Rangan, Geopolymer concrete - sustainable cementless concrete, Am. Concr. Institute, ACI Spec. Publ. (2009) 33–53.
[13] X. Ke, M. Criado, J.L. Provis, S.A. Bernal, Slag-based cements that resist damage induced by carbon dioxide, ACS Sustain. Chem. Eng. 6 (2018) 5067–5075, https://doi.org/10.1021/acssuschemeng.7b04730.
[14] K. Ramujee, K.S. Prasad, B. Narendra Kumar, Durability properties of ternary blended geopolymer concrete under ambient curing, Int. J. Eng. Technol. 7 (2018) 46–50, https://doi.org/10.14419/ijet.v7i2.1.9882.
[15] A. Chithambar Ganesh, M. Muthukannan, Experimental study on the behaviour of hybrid fiber reinforced geopolymer concrete under ambient curing condition, IOP Conf. Ser. Mater. Sci. Eng. 561 (2019), https://doi.org/10.1088/1757-899X/561/1/012014.
[16] N.P. Rajamane, M.C. Nataraja, N. Lakshmanan, J.K. Dattatreya, Rapid chloride permeability test on geopolymer and Portland cement concretes, Indian Concr. J. 85 (2011) 21–26.
[17] G. Mathew, B.M. Issac, Effect of molarity of sodium hydroxide on the aluminosilicate content in laterite aggregate of laterised geopolymer concrete, J. Build. Eng. 32 (2020) 101486, https://doi.org/10.1016/j.jobe.2020.101486.

[18] K. Pandurangan, M. Thennavan, A. Muthadhi, Studies on effect of source of flyash on the bond strength of geopolymer concrete, Mater. Today Proc. 5 (2018) 12725–12733, https://doi.org/10.1016/j.matpr.2018.02.256.
[19] S. Mesgari, A. Akbarnezhad, J.Z. Xiao, Recycled geopolymer aggregates as coarse aggregates for Portland cement concrete and geopolymer concrete: effects on mechanical properties, Constr. Build. Mater. 236 (2020) 117571, https://doi.org/10.1016/j.conbuildmat.2019.117571.
[20] P.K. Prasanna, K. Srinivasu, A.R. Murthy, Compressive strength assessment using GGBS and randomly distributed fibers in concrete, Int. J. Innov. Technol. Explor. Eng. 9 (2019) 1078–1086, https://doi.org/10.35940/ijitee.l3186.129219.
[21] M.A. Kotop, M.S. El-Feky, Y.R. Alharbi, A.A. Abadel, A.S. Binyahya, Engineering properties of geopolymer concrete incorporating hybrid nano-materials, Ain Shams Eng. J. (2021), https://doi.org/10.1016/j.asej.2021.04.022.
[22] A.C. Ganesh, M. Muthukannan, Development of high performance sustainable optimized fiber reinforced geopolymer concrete and prediction of compressive strength, J. Clean. Prod. 282 (2021) 124543, https://doi.org/10.1016/j.jclepro.2020.124543.
[23] S.K. Rahman, R. Al-Ameri, A newly developed self-compacting geopolymer concrete under ambient condition, Constr. Build. Mater. 267 (2021) 121822, https://doi.org/10.1016/j.conbuildmat.2020.121822.
[24] M. Kalaivani, G. Shyamala, S. Ramesh, K. Angusenthil, R. Jagadeesan, Performance evaluation of fly ash/slag based geopolymer concrete beams with addition of lime, Mater. Today Proc. 27 (2020) 652–656, https://doi.org/10.1016/j.matpr.2020.01.596.
[25] T.V. Reshma, M. Manjunatha, A. Bharath, R.B. Tangadagi, J. Vengala, L.R. Manjunatha, Influence of ZnO and TiO2 on mechanical and durability properties of concrete prepared with and without polypropylene fibers, Materialia 18 (2021) 101138, https://doi.org/10.1016/j.mtla.2021.101138.
[26] R.R. Bellum, K. Muniraj, S.R.C. Madduru, Investigation on modulus of elasticity of fly ash-ground granulated blast furnace slag blended geopolymer concrete, Mater. Today Proc. 27 (2020) 718–723, https://doi.org/10.1016/j.matpr.2019.11.299.
[27] J.I.T. Garces, I.J. Dollente, A.B. Beltran, R.R. Tan, M.A.B. Promentilla, Life cycle assessment of self-healing geopolymer concrete, Clean. Eng. Technol. 4 (2021) 100147, https://doi.org/10.1016/j.clet.2021.100147.

KUVEMPU UNIVERSITY

Department of P.G. Studies and Research in Industrial Chemistry,
Jnana Sahyadri, Shankaraghatta-577451, Shivamogga, Karnataka

Certificate

This is to certify that Mr./Ms./Dr./Prof./ V. VEENA, Assistant professor, Ballari Institute of technology and Management, Ballari

has delivered/participated/presented Research paper entitled EFFECTIVE PHOTO-CONTROLLED RELEASE AND SYNERGISTIC ACTIVITY OF ENCAPSULATED CORAGEN-ZnO NANOPESTICIDE

(Oral/Poster) in the Two-day National Conference on "Impact of Chemistry and Biology to the Society and Industry" (ICBSI-2022) held on 20th & 21st May 2022, at Dept. of Industrial Chemistry, Kuvempu University, Shankaraghatta, Shivamogga, Karnataka.

Prof. H.S. Bhojya Naik
Convener

Prof. B.P. Veerabhadrappa
Vice Chancellor

Materials Today: Proceedings 54 (2022) 259–263

Contents lists available at ScienceDirect

Materials Today: Proceedings

journal homepage: www.elsevier.com/locate/matpr

Analysis of strength and durability properties of ternary blended geopolymer concrete

S. Khalid [a], T.V. Reshma [b,*], M.S. Shobha [c], G. Priyanka [a], Vineetha Satyanarayana Siriki [a]

[a] Department of Civil Engineering, BITM, Ballari 583104, India
[b] Department of Civil Engineering, GITAM University, Bengaluru 562163, India
[c] Department of Civil Engineering, RYMEC, Ballari 583104, India

ARTICLE INFO

Article history:
Available online 15 September 2021

Keywords:
Fly ash (FA)
Ground granulated blast furnace slag (GGBS)
Geopolymer concrete (GPC)
Molarity (M)
Metakaolin (MK)

ABSTRACT

Cement is the primary raw material in any construction works, being an indispensable binding material. The production associate degreed consumption of cement is an index of its industrial development. However, excess production of cement pollutes the setting by emotional CO2 gas. So, it is necessary to exchange cement with alternative binding materials. In this study, one such trial is attempted using mineral admixtures like Fly ash, GGBS which are industrial waste byproducts. The concrete specimens are cast using, Fly ash, GGBS, and Metakaolin, with Alkaline liquid like Sodium silicate, and Sodium Hydroxide solution with 10 M, in the ratio of 1:1.5 and 1:2. Fibers such as steel fibers and polypropylene fibers are added with a 0–1.5% percentage to enhance the concrete properties. The moulds are cured under sunlight. The mechanical properties such as flexural strength, compressive strength, and split-tensile strength are performed along with durability tests to evaluate the optimized ratio of using mineral admixtures and fibers. The test results indicate that the combination of Metakaolin and GGBS can be used to develop environmentally friendly geopolymer concrete.

Selection and peer-review under responsibility of the scientific committee of the 5th International Conference on Advanced Research in Mechanical, Materials and Manufacturing Engineering-2021

1. Introduction

Infrastructure development in the modern era has made use of cement concrete in huge quantities. Concrete construction has made to deplete natural resources and causing pollution in the environment. The binding material used in manufacturing concrete is cement, leading to CO2 emission in its manufacturing process, causing environmental pollution. Moreover, the extraction of limestone for cement manufacturing will cause in the reduction of renewable resources like limestone [1]. Hence, it is essential to use environmentally friendly alternative binding cementitious material [2].

This study focuses on the experimental investigation using ternary blended GPC reinforced with steel fibers [34]. The development of ternary GPC consisting of ground granulated blast furnace slag, flyash, and metakaolin as mineral admixture activated with sodium hydroxide & sodium silicate solution [5–7]. To improve the split-tensile strength property of concrete, Steel fibres are also added to this concrete. The minor research studies are done on fiber reinforced ternary blend GPC under sunlight curing. Strength and durability characteristics were also studied. Finally, the test results are analyzed to know the suitability of using this concrete [3].

Past Literatures available on geo-polymer concrete shows that this type of concrete is a good alternative for conventional concrete. Therefore, although very little research study is there on ternary blended geopolymer concrete using fibers [8]. Therefore, this study has been carried out with the gaps present on geopolymer concrete.

Joseph Davidovits [9,10] developed the idea of using polymer concrete as an alternative cement concrete. It can be manufactured by using alumina-silicate materials using alkali activators. It has very good strength & durability properties.

T Bakharev [11] conducted experimental study on durability characteristics of geopolymer concrete such as acid resistance and sulphate resistance. It was found that ternary blended geopolymer concrete showed good performance under these attacks [12–14].

* Corresponding author.
E-mail address: rvishwes@gitam.edu (T.V. Reshma).

https://doi.org/10.1016/j.matpr.2021.08.307

Selection and peer-review under responsibility of the scientific committee of the 5th International Conference on Advanced Research in Mechanical, Materials and Manufacturing Engineering-2021

Sathia and Ganesh Babu [15] investigated durability characteristics of geopolymer concrete. They observed superior durability characteristics under acid attack & absorption characteristics. Raja Mane [16] et al. conducted rapid chloride ion penetration test & concluded that geopolymer concrete has chloride ion penetration with a low permeability. Satish Kumar et al. conducted experimental investigation on ternary blended GPC with different molarities of sodium hydroxide. It was noticed that higher the molarity of sodium hydroxide, higher is the strength of concrete [17–18].

2. Materials and methodology

The materials used in this experimental investigation are ground granulated blast furnace slag, flyash, metakaolin, M-sand, natural 20 mm size aggregate, steel fibers, sodium hydroxide & sodium silicate solution [19]. Fig. 1 exhibits the research methodology for this investigation.

In this study, Low calcium Flyash used was collected from BTPS, Ballari. It is a base binding material, consisting of SiO2 and Al2O3, ground granulated blast furnace slag was collected JSW Steels, Ballari mainly consists of Cao, MgO, and SiO2. Size of particle is less than 30microns.

Metakaolin [7] is used, which is having significant components are SiO2, Al2O3, and Fe2O3. The Filler material used was M−sand. Sieve analysis is conducted, and the fineness modulus of M sand is 2.90 and specific gravity of M sand 2.40.

Coarse aggregate used is natural 20 mm size aggregate and specific gravity 2.78.

Alkali activator solution was prepared using Na2SiO3 and NaOH with 12 M.Fosroc superplasticizer is used to improve the workability of concrete [20].

Crimped steel fibers with aspect-ratio 60 were used in varying volume forming this concrete [20].

3. Mix design

GPC Mix design code yet not specified and formulated. Hence, mix design was done by trial-and-error method. The mix design for the M50 grade of concrete is performed. The trial-and-error method was adopted for various mineral admixture. fibres were used in 0, 0.5, 1, and 1.5% by volume of concrete and named M1, M2, M3, and M4, respectively [21].

The mix proportion adopted in this experimental investigation consisting of GGBS, flyash, and metakaolin [1422]. Some authors have performed evaluation on self-compacting GPC under ambient temperature [23]. Table 1 represents the details of mixed proportions.

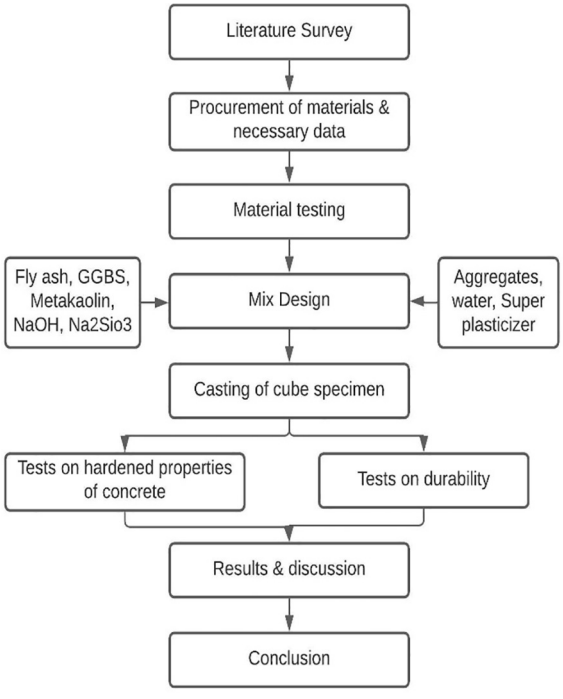

Fig. 1. Methodology.

3.1. Casting of test samples

All the ingredients are mixed in dry condition. Fibers are added uniformly. The alkaline solution with 12 M is used along with Superplasticizer. This Mixture is mix till homogeneity is obtained [24].

Cubes of size 150 mm is used for testing the compressive strength & durability tests. Concrete cylinder moulds of 150 mm diameter and height 300 mm is used for testing of split tensile strength and Beam specimens of size 150 mm* 150 mm* 700 mm for testing the flexural strength. Curing of the samples is carried out under sunlight for 28 days. Fig. 2 shows the casted specimens of GPC.

3.2. Tests conducted

The casted samples after curing are tested for mechanical, and durability properties. Mechanical properties include determining compressive strength, splitting tensile strength, and flexural strength. Also, durability properties include testing for acid Resistance, chloride attack, sulphate attack [25].

4. Result and discussions

4.1. Compressive strength

Cubes of 150 mm*150 mm size were tested for compression to find out the concrete's compressive strength. The test is performed

Table 1
Mix proportion.

Constituent used	Quantity used (kg/m^3)
Flyash	120.35
Ground granulated blast furnace slag	283.25
Metakaolin	72.46
M−sand	676.26
Natural Coarse aggregate	1396.25
NaOH solution	42.06
Na_2SiO_3 solution	108.64
Superplasticizer	6.00
Water	92.36

Fig. 2. Casted Specimen.

Table 2
Mechanical properties test results after 28, and 90 days of curing.

Mix ID	Compressive strength (MPa)		Split-tensile strength (MPa)		Flexural strength (MPa)	
	28 days	90 days	28 days	90 days	28 days	90 days
M1	50.43	53.68	3.72	3.86	4.72	4.96
M2	52.62	55.42	3.89	4.08	5.26	5.42
M3	54.30	58.57	3.98	4.18	6.22	6.45
M4	58.65	61.34	4.24	4.35	7.40	7.62

as per IS:516–1959 at 28 and 90 days of curing. Table 2 shows compressive strength at different curing days. From results it was observed that increase in fiber volume increases the compressive strength of concrete. An increase in strength is noticed with an increase in fibres at both the curing ages. Fig. 3 represents the graphical variation of compressive strength of concrete at both curing ages. Maximum strength is noticed at M4 mix comprising 1.5% of steel fibres. [14]

4.2. Splitting tensile strength

Cylinder of 150 mm*300 mm size casted & after curing it is tested for split tensile strength. The maximum load is noted when the specimens breaks or splits into two halves. The test is performed as per IS:516–1959 at 28 and 90 days of curing. Table 2 shows split tensile strength at different curing days. From results it was observed that enhancement in fiber volume enhances the split tensile strength of concrete. An increase in strength is noticed with an increase in fibres at both the curing ages. Fig. 4 represents the graphical representation of concrete's split-tensile strength at twain curing ages. Maximum strength is noticed at M4 mix comprising of higher volume fraction of fibers.

4.3. Flexural strength

Beam of 150 mm*150 mm*700 mm size casted & after curing it is tested for flexural strength under two-point loading. The test is performed as per IS:516–1959 at 28 and 90 days of curing. Table 2 shows flexural strength at different curing days. From results it was observed that rise in fiber volume increases the flexural strength of concrete Fig. 5 represents the graphical representation of concrete's flexural strength at twain curing ages. Maximum strength is noticed at M4 mix comprising 1.5% of steel fibres [3].

Durability properties are analyzed by considering weight loss on the concrete specimens immersed in sulphuric acid, Magnesium sulphate and hydrochloric acid. This test helps determine the long-term variation in the weight of concrete and, thereby, the strength of concrete.

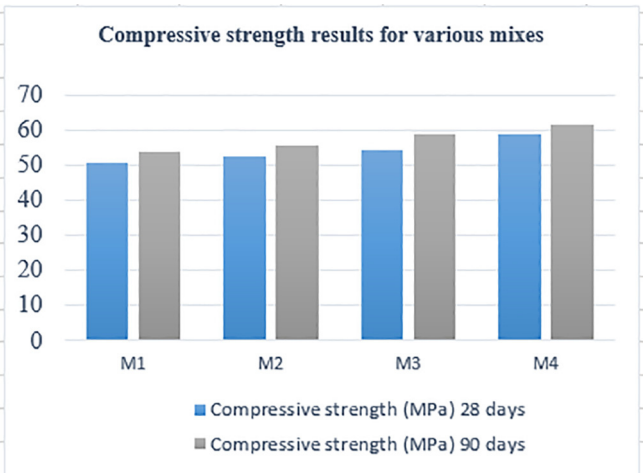

Fig. 3. Compressive strength at 28 and 90 days of curing.

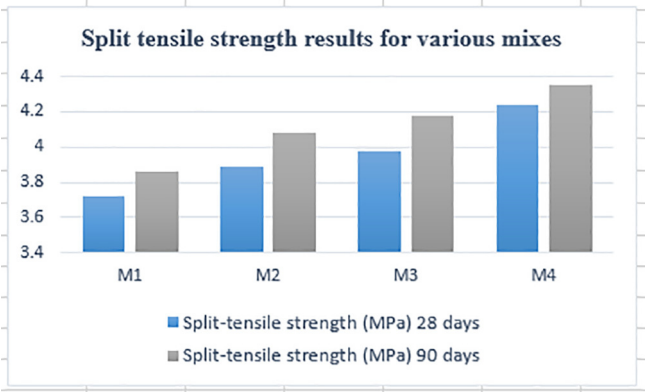

Fig. 4. Split-tensile strength at 28, and 90 days of curing.

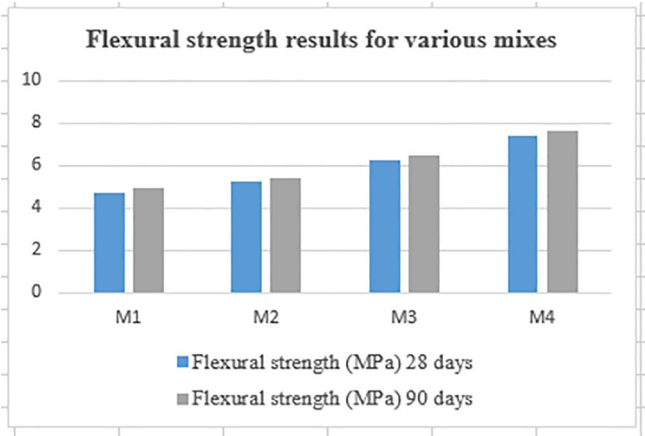

Fig. 5. Flexural strength at 28, and 90 days of curing.

4.4. Sulphuric acid resistance

Cubes after 28 days of curing period were kept in 5% concentrated sulphuric acid solution. To prepare, 5% concentration sulphuric acid, 95 g of water and 5 g (by weight) of H2So4 are mixed. Loss in weight of specimens when it is subjected to sulphuric acid is tabulated below in Table 3. Percentage loss in weight is found to be declining with an increase in fibres. Hence, we can say that using GPC we can achieve better strength and durability even after 90 days.

4.5. Chloride attack

Chloride especially in groundwater contact with concrete causing deterioration. Cubes after 28 days of curing period were kept in

Table 3
% Loss in weight after 90 days in when immersed in H_2SO_4.

Mix	Initial Weight (kg)	Final Weight (kg)	% Loss in weight (90 days)
M1	7.56	6.79	10.18
M2	7.68	6.89	10.28
M3	7.65	6.92	9.28
M4	7.58	6.88	9.23

Table 4
% Loss in weight after 90 days in when immersed in HCL.

Mix	Initial weight (kg)	Final Weight (kg)	% Loss in weight (90 days)
M1	7.80	7.62	2.30
M2	7.74	7.60	1.80
M3	7.78	7.62	2.05
M4	7.75	7.60	1.93

Table 5
% Loss in weight after 90 days in when immersed in $MgSo_4$.

Mix	Initial weight (kg)	Final Weight (kg)	% Loss in weight (90 days)
M1	7.74	7.60	1.80
M2	7.79	7.69	1.28
M3	7.72	7.64	1.03
M4	7.80	7.69	1.41

5% concentrated HCL solution. To prepare, 5% solution of concentrated hydrochloric acid, 95 g of water, and 5 g (by weight) of Hydrochloric acid is added. Loss in weight of specimens when it is subjected to HCL is tabulated below in Table 4. Percentage loss in weight is found to be fluctuating with an increase in fibres, and we can notice maximum resistance to chloride attack is noticed. Also, minimum weight loss is at 0.5% of fibres. Hence, we can say that using GPC, we can achieve better strength and durability even after 90 days.

4.6. Sulphate resistance

Some soil containing sulphate or groundwater containing sulphate contact with concrete causing deterioration. Cubes after 28 days of curing period were kept in 5% concentrated magnesium sulphate solution. To prepare, 5% solution of concentrated magnesium sulphate, 95 g of water, and 5 g (by weight) of Magnesium sulphate is added. Loss in weight of specimens when it is subjected to magnesium sulphate solution. is tabulated below in Table 5. Percentage loss in weight is found to be fluctuating with an increase in fibres, and we can notice that maximum resistance to sulphate attack is observed. Also, minimum weight loss is at 0.5 and 1% of fibres. Hence, we can say that using GPC, we can achieve better strength and durability even after 90 days.

5. Conclusion

Ternary blended geopolymer concrete with the incorporation of steel fibres shows superior strength & durability properties both 28 and 90 days of curing. Concrete mix with higher volume fraction of steel fibres has shown the maximum increase in the mechanical properties of GPC. 14.27% increase in compressive strength at 90 days of curing. Similarly, 12.69% increase in flexural strength and 53.63% increase in split tensile strength is observed at 90 days of curing. It also gives good results when it is subjected to chemical attacks. GPC performed well against chloride and sulphate attack with minimum reduction in its weight even after 90 days of exposure. It also reduces the wastage of thermal power plant production and is found to be environment friendly.

The scope of this study on GPC can be explored to determine the microstructural properties and cement binding using SEM, XRD tests. Moreover, additional tests on durability, such as water absorption, reduced compressive strength after 90 days of exposure to chemicals. Also, modulus of elasticity [26] can be determined by considering various admixtures along with life cycle assessment [27] of GPC.

CRediT authorship contribution statement

S Khalid: Investigation, Methodology. **Reshma T V:** Writing review & editing. **M S Shobha:** Supervision, Validation. **G Priyanka:** Investigation, Writing original draft. **Vineetha Satyanarayana Sirki:** Investigation, Writing original draft.

Declaration of Competing Interest

The authors declare that they have no known competing financial interests or personal relationships that could have appeared to influence the work reported in this paper.

References

[1] T.V. Reshma, M. Manjunatha, S. Sankalpasri, H.M. Tanu, Effect of waste foundry sand and fly ash on mechanical and fresh properties of concrete, Mater. Today Proc. (2021), https://doi.org/10.1016/j.matpr.2020.12.821.
[2] L.N. Assi, K. Carter, E. Deaver, P. Ziehl, Review of availability of source materials for geopolymer/sustainable concrete, J. Clean. Prod. 263 (2020) 121477, https://doi.org/10.1016/j.jclepro.2020.121477.
[3] D. Leela, S. Manjula, Mechanical strength characteristics of ternary blend geopolymer concrete with steel fibres under ambient curing, Int. J. Recent Technol. Eng. 8 (2020) 3013–3016, https://doi.org/10.35940/ijrte.e6103.018520.
[4] N. Ganesan, R. Abraham, S. Deepa Raj, Durability characteristics of steel fibre reinforced geopolymer concrete, Constr. Build. Mater. 93 (2015) 471–476, https://doi.org/10.1016/j.conbuildmat.2015.06.014.
[5] K. Singh, Experimental study on metakolin and baggashe ash based geopolymer concrete, Mater. Today Proc. 37 (2020) 3289–3295, https://doi.org/10.1016/j.matpr.2020.09.116.
[6] F.-Z. Refaie, R. Abbas, F.H. Fouad, Sustainable construction system with Egyptian metakaolin based geopolymer concrete sandwich panels, Case Stud. Constr. Mater. 13 (2020) e00436, https://doi.org/10.1016/j.cscm.2020.e00436.
[7] H.Y. Zhang, G.H. Qiu, V. Kodur, Z.S. Yuan, Spalling behavior of metakaolin-flyash based geopolymer concrete under elevated temperature exposure, Cem. Concr. Compos. 106 (2020) 103483, https://doi.org/10.1016/j.cemconcomp.2019.103483.
[8] Y.H.M. Amran, R. Alyousef, H. Alabduljabbar, M. El-Zeadani, Clean production and properties of geopolymer concrete; a review, J. Clean. Prod. 251 (2020) 119679, https://doi.org/10.1016/j.jclepro.2019.119679.
[9] J. Davidovits, S. France, Geopolymer chemistry and sustainable development. "The Poly (s ialate) term inology : a very useful and simp le model for th e p rom otion and understanding of green-chemistry", Conf. Pap. (2019).
[10] J. Davidovits, Geopolymer Chemistry and Applications. 5-th edition, 2020.
[11] T. Bakharev, Resistance of geopolymer materials to acid attack, Cem. Concr. Res. 35 (2005) 658–670, https://doi.org/10.1016/j.cemconres.2004.06.005.
[12] N. Lloyd, V. Rangan, Geopolymer concrete - sustainable cementless concrete, Am. Concr. Institute, ACI Spec. Publ. (2009) 33–53.
[13] X. Ke, M. Criado, J.L. Provis, S.A. Bernal, Slag-based cements that resist damage induced by carbon dioxide, ACS Sustain. Chem. Eng. 6 (2018) 5067–5075, https://doi.org/10.1021/acssuschemeng.7b04730.
[14] K. Ramujee, K.S. Prasad, B. Narendra Kumar, Durability properties of ternary blended geopolymer concrete under ambient curing, Int. J. Eng. Technol. 7 (2018) 46–50, https://doi.org/10.14419/ijet.v7i2.1.9882.
[15] A. Chithambar Ganesh, M. Muthukannan, Experimental study on the behaviour of hybrid fiber reinforced geopolymer concrete under ambient curing condition, IOP Conf. Ser. Mater. Sci. Eng. 561 (2019), https://doi.org/10.1088/1757-899X/561/1/012014.
[16] N.P. Rajamane, M.C. Nataraja, N. Lakshmanan, J.K. Dattatreya, Rapid chloride permeability test on geopolymer and Portland cement concretes, Indian Concr. J. 85 (2011) 21–26.
[17] G. Mathew, B.M. Issac, Effect of molarity of sodium hydroxide on the aluminosilicate content in laterite aggregate of laterised geopolymer concrete, J. Build. Eng. 32 (2020) 101486, https://doi.org/10.1016/j.jobe.2020.101486.

[18] K. Pandurangan, M. Thennavan, A. Muthadhi, Studies on effect of source of flyash on the bond strength of geopolymer concrete, Mater. Today Proc. 5 (2018) 12725–12733, https://doi.org/10.1016/j.matpr.2018.02.256.
[19] S. Mesgari, A. Akbarnezhad, J.Z. Xiao, Recycled geopolymer aggregates as coarse aggregates for Portland cement concrete and geopolymer concrete: effects on mechanical properties, Constr. Build. Mater. 236 (2020) 117571, https://doi.org/10.1016/j.conbuildmat.2019.117571.
[20] P.K. Prasanna, K. Srinivasu, A.R. Murthy, Compressive strength assessment using GGBS and randomly distributed fibers in concrete, Int. J. Innov. Technol. Explor. Eng. 9 (2019) 1078–1086, https://doi.org/10.35940/ijitee.l3186.129219.
[21] M.A. Kotop, M.S. El-Feky, Y.R. Alharbi, A.A. Abadel, A.S. Binyahya, Engineering properties of geopolymer concrete incorporating hybrid nano-materials, Ain Shams Eng. J. (2021), https://doi.org/10.1016/j.asej.2021.04.022.
[22] A.C. Ganesh, M. Muthukannan, Development of high performance sustainable optimized fiber reinforced geopolymer concrete and prediction of compressive strength, J. Clean. Prod. 282 (2021) 124543, https://doi.org/10.1016/j.jclepro.2020.124543.
[23] S.K. Rahman, R. Al-Ameri, A newly developed self-compacting geopolymer concrete under ambient condition, Constr. Build. Mater. 267 (2021) 121822, https://doi.org/10.1016/j.conbuildmat.2020.121822.
[24] M. Kalaivani, G. Shyamala, S. Ramesh, K. Angusenthil, R. Jagadeesan, Performance evaluation of fly ash/slag based geopolymer concrete beams with addition of lime, Mater. Today Proc. 27 (2020) 652–656, https://doi.org/10.1016/j.matpr.2020.01.596.
[25] T.V. Reshma, M. Manjunatha, A. Bharath, R.B. Tangadagi, J. Vengala, L.R. Manjunatha, Influence of ZnO and TiO2 on mechanical and durability properties of concrete prepared with and without polypropylene fibers, Materialia 18 (2021) 101138, https://doi.org/10.1016/j.mtla.2021.101138.
[26] R.R. Bellum, K. Muniraj, S.R.C. Madduru, Investigation on modulus of elasticity of fly ash-ground granulated blast furnace slag blended geopolymer concrete, Mater. Today Proc. 27 (2020) 718–723, https://doi.org/10.1016/j.matpr.2019.11.299.
[27] J.I.T. Garces, I.J. Dollente, A.B. Beltran, R.R. Tan, M.A.B. Promentilla, Life cycle assessment of self-healing geopolymer concrete, Clean. Eng. Technol. 4 (2021) 100147, https://doi.org/10.1016/j.clet.2021.100147.

Materials Today: Proceedings 66 (2022) 2315–2321

Contents lists available at ScienceDirect

Materials Today: Proceedings

journal homepage: www.elsevier.com/locate/matpr

Performance of rice husk ash, silica fume, and quarry dust based glass fibre reinforced concrete subjected to acid attack

Sachin Patil [a,*], T.H. Patel [b]

[a] Department of Civil Engineering, RYMEC, Ballari 583104, Karnataka, India
[b] Department of Civil Engineering, BITM, Ballari 583104, Karnataka, India

ARTICLE INFO

Article history:
Available online 24 June 2022

Keywords:
Acid attack
Glass fiber
Rice husk ash
Silica fume
Quarry dust

ABSTRACT

In this analysis silica fume, quarry dust, and rice husk ash were used as partial replacement for cement. To create advanced concrete, glass fibers were added. The experiment is looking into the effect of HCl and H_2SO_4 acid attack on concrete cured at 30, 60, and 90 days. Concrete mix was designed for 0.4 water binder ratio by keeping quarry dust replacement at 20 percentiles. Silica fume and rice husk ash was replaced in 10, 20 and 30 percentage each in proportions. 0.25, 0.5, and 0.75 percent of the total volume was the percentages of glass fibers added in the mix. It has been discovered that replacing cement with 20 percentage each of rice husk ash, silica fume, and quarry dust, along with 0.75 percent glass fibre, delivers the best acid resistance. Through its use, offered concrete making reduces cement production and minimizes damage to the environment.

Selection and peer-review under responsibility of the scientific committee of 2022 International Conference on Recent Advances in Engineering Materials.

1. Introduction

For its stronger strength and reduced thicknesses, which marks in thinner sections and lesser construction load, HPC has seen a growth in demand as a result of development and a rising need for concrete. HPC is utilized to build many infrastructure projects, among other things, thus this is cost-effective for consumers. According to recent studies, the production of Portland cement emits greenhouse gases. In 2018, global cement production was at 4.05 BT. Investigators have proposed a number of cement substitutes that can assist reduce cement use, pollutants, and energy consumption. Furthermore, this design strengthens concrete characteristics.

Rice husk (RHA) was manufactured as a pozzolana using a unique procedure that ensured its physiochemical properties matched technical standards while keeping the silica in an amorphous condition with a small amount of carbon waste. The findings revealed that pozzolanic efficacy differs based on the fineness with which the pozzolana is crushed and the temperatures at which it is burned. The latter obtained by addition of rice husk ash (RHA) to concrete mixtures on compressive strength and volume was investigated. Compared to control mix, a significant compression strength was achievable, with a level of 40% replacement. Even though the American Standard has limited volume changes, they are well within the estimated range [1]. According to studies, adding silica fume (SF) to concrete improves water penetration resistance, which in turn improves resistance to chloride ion penetration. The outcomes of current investigations on SF concrete have affected the substantial use of SF in the building sector over the last 20 years. The outcome of utilising SF and glass fibre mixed HPC was also investigated by the authors, who discovered that the enhanced strength and durability are potential possibilities in the production of HPC [2–5].

In comparison to concrete mixes lacking GF fibre, studies indicated that incorporating GF fibre into concrete created tougher M20 graded concrete mixtures with a 15–20% improvement in compressive strength. All the possible properties has been studied in depth and found to be improved by the use of fibres, especially the light, tough, and economical fibre known as glass. The addition of GF improves the part's resistance to shrinkage-related cracks by allowing it to twist and stretch more. Even yet, if fibres are utilised at a concentration of more than 1% by volume, the concrete will be lumpy and difficult to work with. Researchers have discovered that quarry dust (QD) can improve the strength of concrete [6–11].

In comparison to normal Portland cement, the scientific group has not spent much time investigating the durability of HPC, which uses RHA, SF, and QD as replacements, as well as GF with super-

* Corresponding author.
E-mail address: sachinpatil.akruthi@gmail.com (S. Patil).

https://doi.org/10.1016/j.matpr.2022.06.231
2214-7853/
Selection and peer-review under responsibility of the scientific committee of 2022 International Conference on Recent Advances in Engineering Materials.

plasticizers. As a result, there is a scarcity of study materials. The findings of experimental investigation into the acid attack resistance of RHA, SF, and QD based GF reinforced HPC, also known as glass fibre reinforced ternary blended concrete, are presented in this article (GFRTBC).

2. Materials and their characteristics

The cement used was grade 53 OPC with a specific gravity of 3.15. Fine aggregates(FA) with a specific gravity of 2.60 were utilised to get the appropriate concrete mix. The coarse aggregates (CA) utilised have a specific gravity of 2.65. RHA has a specific gravity of 2.30 and a specific surface area of 55.4 m^2/g, with SiO_2 accounting for 88.32 percent of its composition. The SF utilised had a specific gravity of 2.20, a specific surface area of 22.2 m^2/g, and 91.36 percent SiO_2. The QD in question is round, white, and has a specific gravity of 2.60. CemFil AntiCrack HD Glass fibre with a diameter of 14 μm and a length of 12 mm was employed in this concrete production. These fibres are water dispersible, which means they may totally disperse when mixed with water, allowing them to maintain each GF isolated from the others. Concrete is mixed with fresh, potable water that is devoid of organic and acid contaminants. Superplasticizer with a specific gravity of 1.18 is used to improve the workability of concrete. Hydrochloric acid (HCl) and sulfuric acid (H_2SO_4) in 5 percent concentration solutions were used in the investigation since this concentration had the necessary pH and had a deteriorating effect on materials.

3. Methodology for the study

3.1. Proportions of the mixture

To evaluate the behaviour of GFRTBC, 9 combinations with 0.4 proportion of water to binders were prepared in the lab and compared to a control mixture of M20 grade plain concrete. RHA and SF were substituted at 10%, 20%, and 30%, respectively, although QD maintained at 20%. 0.25, 0.5, and 0.75 percentages GF were introduced to the mix as volume percentages. The SP content in the binder was 0.8 weighted percentage. The percentages were worked out using the volume approach, which involves evaluating volume rather than weight. The cement being used is standard Portland cement with a grade of 53, which was manufactured in a single batch lately. The first digit in the mix designation is the proportion of cement replacement, indicating how much RHA and SF is included. R stands for RHA, and S stands for SF. The next number depicts the amount of cement that was substituted with QD. Succeeding Q designates QD. The concluding letter denotes the proportion of glass fiber ingredients, such as A = 0.25 percent GF, B = 0.50 percent GF, and C = 0.75 percent GF. 10RS20QA is a GFRTBC mix of 10% RHA and SF cement replacement each, 20% cement substitution of QD, and 0.25 percent GF for a water - binder of 0.4, with 394 kg/m^3 cement and 49.25 kg/m^3 RHA and SF, and 120 kg/m^3 QD. The amount of ingredients and mixing compositions used are shown in Tables 1 and 2.

3.2. Preparing, curing, and testing samples

The samples were made by manually combining cement, fine aggregate, RHA, SF, and QD to make a homogeneous mix, and then adding glass fibres. At the end of the process, coarse aggregates, water, and a superplasticizer were added to the mix. A total of 18 samples of 100 mm cube were made for each of the nine mixes in the investigation. With 21 specimens, one M20 grade mixture was made as a control mixture. At 30, 60, & 90 days, each sample was evaluated. Following the concrete setting process, samples were taken from the mould and nine M20 grade cubes were placed in tanks with 5% HCl and H_2SO_4 solutions to cured them until testing. Remaining 3 cubes of M20 grade mix were cured in normal water to test at 28 days, which is required for calculating residual compressive strength. 9 cubes out of 18 cubes each (cast for each GFRTBC mix) were submerged in HCl & H_2SO_4 solutions at a dosage of 5%. Out of a total of 9 cubes, three were submerged in each acid for 30, 60, and 90 days. A curing duration based on the test's intended age was followed by samples being dried under shade after being removed from water. The specimen was compressed on the 3000 kN machine to failure under constant load. A compression testing machine is calibrated to within 1% of its maximum value according to IS: 14858(2000) and all the recommendations outlined in 1828(Class1). The samples were loaded into the device, and the cubes were loaded gradually until they failed in the compression test as shown in Fig. 1. Every one of the group's samples was examined in the very same batches, so the results represent an average of the result of each.

4. Discussion of the findings

4.1. Impact of rice husk ash, silica fume, and quarry dust as cement substitutes on acid attack resistance of GFRTBC

As shown in Fig. 2(a) and (b), cement substitution rate by RHA, SF and QD has an impact on the HCl and H_2SO_4 acid attack resistance of GFRTBC. Fig. 2(a) and (b) show how the acid attack resistance of GFRTBC is affected by the percent substitution of cement by RHA, SF, and QD. These statistics show that when RHA, SF, and QD were added to GFRTBC, the residual compressive strength rose for 10% RHA and SF replacement levels, respectively and for 20 % QD. The highest residual compressive strength is reached when RHA, SF, and QD each replace 20% of the cement. The residual compressive strength began to decrease as the admixture level increased, i.e. at 30% RHA, SF, and 20% QD. This is true for each of the three glass fibre dosages tested in this study. The residual compressive strengths of GFRTBC immersed in HCl and H_2SO_4 acid

Table 1
Quantities of the ingredients.

Mix	W/B	SP	RHS	SF	QD	GF
				(%)		
10RS20QA	0.4	0.8	10	10	20	0.25
20RS20QA	0.4	0.8	20	20	20	0.25
30RS20QA	0.4	0.8	30	30	20	0.25
10RS20QB	0.4	0.8	10	10	20	0.50
20RS20QB	0.4	0.8	20	20	20	0.50
30RS20QB	0.4	0.8	30	30	20	0.50
10RS20QC	0.4	0.8	10	10	20	0.75
20RS20QC	0.4	0.8	20	20	20	0.75
30RS20QC	0.4	0.8	30	30	20	0.75

Table 2
Amounts per cubic meter of the mixture.

Mix	Cement (Kg)	RHS (Kg)	SF (Kg)	QD (Kg)	Water (Lts)	CA (Kg)	FA (Kg)
10RS20QA	394.00	49.25	49.25	120.00	197.00	1054.00	479.00
20RS20QA	295.50	98.50	98.50	118.00	197.00	1036.00	470.00
30RS20QA	197.00	147.75	147.75	115.00	197.00	1013.00	460.00
10RS20QB	394.00	49.25	49.25	120.00	197.00	1054.00	479.00
20RS20QB	295.50	98.50	98.50	118.00	197.00	1036.00	470.00
30RS20QB	197.00	147.75	147.75	115.00	197.00	1013.00	460.00
10RS20QC	394.00	49.25	49.25	120.00	197.00	1054.00	479.00
20RS20QC	295.50	98.50	98.50	118.00	197.00	1036.00	470.00
30RS20QC	197.00	147.75	147.75	115.00	197.00	1013.00	460.00

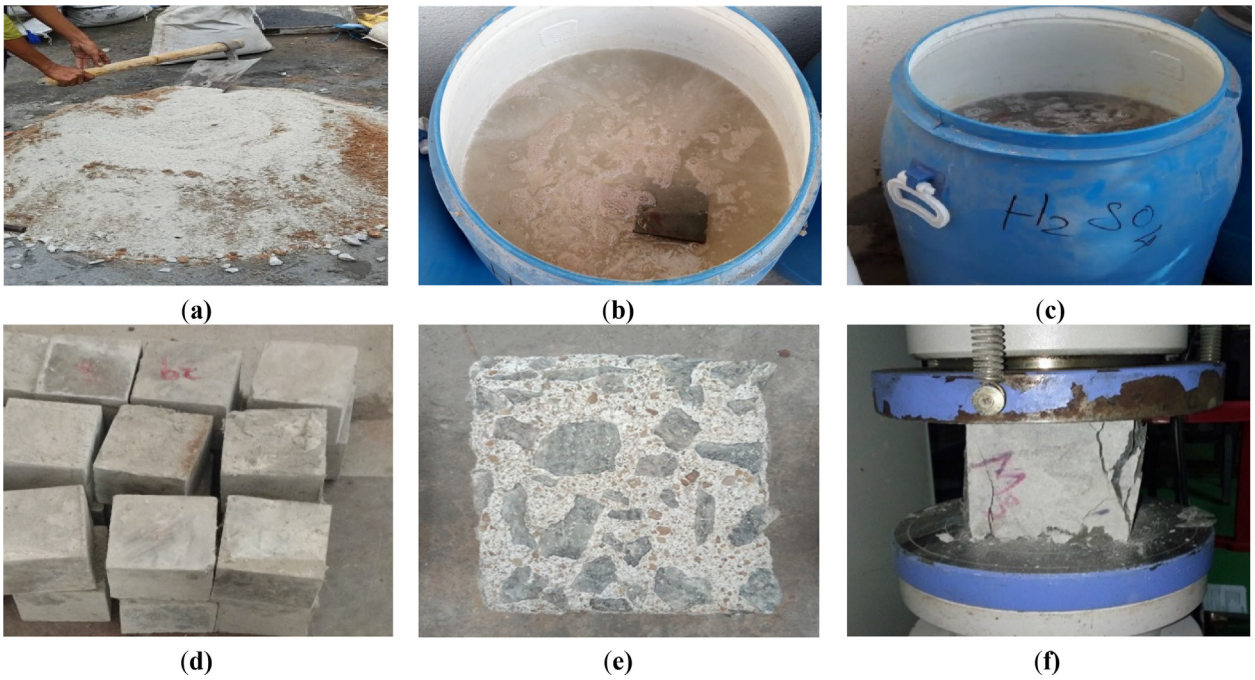

Fig. 1. (a) Mixing; (b) Curing samples in HCl solution; (c) Curing samples in H_2SO_4 solution; (d) Sample following 90 days of HCl cure; (e) Sample after ninety days H_2SO_4 curing; (f) Following ninety days of HCl cure, testing and failure patterns of the sample examined.

is much greater than residual compressive strength of reference mix of M20 grade cured in HCl and H_2SO_4 acid at all replacement levels. All three glass fibre dosages studied show a similar pattern.

The residual compressive strength of 10RS20QA treated in HCl at ninety days was raised by 96.29 percent when compared with M20 grade concrete cured in same acid and curing age. With a 20 percent rise in RHA, SF, & QD, residual compressive strength rose by 1.72 percent when compared to the 10RS20QA mix. Furthermore, the compressive strength of the 30RS20QA mix fell by 7.49 percent when compared to the 20RS20QA mixture. All doses of glass fibres and curing ages showed a similar tendency.

The residual strength of 10RS20QA concrete cured in H_2SO_4 at 90 days was raised by 115 percent when compared to M20 grade concrete cured in H_2SO_4 at ninety days. RHA, SF, and QD were further increased to 20%, resulting in a 0.73 percent enhancement in residual compressive strength competed to the 10RS20QA mix. Furthermore, the compressive strength of the 30RS20QA mix was 5.17 percent lower than the 20RS20QA mix.

As a result, it can be inferred that adding RHA,SF, and QD to GFRTBC at 20% replacement levels improves the microstructure of HPC by increasing density the transition zone, resulting in the greatest gain in acid attack resistance in the current study.

4.2. Impact of glass fiber volumes on acid attack resistance of GFRTBC

To analyse the outcome of the percentage of glass fibres for HCl and H_2SO_4 attacks on the HCl and H_2SO_4 acid attack resistance for each mix, the residual compressive strengths are charted versus the proportions of glass fibres for all three ages of testing cured in HCl and H_2SO_4 acids in Fig. 3(a), and (b), respectively. Fig. 3 indicates that introducing 0.25, 0.5, and 0.75 percent glass fibres to GFRTBC mixtures enhanced the residual compressive strength after 30, 60, and 90 days, respectively. The plot clearly illustrates that 0.75 percent glass fibre inclusion resulted in the highest residual compressive strength for varied curing ages.

For HCl curing, the 90 days residual compressive strength of 20RS20QA, 20RS20QB, and 20RS20QC mixtures was amplified by 99.68%, 105.03%, and 110.10% respectively with respect to M20 reference mix concrete cured in HCl at 90 days. For H_2SO_4 curing, the 90 days residual compressive strength of 20RS20QA, 20RS20QB, and 20RS20QC mixes was increased by 116.56%, 125.23%, and 135.60% correspondingly inline with M20 control mixture concrete cured in H_2SO_4 at 90 days. All ages of curing showed a similar pattern.

Since these fibres can act as reinforcements both at the microscopic and macroscopic scales, this functionality is possible. These

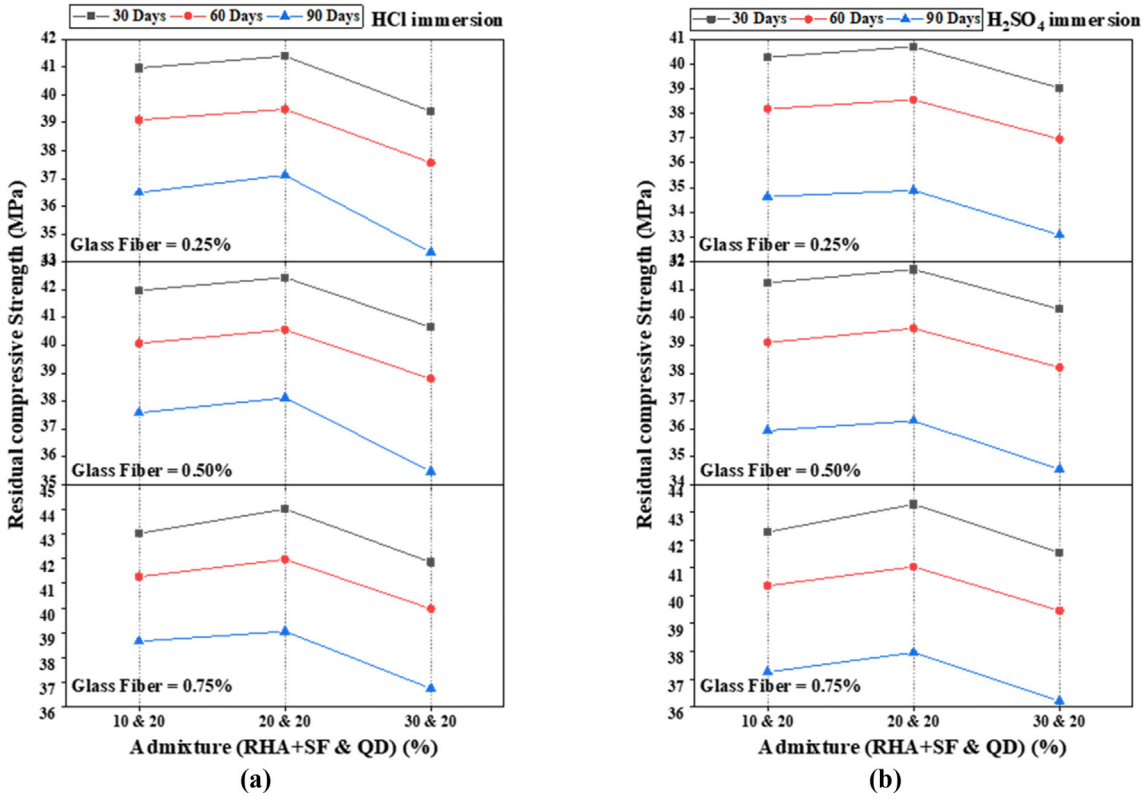

Fig. 2. (a) Residual compressive strength versus RHA, SF, and QD portions for diverse GFRTBC mixes cured in HCl; (b) Residual compressive strength versus RHA, SF, and QD portions for diverse GFRTBC mixes cured in H_2SO_4.

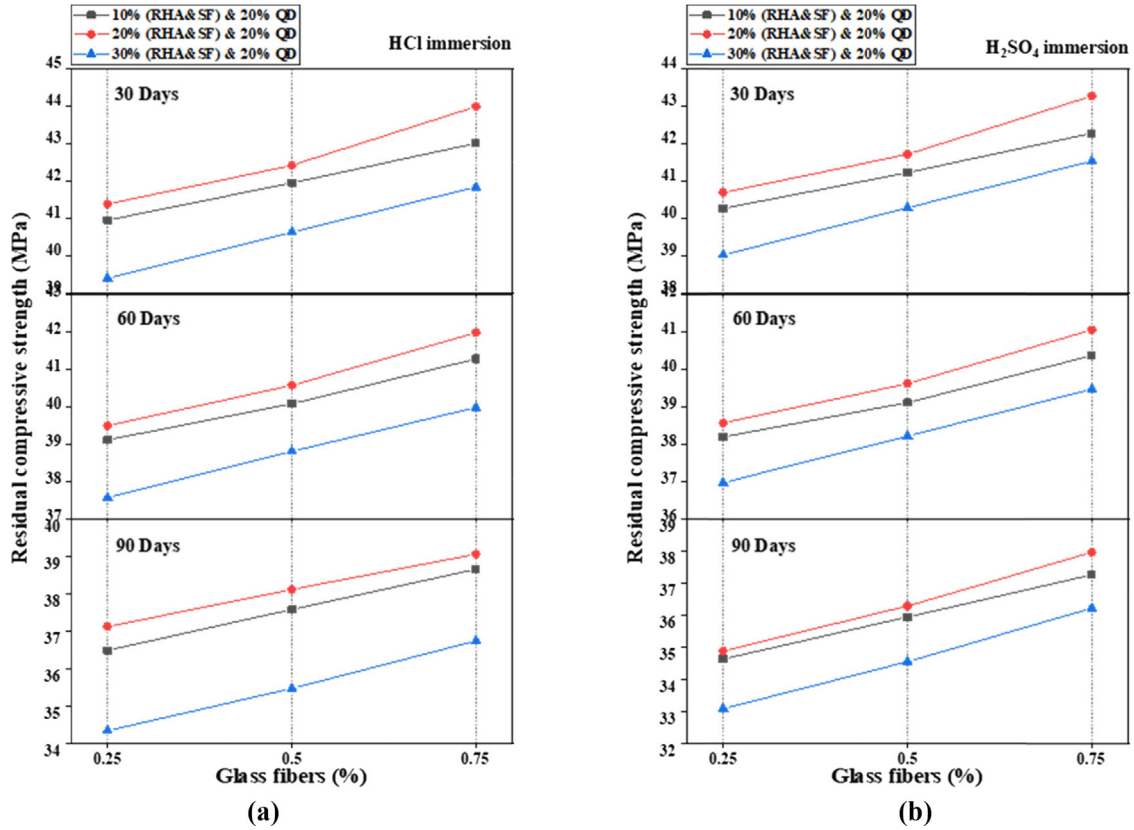

Fig. 3. (a) Residual compressive strength vs. glass fiber proportions for diverse GFRTBC mixtures cured in HCl; (b) Residual compressive strength vs. glass fiber proportions for diverse GFRTBC mixtures cured in H_2SO_4.

fibres avoid micro-cracks from forming on a microscopic scale. The quantity of fibres available in the matrix has a significant influence on the development of microscopic cracks. These fibres promote better strength by avoiding fracture openings from widening further and enhancing energy absorption capacity at macroscopic levels. As a result, almost impenetrable concrete can be manufactured, and minute and macro fractures are less probable to form, assuring long-term concrete durability.

Only by the incorporation of glass fibres improves the flexibility of normal concrete. Because of the strain hardening reaction of GFRTBC, this work included fibre glass and additives, which resulted in a significant enhancement in acid attack resistance.

4.3. Impact of period of curing on acid attack resistance of GFRTBC

To determine how the age of curing affects the development of residual compressive strength for every mix, the results of all three aging tests cured in HCl & H_2SO_4 acid in Fig. 4(a) and (b) respectively against the curing days for different proportions of glass fibers, RHA, SF, and QD are shown. The residual compressive strength diminishes with time of curing, as shown in the graph.

20RS20QA mix at 30 days had a residual compressive strength of 41.40 MPa after HCl curing. Further at 60 days, the residual compressive strength decreased by 4.68% and by 8.60% at 90 days with respect to 30 day residual compressive strength of same mix. 20RS20QB mix at 30 days had a residual compressive strength of 42.44 MPa after HCl curing. Further at 60 days, the residual compressive strength decreased by 4.41% and by 6.04% at 90 days with respect to 30 day residual compressive strength of same mix. Similarly, 20RS20QC mix at 30 days had a residual compressive strength of 44 MPa after HCl curing. Further at 60 days, the residual compressive strength decreased by 4.62% and by 6.34% at 90 days with respect to 30 day residual compressive strength of same mix.

20RS20QA mix at 30 days had a residual compressive strength of 40.71 MPa after H_2SO_4 curing. Further at 60 days, the residual compressive strength decreased by 5.32% and by 10.49% at 90 days with respect to 30 day residual compressive strength of same mix. 20RS20QB mix at 30 days had a residual compressive strength of 41.73 MPa after H_2SO_4 curing. Further at 60 days, the residual compressive strength decreased by 5.07% and by 8.40% at 90 days with respect to 30 day residual compressive strength of same mix. Similarly, 20RS20QC mix at 30 days had a residual compressive strength of 43.29 MPa after H_2SO_4 curing. Further at 60 days, the residual compressive strength decreased by 5.19% and by 7.68% at 90 days with respect to 30 day residual compressive strength of same mix.

The residual compressive strength degrades due to the formation of ettringites over time in the acid immersion, and this deterioration reaches its maximum at ninety days in all two acid curings.

4.4. Impact of type of acid on acid attack resistance of GFRTBC

GFRTBC mixtures were exposed to concentrated HCl and H_2SO_4 solutions at 5 percent strength. In Fig. 5(a), (b), and (c), we can see the impact of these acids on residual compressive strength of GFRTBC mixes in W/B of 0.4 for 10 percent RHA, SF, & 20 percent QD, 20 percent RHA, SF, & 20 percent QD, and 30 percent RHA, SF, and 20 percent QD.

It is clear from the results that cubes treated with H_2SO_4 acid immersion had the highest levels of compressive strength depreciation compared to cubes treated with HCl. The current investigation revealed that the three mineral admixture doses followed the same pattern. Cement substitution rate for all mineral admixtures and the inclusion of glass fibres, the HCl acid curing had the least degradation of compressive strength of the two acids, HCl and H_2SO_4.

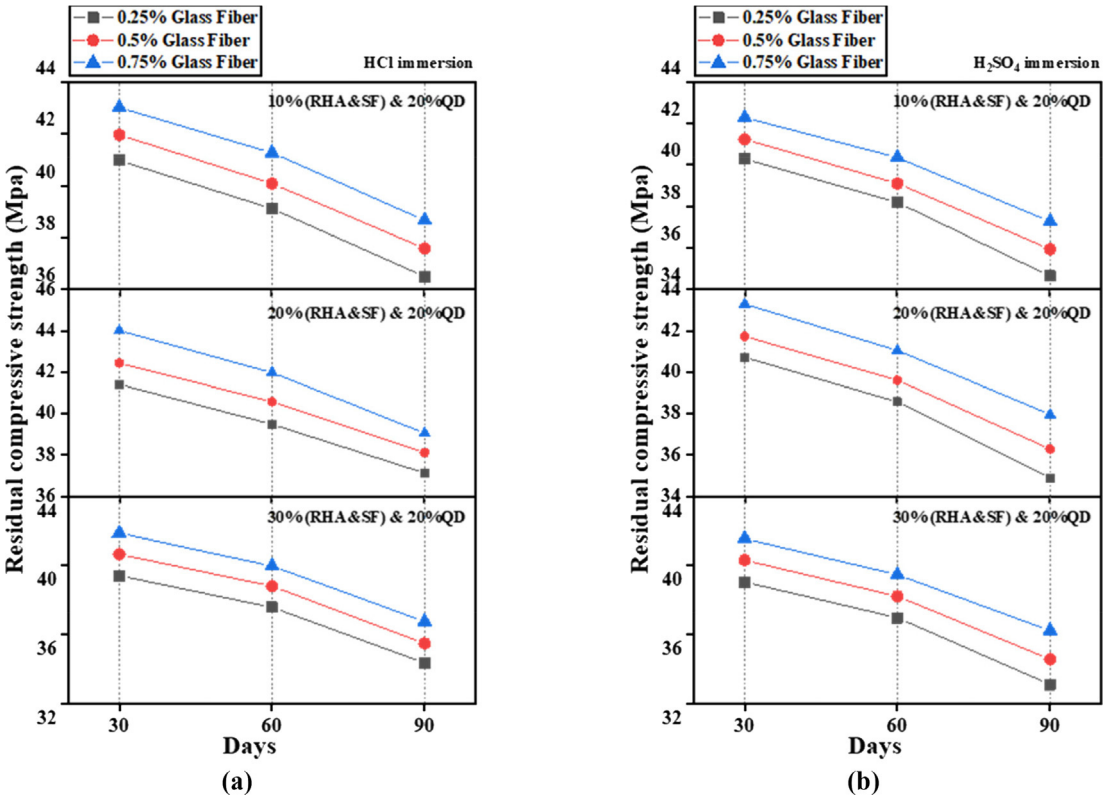

Fig. 4. (a) Residual compressive strength vs. periods curing for diverse GFRTBC mixtures cured in HCl; (b) Residual compressive strength vs. periods curing for diverse GFRTBC mixtures cured in H_2SO_4.

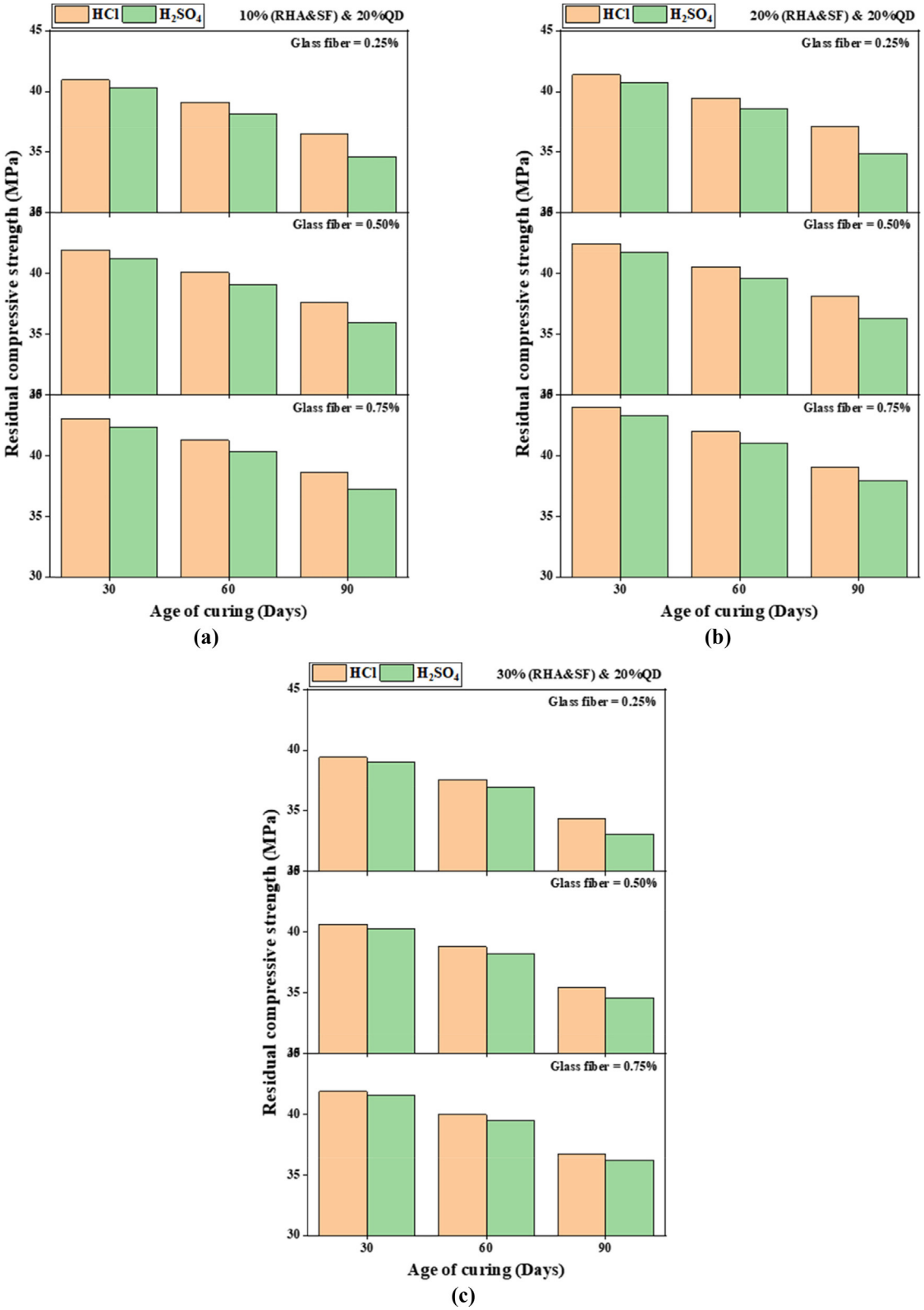

Fig. 5. (a) Residual compressive strength against periods of acid curing for diverse GFRTBC mixtures thru 10% RHA,SF and 20% QD; (b) Residual compressive strength against periods of acid curing for diverse GFRTBC mixtures thru 20% RHA,SF and 20% QD; (c) Residual compressive strength against periods of acid curing for diverse GFRTBC mixtures thru 30% RHA,SF and 20% QD.

The residual compressive strength of the 20RS20QC mix that had been treated with 30 days of HCl was 44 MPa, but for the same mix when treated with 30 days of H_2SO_4 the residual compressive strength decreased to 43.29 MPa, which reduced by 1.63%. The $CaSO_4$ created due to H_2SO_4 had a bad outcome on the compressive strength of concrete as its 60-day and 90-day strength also reduced

by 2.21% and 2.82%, respectively, showing how badly the $CaSO_4$ reacted with the C3A to form expansive ettringite, resulting in the concrete's loss of compressive strength. The same results were found for other mixes. This study found that H_2SO_4 is more powerful at degrading GFRTBC, while HCl is least effective.

5. Conclusions

The effectiveness of these acid attack tests was studied to see how GFRTBC generated using RHA, SF, QD, and GF held up for resistance to HCl and H_2SO_4 acids. The following points are obtained from the findings:

- Compared to a plain M20 grade reference mix, RHA, SF, and QD based GFRTBC mix counterattacked the acids more effectively and was effective across all ages of exposure to HCl and H_2SO_4.
- It can be arrived at the conclusion from the test performed on concrete of different ages that if substitution of cement is retained underneath 20%, the residual compressive strength will upsurge with an increase in RHA, SF, and QD replacement; however, once this level is exceeded, the residual compressive strength started to decline. For all ages of assessment, a 20 percent mineral admixture replacement level on GFRTBC provides the best residual compressive strength.
- When glass fibres were introduced to all three concrete testing ages, the acid attack resistance of the GFRTBC mixes improved vastly. The acid attack resistance of GFRTBC mixtures with 0.75 percent glass fibre was the highest, and they were suitable for all ages of testing.
- An escalation in the period of acid curing caused the compressive strength of GFRTBC to decrease. 90 days of acid immersion produces the greatest possible loss of compressive strength. All acids tested had the same behavior.
- Compressive strength took the greatest hit when using H_2SO_4 acid curing versus HCl. The least amount of compressive strength loss was noted when HCl acid immersion was used.
- As a result, the ideal cement replacement is 20% RHA, 20% SF, and 20% QD, with 0.75 percent glass fibre added at a W/B of 0.4 to achieve greatest acid attack resistance for GFRTBC.
- These findings demonstrated the feasibility of employing RHA, SF, QD, and GF in GFRTBC manufacturing, as well as the ability to reduce cement output while preserving the environment from pollutants.

Rice husk ash, silica fume, and quarry dust, as well as glass fibre, were used in the production of GFRTBC in this study which can be used for structures of importance like bridges, dams etc. New research in the future could use a mixture of metakaolin, silica fume, and stone dust to manufacture GFRTBC, with steel fibres replacing the glass fibres used in this investigation.

CRediT authorship contribution statement

Sachin Patil: Conceptualization, Investigation, Methodology, Writing – original draft. **T.H. Patel:** Supervision, Writing – review & editing.

Declaration of Competing Interest

The authors declare that they have no known competing financial interests or personal relationships that could have appeared to influence the work reported in this paper.

References

[1] M.N. Al-Khalaf, H.A. Yousif, Use of rice h u s k ash in concrete, Int. J. Cem. Compos. Light. Concr. 6 (4) (1984) 241–248.
[2] R. Siddique, Utilization of silica fume in concrete: Review of hardened properties, Resour. Conserv. Recycl. 55 (11) (2011) 923–932, https://doi.org/10.1016/j.resconrec.2011.06.012.
[3] M.I. Khan, R. Siddique, Utilization of silica fume in concrete: Review of durability properties, Resour. Conserv. Recycl. 57 (2011) 30–35, https://doi.org/10.1016/j.resconrec.2011.09.016.
[4] S. Patil, H.M. Somasekharaiah, H. Sudarsana Rao, V.G. Ghorpade, Behaviour of Fly Ash and Silica Fume based Composite Fiber (Glass and Polypropylene) reinforced High-Performance Concrete under Acid Attack, IOP Conf. Ser. Earth Environ. Sci. 822 (1) (2021) 012030, https://doi.org/10.1088/1755-1315/822/1/012030.
[5] S. Patil, H.M. Somasekharaiah, H.S. Rao, V.G. Ghorpade, Effect of Fly ash, Silica fume, Glass Fiber and Polypropylene Fiber on Strength Properties of Composite Fiber Reinforced High Performance, Concrete 69 (2021) 69–84, https://doi.org/10.14445/22315381/IJETT-V69I5P212.
[6] D. Kumar, L.K. Rex, V.S. Sethuraman, V. Gokulnath, B. Saravanan, High performance glass fiber reinforced concrete, Mater. Today Proc. 33 (2020) 784–788, https://doi.org/10.1016/j.matpr.2020.06.174.
[7] G. Barluenga, F. Hernández-Olivares, Cracking control of concretes modified with short AR-glass fibers at early age. Experimental results on standard concrete and SCC, Cem. Concr. Res. 37 (12) (2007) 1624–1638, https://doi.org/10.1016/j.cemconres.2007.08.019.
[8] S. Patil, H.M. Somasekharaiah, H. Sudarsana Rao, Evaluation of strength properties of fly ash and metakaolin based composite fiber (glass and polypropylene) reinforced high-performance concrete, Int. J. Eng. Trends Technol. 69 (2021) 188–203, https://doi.org/10.14445/22315381/IJETT-V69I4P227.
[9] S. Patil, H.M. Somasekharaiah, H.S. Rao, V.G. Ghorpade, Behaviour of fly ash and metakaolin based composite fiber (Glass and polypropylene) reinforced high performance concrete under acid attack, Civ. Eng. Archit. 9 (2021) 1026–1047, https://doi.org/10.13189/cea.2021.090406.
[10] S. Patil, H.M. Somasekharaiah, H. Sudarsana Rao, Chloride penetration resistance and behaviour under acid attack of metakaolin and silica fume based composite fiber (glass and polypropylene) reinforced high performance concrete, Int. J. Eng. Trends Technol. 69 (2021) 146–161, https://doi.org/10.14445/22315381/IJETT-V69I4P222.
[11] S. Patil, T.H. Patel, E. Yashodha, The effect of rice husk ash, silica fume, and quarry dust on glass fibre reinforced concrete's strength properties, Mater. Today:. Proc. 59 (2022) 918–925.

Ricerche di Matematica
https://doi.org/10.1007/s11587-022-00687-4

Heat and mass transport nature of MHD nanofluid flow over a magnetized and convectively heated surface including Hall current, magneto and thermo diffusions impacts

Jitendra Kumar Singh[1,2] · **Suneetha Kolasani**[1,3] · **G. S. Seth**[4]

Received: 8 October 2021 / Revised: 10 December 2021 / Accepted: 14 March 2022

Abstract
The key interest in this paper to examine the heat and mass transport nature of Ti_6Al_4V–H_20 based nanofluid flow and its interaction with a strong magnetic field. In this study significances of Hall current, magneto and thermo diffusions on the flow behavior are included. The induced magnetic field (IMF) and its consequences on the flow-field are also examined. The non-dimensional flow model is solved analytically by use of perturbation method. In order to scrutinize the effects of relevant flow parameters to the flow nature, the numerical values of flow behaviors corresponds to these parameters are depicted, and graphically and tabuly presented. This kind of a study has significant applications in nano science to explore the heat and mass transport characteristic of electrically conducting nanofluids. An important result noted from this study that, on incrementing the volumetric concentration of nanoparticles in the fluid employing resistance force which cause to reduce the flow velocity and enhance the temperature. The mass diffusion factor grows the flow velocity while it reduces the IMF along the main flow. A key fact noted that Hall current generates IMF by modifying the existing magnetic field.

Keywords Nanofluid · Heat and mass transport · Hall current · Magneto diffusion · Thermo diffusion

✉ Jitendra Kumar Singh
s.jitendrak@yahoo.com

1 Department of Mathematics, Vijayanagara Sri Krishnadevaraya University, Ballari 583105, India

2 Present Address: Department of Mathematics, Siddharth University Kapilvastu, Siddharthnagar 272202, India

3 Department of Mathematics, Ballari Institute of Technology and Management, Ballari 583105, India

4 Department of Applied Mathematics, Indian Institute of Technology (ISM), Dhanbad 826004, India

Published online: 04 April 2022

Mathematics Subject Classification 76R10 · 76S05 · 76U05 · 76W05

Abbreviations

Bi	Biot number
C_p	Specific heat at constant pressure
D	Chemical molecular diffusivity
Fi	Solutal biot number
g	Acceleration due to gravity
g_Θ	Thermal grashof number
g_Φ	Solutal grashof number
c_m	Coefficient of convective mass transfer
c_h	Coefficient of convective heat transfer
hc	Hall current parameter
$\vec{v}$	Velocity field
$\vec{h}$	Induced magnetic field
Hp	Chemical reaction parameter
h_1, h_2, h_3	Non-dimensional magnetic field components along x_1', x_2' and x_3' directions
(h_1', h_0, h_3')	Induced magnetic field components along x_1', x_2' and x_3' directions
$(j_1, 0, j_3)$	Non-dimensional current density components along x_1', x_2' and x_3' directions
k	Permeability parameter
k'	Permeability of the porous medium
Mg^2	Magnetic parameter
Su	Suction parameter
Ro	Rotation parameter
R_1	Magnetic viscosity
S_1	Heat absorption coefficient
S_2	Thermal reaction constant
v_1, v_2, v_3	Non-dimensional velocity components along x_1', x_2' and x_3' directions
$(v_1', -V_0, v_3')$	Velocity components along x_1', x_2' and x_3' directions
v_0	Characteristic velocity
V_0	Transpiration velocity
(x_1', x_2', x_3')	Cartesian coordinates

Greek symbols

α	Thermal diffusivity
β	Volumetric thermal expansion coefficient
β^*	Coefficient of chemical molecular expansion
μ	Dynamic viscosity
μ_e	Magnetic viscosity
υ	Coefficient of viscosity

υ_m	Magnetic viscosity
φ	Volume fraction coefficient of nanofluid
Φ	Non-dimensional species concentration
ϕ'	Species concentration
ϕ'_w	Concentration near wall
ϕ'_∞	Ambient concentration
ρ	Fluid density
σ	Electrical conductivity
Θ	Non-dimensional fluid temperature
θ'	Fluid temperature
θ'_w	Wall temperature
θ'_∞	Ambient temperature
$(\tau_1, 0, \tau_3)$	Non-dimensional skin friction components

Subscripts

f	Quantities for base fluid
nf	Quantities for nanofluid

1 Introduction

The area of nanoscience and nanotechnology attracted the attention of the researchers since its emergence due its tremendous applications such as thermal industry, nuclear reactors, powder technology, biomedical industry etc. During the experimental investigation of the heat transport behavior of aqueous sodium chloride with suspended polystyrene sphere, Ahuja [1] observed that the effective thermal conductivity of suspension is 3 times higher than the effective thermal conductivity of the aqueous sodium chloride. Further he revealed that the thermal conductivity of the suspension depends on various thermo physical properties like particle size, concentration of the liquid, shear rate, viscosity, thermal diffusivity etc. Choi and Eastman [2] were first who introduced this new class of fluid and named it nanofluid. They found that the thermal performance of fluid can be enhanced by emerging nano size particles in them called nanoparticles. Pak and Cho [3] experimentally examined the heat transfer and turbulent friction nature of ultrafine metallic oxide suspended water flowing through a circular tube. They revealed from their investigation that the convective heat transfer in water is higher than the dispersed fluid and for enhancing the thermal performance of the dispersed fluid large number of particles to be added to the water. A method for measuring the thermal conductivity of oxide nanofluids is developed by Lee et al. [4]. Through the results they verified that the thermal conductivity of the nanofluid is neither depends only on the shape of the nanoparticles but theirs size also. A systematic procedure for preparing the nanofluid is presented in the research paper of Xuan and Li [5]. Moreover, they scrutinized the thermal performance of nanofluid in a tube. Soon after these pioneer research investigations researchers started to explore the heat and

mass transfer behavior of nanofluids under diverse flow conditions and configurations. It is a well known fact that the emergence of large size of nanoparticles to a base fluid produces drag force which reduces the flow velocity and enhance the fluid temperature. Similar to this fact, the flow of an electrically conducting fluid under the appearance of a magnetic field also produces a drag force as a result reduces the flow velocity and enhance the fluid temperature. The presence of magnetic field domain significantly affecting the nanofluid flows. In view of these facts many scientists investigated the flow of nanofluids in connection with MHD. Some recent excellent research works which captures the heat transfer aspects in MHD nanofluid flows are due to Sheikholesami and Rokni [6], Muhammad et al. [7], Durga Prasad et al. [8], Dutta et al. [9], Das et al. [10], Khan et al. [11], Mkhatshwa et al. [12], Sreedevi et al. [13] and Khan et al. [14]. An insightful review of literatures on MHD flow reports that most of the studies either consider the flow surface to be non-conducting or infinitely conducting. However, in many industrial applications the flow surface may be magnetized which significantly alter the consequence of the applied magnetic field. Stimulated from these facts Seth et al. [15] and Singh et al. [16, 17] examined the hydromagnetic flow problems over the magnetized surface. Furthermore it is seen that the majority of the research papers neglect the IMF effect to the MHD flow problems by considering the large magnetic viscosity. But when we are dealing with such a working fluid for which the magnetic viscosity is very small ($\upsilon_m \ll 1$ or $Rm \gg 1$) in that condition we cannot ignore the IMF effect. The generated magnetic field also has considerable influence on the flow nature. Singh et al. [18] examined the significances of wall conductivity on mixed convective flow within a porous channel with induced magnetic field. They scrutinized that the wall conductivity notably affecting the induced magnetic field and it tend to enhance the IMF along the principal flow direction. Subsequently, Kumar et al. [19] analyzed the impacts of viscous dissipation and thermal radiation on mixed convective flow over a vertical surface and seen that the buoyancy force and viscous dissipation have tendency of incrementing the IMF. The role of IMF on MHD mixed convective flow in a microchannel with radially applied magnetic field is presented in the paper of Jha and Aina [20]. Kumar et al. [21] analyzed the MHD natural convective flow within a vertical channel consisting of a conducting and a non-conducting wall. An interesting result noted that the magnetic parameter considerably improves the constituent of the IMF. The nature of heat and mass transport in MHD dissipative boundary layer flow over a vertically oriented surface including IMF effect is investigated by the research team of Poddar [22]. It is seen that the magnetic parameter leads to decrease the induced magnetic field. Similar behavior of magnetic parameter on IMF is recorded in the paper of Alharbi [23]. Askari et al. [24] discussed the heat transfer behavior of MHD water-graphene based nanofluid flow within a channel with viscous dissipation and IMF effects. They observed that the absolute value of the induced magnetic field increases when the Hartmann number rises. The phenomena Hall and ion-slip appears in electrodynamics due to wandering of ions and charge particles about the electromagnetic field lines. The phenomenon of ion-slip current may be neglected in many of the cases because the mass of the ions are much larger than the mass of the electrons and hence the velocity of ions is much smaller than the velocity of electrons. These phenomena place a decisive role in scrutinizing flow features of many problems. Sato [25] was first who successfully applied the Hall phenomenon

in examining the flow behavior of ionized gases flowing within a parallel plate channel. Soon after Sato [25], Datta and Jana [26], Krishnam Raju and Ramana Rao [27], Hossain and Rashid [28], Linga Raju and Ramana Rao [29] and Nagy and Demendy [30] studied the Hall phenomenon in MHD flow problems. The significances of Hall phenomenon on the MHD nanofluid flow under various geometrical configurations are excellently presented in the papers of Shah et al. [31], Reddy et al. [32], Bishnoi et al. [33] and Singh et al. [34]. The combined impacts of Hall and ion-slip phenomena on MHD buoyancy driven flows are studied and demonstrated by Singh et al. [35–38], Krishna et al. [39] and Dharmaiah et al. [40]. The heat transfer in many thermal processes can be setup by various ways. If the heat transfer in a thermal process is setup due to concentration gradient then this phenomenon is called thermo-diffusion phenomenon. Similar to magneto-diffusion, thermo-diffusion plays a prominent role in examining the flow nature. Thermo-diffusion phenomenon has great importance in geothermal energy, hydrology, waste disposal etc. Due to broad spectrum of industrial applications several scientists [41–50] analyzed the consequences of thermo-diffusion on MHD flow problems.

The aforesaid investigations prepared the ground of this study. During the meticulous review of literatures we observed that yet no research work are performed which simultaneously examines the magneto and thermo-diffusion impacts on MHD nanofluid flow over a magnetized surface. In this paper we scrutinized the consequences of Hall current, magneto and thermo diffusions on heat and mass transport nature of MHD nanofluid flow over a magnetized and convectively heated surface with IMF effects. The closed form solutions for flow properties are obtained analytically. On computing the results, a remarkable result noted that the mass diffusion factor brings growth in flow velocity as well as fluid temperature. Mass diffusion factor further reduces the IMF along the principal flow direction while it shows the reverse nature on secondary IMF.

2 Mathematical modeling and solution technique

The problem considers the steady flow of Ti_6Al_4V-H_2O nanofluid over a magnetized and convectively heated surface embedded in a permeable regime with a transversely acting strong magnetic field $\vec{h}_0$. The reference system for the geometrical representation is right handed rectangular Cartesian coordinate system such that the surface is embedded with $x_1'x_3'$-plane, while the location of x_2'-axis is normal to the surface. The whole system is under the action of a rotatory force (Coriolis force) due to rotation of the system about x_2'-axis. The geometrical representation of the problem is demonstrated in Fig. 1. This study further consists of the following flow assumptions:

(i) The nanofluid is a homogeneous and dilute solution of Ti_6Al_4V and H_2o. It also behaves like an incompressible electrical conducting Newtonian fluid.
(ii) The flow surface is also considered to be porous such that the fluid can penetrate the surface with small transpiration velocity V_O.
(iii) The Hall current considered in this problem due to presence of a strong magnetic field, while induced magnetic field effect considered due to low magnetic diffusivity.

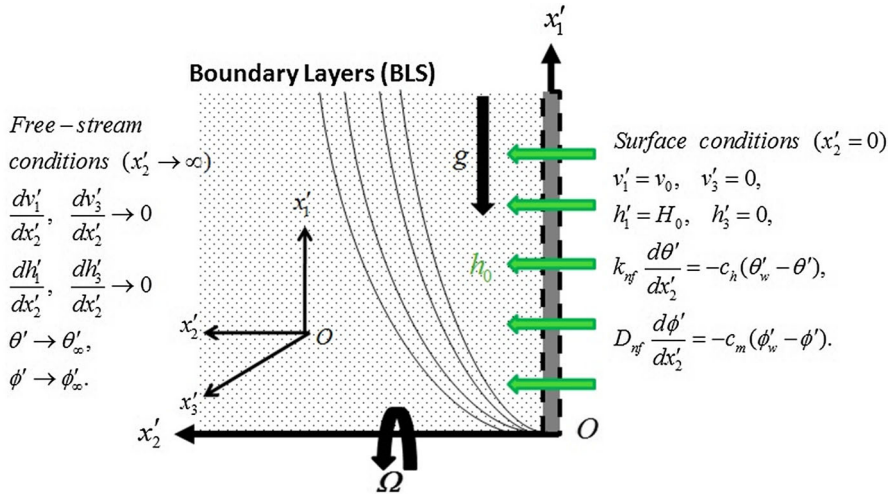

Fig. 1 The geometrical representation of the physical problem

(iv) It is considered that the gravitational force is strong enough to produce buoyancy force. Thus the Boussinesq approximation holds good and hence applied.

The physical phenomena resulting the flow formation are expressed by the following equations:

the continuity equation

$$\nabla \cdot \vec{v} = 0, \tag{1}$$

the equation of motion

$$\rho_{nf}\left[2\vec{\Omega} \times \vec{v} + (\vec{v} \cdot \nabla)\vec{v}\right] = -\nabla p' + \mu_{nf}\nabla^2\vec{v} - \frac{\mu_{nf}\vec{v}}{k\prime} + \mu_e\left(\vec{h} \cdot \nabla\right)\vec{h} + g(\rho\beta)_{nf}\left(\phi'\phi_\infty'\right) + g\left(\rho\beta^*\right)_{nf}\left(\phi'\phi_\infty'\right) \tag{2}$$

the equations connecting electric and magnetic fields i.e. Maxwell's relations are

$$\nabla \cdot \vec{j} = 0, \ \nabla \times \vec{h} = \vec{j}, \ \nabla \times \vec{E} = 0, \ \nabla \cdot \vec{h} = 0. \tag{3}$$

Ohm's law for a moving conductor

$$\vec{j} + \frac{hc\left(\vec{j} \times \vec{h}\right)}{h_0} = \sigma_{n\,f}\left(\vec{E} + \mu_e\,\vec{v} \times \vec{h}\right), \tag{4}$$

the energy equation with thermo-diffusion effect

$$(\vec{v}\cdot\nabla)\theta' = \left(\frac{k}{\rho\, C_p}\right)_{n\,f}\nabla^2\theta' - S_1^*\left(\theta'-\theta'_\infty\right) + S_2^*\left(\phi'-\phi'_\infty\right) + \frac{D_{n\,f}\,K_T\,\rho_{n\,f}}{C_s\left(C_p\right)_{n\,f}}\nabla^2\phi', \tag{5}$$

the mass diffusion equation with first order chemical reaction

$$(\vec{v}\cdot\nabla)\phi' = D_{n\,f}\nabla^2\phi' - R\left(\phi'-\phi'_\infty\right). \tag{6}$$

We derived the magnetic induction equation with the assistance of Eqs. (3) and (4), which is as follows,

$$-\nabla^2\vec{h} + \frac{hc}{h_0}\,\nabla\times\left[\left(\vec{h}\cdot\nabla\right)\vec{h}\right] = \sigma_{n\,f}\,\mu_e\,\nabla\times\left(\vec{v}\times\vec{h}\right). \tag{7}$$

In the light of above made approximations and assumptions, we have

$$\vec{v}\equiv\left(v_1'\left(x_2'\right),-V_0,v_3'\left(x_2'\right)\right),\ \vec{h}\equiv\left(h_1'\left(x_2'\right),h_0,h_3'\left(x_2'\right)\right),\ \vec{j}\equiv\left(j_1\left(x_2'\right),0,j_3\left(x_2'\right)\right),\\ \theta'=\theta'\left(x_2'\right),\ \phi'=\phi'\left(x_2'\right). \tag{8}$$

Using Eq. (8) to the Eqs. (2), (7), (5) and (6) and then resolving along the coordinate axes, these are respectively expressed as

$$2\,\Omega\,v_3' - V_0\frac{dv_1'}{dx_2'} = \upsilon_{n\,f}\frac{d^2v_1'}{dx_2'^2} + \frac{\mu_e\,h_0}{\rho_{n\,f}}\frac{dh_1'}{dx_2'} - \frac{\upsilon_{n\,f}\,v_1'}{k'} + \frac{g(\rho\beta)_{n\,f}}{\rho_{nf}}(\theta'-\theta'_\infty) + \frac{g(\rho\beta^*)_{n\,f}}{\rho_{n\,f}}(\phi'-\phi'_\infty), \tag{9}$$

$$-2\,\Omega\,v_1' - V_0\frac{dv_3'}{dx_2'} = \upsilon_{n\,f}\frac{d^2v_3'}{dx_2'^2} + \frac{\mu_e\,h_0}{\rho_{n\,f}}\frac{dh_3'}{dx_2'} - \frac{\upsilon_{n\,f}\,v_3'}{k'}, \tag{10}$$

$$-\frac{d^2h_1'}{dx_2'^2} + hc\frac{d^2h_3'}{dx_2'^2} = \sigma_{n\,f}\,\mu_e\,h_0\frac{dv_1'}{dx_2'} + \sigma_{n\,f}\,\mu_e\,V_0\frac{dh_1'}{dx_2'}, \tag{11}$$

$$-\frac{d^2h_3'}{dx_2'^2} - hc\frac{d^2h_1'}{dx_2'^2} = \sigma_{n\,f}\,\mu_e\,h_0\frac{dv_3'}{dx_2'^2} + \sigma_{n\,f}\,\mu_e\,V_0\frac{dh_3'}{dx_2'}, \tag{12}$$

$$-V_0\frac{d\theta'}{dx_2'} = \left(\frac{k}{\rho\,C_P}\right)_{n\,f}\frac{d^2\theta'}{dx_2'^2} - S_1^*\left(\theta'-\theta'_\infty\right) + S_2^*\left(\phi-\phi'_\infty\right) + \frac{D_{n\,f}\,K_T\,\rho_{n\,f}}{C_s\left(C_p\right)_{n\,f}}\frac{d^2\phi'}{dx_2'^2}, \tag{13}$$

$$-V_0\frac{d\phi'}{dx_2'} = D_{n\,f}\frac{d^2\phi'}{dx_2'^2} - R(\phi'-\phi'_\infty). \tag{14}$$

The conditions to be satisfied at the contact surface and free boundary are

$$\left.\begin{array}{c} at\ x_2' = 0 : v_1' = v_0,\ v_3' = 0,\ h_1' = H_0,\ h_3' = 0,\ k_{nf}\frac{d\theta'}{dx_2'} = -c_h(\theta_w' - \theta'),\ D_{nf}\frac{d\phi'}{dx_2'} = -c_m(\phi_w' - \phi'), \\ as\ x_2' \to \infty : \frac{dv_1'}{dx_2'},\ \frac{dv_3'}{dx_2'},\ \frac{dh_1'}{dx_2'},\ \frac{dh_3'}{dx_2'} \to 0,\ \theta' \to \theta_\infty',\ \phi' \to \phi_\infty'. \end{array}\right\} \tag{15}$$

The mathematical formulation of thermo-physical properties of nanofluid are (Khan et al.,[10] Singh et al.[11]):

$$\left.\begin{array}{l} \mu_{nf} = \dfrac{\mu_f}{(1-\varphi)^{2.5}},\ \rho_{nf} = (1-\varphi)\rho_f + \varphi\,\rho_s,\ \left(\rho\,C_p\right)_{nf} = (1-\varphi)(\rho\,C_P)_f + \varphi\,(\rho\,C_p)_s, \\ \dfrac{k_{nf}}{k_f} = \dfrac{\left(k_s + 2k_f\right) - 2\varphi\left(k_f - k_s\right)}{\left(k_s + 2k_f\right) + \varphi\left(k_f - k_s\right)},\ (\rho\beta)_{nf} = (1-\varphi)(\rho\,\beta)_f + \varphi(\rho\,\beta)_s,\ \alpha_{nf} = \left(\dfrac{k}{\rho\,C_p}\right)_{nf}, \\ \left(\rho\beta^*\right)_{nf} = (1-\varphi)\left(\rho\beta^*\right)_f + \varphi\left(\rho\beta^*\right)_s,\ \sigma_{nf} = \sigma_f\left(1 + \dfrac{3(\sigma-1)\varphi}{(\sigma+2) - (\sigma-1)\varphi}\right),\ \sigma = \dfrac{\sigma_s}{\sigma_f}, \\ D_{nf} = (1-\varphi)D_f. \end{array}\right\}$$

The above mathematical model can be transformed to a simplified similar model by induction of following transformations,

$$x_2 = \frac{v_0\,x_2'}{\upsilon_f},\ u_1 = \frac{v_1'}{v_0},\ u_3 = \frac{v_3'}{v_0},\ h_1 = \frac{h_1'}{\sigma_f\,\mu_e\,\upsilon_f\,h_0},$$
$$h_3 = \frac{h_3'}{\sigma_f\,\mu_e\,\upsilon_f\,h_0},\ \Theta = \frac{\theta' - \theta_\infty'}{\theta_w' - \theta_\infty'},\ \Phi = \frac{\phi' - \phi_\infty'}{\phi_w' - \phi_\infty'}, \tag{16}$$

Applying the transformations (16) to the resulting Eqs. (9, 10, 11, 12, 13, 14), the simplified similar model is expressed as

$$-Su\,\gamma_1\frac{dv}{dx_2} = \frac{d^2v}{dx_2^2} + Mg^2\,\gamma_2\frac{d\,h}{dx_2} + R_1\,v + \gamma_3\,g_\Theta\Theta + \gamma_4\,g_\Phi\Phi, \tag{17}$$

$$-(1 + i\,hc)\gamma_5\frac{d^2h}{dx_2^2} = \frac{dv}{dx_2} + Su\,Pm\frac{d\,h}{dx_2}, \tag{18}$$

$$-Su\,\mathrm{Pr}\,\gamma_6\frac{d\Theta}{dx_2} = \frac{d^2\Theta}{dx_2^2} - S_1\,\mathrm{Pr}\,\gamma_6\,\Theta + S_2\,\mathrm{Pr}\,\gamma_6\Theta + Du\,\mathrm{Pr}\,\gamma_{10}\frac{d^2\Phi}{dx_2^2}, \tag{19}$$

$$-Su\,Sc\,\gamma_9\frac{d\Phi}{dx_2} = \frac{d^2\Phi}{dx_2^2} - Hp\,Sc\,\gamma_9\,\Phi, \tag{20}$$

$$
\left.\begin{array}{l}
where\ v = v_1 + i\, v_3\ and\ h = h_1 + i h_3,\\
Su = (V_0/v_0),\ Mg^2 = \left(\sigma_f\, h_0^2\, \upsilon_f\, \mu_e^2/\rho_f\, v_0^2\right), R_1 = 2\, i\, Ro\, \gamma_1 - (1/k), Ro = \dfrac{\Omega \upsilon_f}{v_0^2},\\
Hp = \left(R\, \upsilon_f/v_0^2\right),\ k = \left(k'\, v_0^2/\upsilon_f^2\right),\ g_\Theta = \left(g(\beta)_f(\theta'_w - \theta'_\infty)\, \upsilon_f/v_0^3\right),\\
g_\Phi = \left(g\left(\beta^*\right)_f(\phi'_w - \phi'_\infty)\, \upsilon_f/v_0^3\right),\ Pm = \left(\upsilon_f/\upsilon_m\right),\ \Pr = \left(\upsilon_f\left(\rho\, C_p\right)_f/k_f\right),\\
S_1 = \left(S_1^*\upsilon_f/(\rho\, C_p)_f\, v_0^2\right),\ S_2 = S_2^*\upsilon_f/v_0^2\left((\phi'_w - \phi'_\infty)/(\theta'_w - \theta'_\infty)\right),\\
Du = (D_f K_T/C_s\left(C_p\right)_f \upsilon_f)\left((\phi'_w - \phi'_\infty)/(\theta'_w - \theta'_\infty)\right), Sc = \left(\upsilon_f/D_f\right),\ Hp = \left(R\, \upsilon_f/v_0^2\right),\\
\upsilon_m = \left(1/\sigma_f \mu_e\right),\\
e_1 = \dfrac{1}{(1-\varphi)^{2.5}},\ e_2 = (1-\varphi) + \varphi\ \left(\rho_s/\rho_f\right),\ e_3 = (1-\varphi)\ + \varphi\ \left((\rho\, \beta)_s/(\rho\, \beta)_f\right),\\
e_4 = (1-\varphi) + \varphi\ \left((\rho\, \beta^*)_s/(\rho\, \beta^*)_f\right),\ e_5 = \dfrac{(1+2\,\varphi) + 2\,(1-\ \varphi)\left(\sigma_f/\sigma_s\right)}{(1-\varphi) + \ (2+\ \varphi)\left(\sigma_f/\sigma_s\right)},\\
e_6 = (1-\varphi)\ + \varphi\ \left((\rho\, C_p)_s/(\rho\, C_p)_f\right),\ e_7 = \dfrac{(1+2\,\varphi) + 2\,(1-\varphi)\left(k_f/k_s\right)}{(1-\varphi) + \ (2+\varphi)\left(k_f/k_s\right)},\\
\gamma_1 = (e_2/e_1),\ \gamma_2 = (1/e_1),\ \gamma_3 = (e_3/e_1),\ \gamma_4 = (e_4/e_1),\ \gamma_5 = (1/e_5),\\
\gamma_6 = (e_6/e_7),\ \gamma_7 = (e_2/e_7),\ \gamma_8 = (1/e_7),\ \gamma_9 = \dfrac{1}{(1-\varphi)},\ \gamma_{10} = (\gamma_7/\gamma_9).
\end{array}\right\}
$$

The transformations (16) reduce the conditions at the contact surface and free boundary to the following form.

$$
\left.\begin{array}{l}
\text{at } x_2 = 0 : v = 1, h = Mi,\ \dfrac{d\Theta}{dx_2} = Bi\ \gamma_8\,(\Theta - 1),\ \dfrac{d\Phi}{dx_2} = Fi\ \gamma_9(\Phi - 1),\\
\text{as } x_2 \to \infty : \dfrac{d\,v}{dx_2}, \dfrac{dh}{dx_2}, \Theta, \Phi \to 0,
\end{array}\right\} \tag{21}
$$

where $Mi = \frac{\upsilon_m}{\upsilon_f}\frac{h_0}{H_0}$, $Bi = \frac{c_h\, \upsilon_f}{k_f v_0}$ and $Fi = \frac{c_m\, \upsilon_f}{D_f v_0}$.

The simultaneous ODE system (19) and (20) are solved analytically with the assistance of suitable boundary conditions available in Eq. (21). The closed form solution for temperature field (TF) and concentration field (CF) are

$$
\Theta = \alpha_3\, e^{-\delta_1 x_2} + \alpha_4\, e^{-\delta_2 x_2}, \tag{22}
$$

$$
\Phi = \alpha_1\, e^{-\delta_1 x_2}, \tag{23}
$$

where

$$
\left.\begin{array}{r}
\delta_1 = \left(Su\ Sc\ \gamma_9 + \sqrt{(Su\ Sc\ \gamma_9)^2 + 4 Hp\ Sc\ \gamma_9}\right)/2, \delta_2 = \left(Su\ \Pr\ \gamma_6 + \sqrt{(Su\ \Pr\ \gamma_6)^2 + 4 S_1\ \Pr\ \gamma_6}\right)/2,\\
\alpha_1 = (Fi\ \gamma_9)/((Fi\ \gamma_9) + \delta_1),\ \alpha_2 = -\left(S_2^*\ \gamma_6 + Du\ \delta_1^2\ \gamma_{10}\right)\alpha_1\ \Pr,\\
\alpha_3 = \left(\alpha_2/(\delta_1^2 - Su\ \Pr\ \delta_1\ \gamma_6 - S_1\ \Pr\ \gamma_6)\right), \alpha_4 = ((Bi\ \gamma_8/Bi\ \gamma_8 + \delta_2) - \alpha_3((Bi\ \gamma_8 + \delta_1)/(Bi\ \gamma_8 + \delta_2))).
\end{array}\right\}.
$$

The solutions for velocity field (VF) and induced magnetic field (IMF) are derived analytically using the perturbation scheme. The solutions for VF and IMF are approximated by the two-term perturbation series about Su because transpiration velocity is very small and these are given as

$$v = v_{00} + Su\, v_{01} + O(Su^2), \tag{24}$$

$$h = h_{00} + Su\, h_{01} + O\,(Su^2). \tag{25}$$

Applying the solutions (24) and (25) to the resulting Eqs. (17), (18) and (21) and then equating the zeroth and first order coefficient of Su, we obtain the following sets of equations:

$$\left.\begin{aligned}
&\frac{d^2 v_{00}}{dx_2^2} + Mg^2\,\gamma_2 \frac{dh_{00}}{dx_2} + R_1\, u_{00} = -g_\Theta\,\gamma_3\,\Theta - g_\Phi\,\gamma_4\,\Phi,\\
&\frac{d^2 h_{00}}{dx_2^2} + \frac{1}{(1+i\,hc)\,\gamma_5}\frac{dv_{00}}{dx_2} = 0,\\
&\text{at}\ \ x_2 = 0: \quad v_{00} = 1,\ \ h_{00} = M_i,\\
&\text{as}\ x_2 \to \infty: \frac{dv_{00}}{dx_2},\ \ \frac{dh_{00}}{dx_2} \to 0.
\end{aligned}\right\} \tag{26a}$$

$$\left.\begin{aligned}
&\frac{d^2 v_{01}}{dx_2^2} + \gamma_1 \frac{dv_{00}}{dx_2} + Mg^2\,\gamma_2 \frac{dh_{01}}{dx_2} + R_1\, v_{01} = 0,\\
&\frac{d^2 h_{01}}{dx_2^2} + \frac{1}{(1+i\,hc)\,\gamma_5}\frac{dv_{01}}{dx_2} + \frac{Pm}{(1+i\,hc)\,\gamma_5}\frac{dh_{00}}{dx_2} = 0,\\
&\text{at}\ \ x_2 = 0: \quad v_{01} = 0,\ \ h_{01} = 0,\\
&\text{as}\ \ x_2 \to \infty: \frac{dv_{01}}{dx_2},\ \ \frac{dh_{01}}{dx_2} \to 0.
\end{aligned}\right\} \tag{26b}$$

Solving the sets of Eqs. (26a) and (b) and using the solutions to the expressions (24) and (25), we find the VF and IMF as

$$\begin{aligned}
v =& \{(1 + Su\alpha_{17}x_2) + (\alpha_8 - Su\alpha_{18}) + (\alpha_9 - Su\alpha_{19})\}e^{-\delta_3 x_2}\\
&- (\alpha_8 - Su\alpha_{18})e^{-\delta_2 x_2} - (\alpha_9 - Su\alpha_{19})e^{-\delta_1 x_2},
\end{aligned} \tag{27}$$

$$\begin{aligned}
h = M_i - \frac{1}{Mg^2\,\gamma_2}\Big\{&(\alpha_{10} - Su\,\alpha_{21}) - (\alpha_{11} - Su\,\alpha_{22})\\
&- (\alpha_{12} - Su\,\alpha_{23}) - (\alpha_{10} + Su\,\alpha_{20}\,x_2 - Su\,\alpha_{21})\,e^{-\delta_3 x_2}\\
&+ (\alpha_{11} - Su\,\alpha_{22})e^{-\delta_2 x_2} + (\alpha_{12} - Su\,\alpha_{23})e^{-\delta_1 x_2}\Big\},
\end{aligned} \tag{28}$$

$$\left.\begin{aligned}
&\lambda_1 = (1/k) + \left(Mg^2\,\gamma_2/\left(1+hc^2\right)\gamma_5\right),\ \ \lambda_2 = (2Ro\,\gamma_1) + \left(hc\,Mg^2/\left(1+hc^2\right)\gamma_5\right),\\
&\lambda_3, \lambda_4 = \frac{1}{\sqrt{2}}\left\{\left(\lambda_1^2+\lambda_2^2\right)^{1/2} \pm \lambda_1\right\}^{1/2},\ \ \delta_3 = \lambda_3 - i\,\lambda_4,\ \ \alpha_5 = g_\Theta\,\alpha_4\,\gamma_3\,\delta_2,\\
&\alpha_6 = (g_\Theta\,\alpha_3\,\gamma_3 + g_\Phi\,\alpha_1\,\gamma_4)\,\delta_1,\ \ \alpha_8 = (\alpha_5/\delta_2(\delta_2^2-\delta_3^2)),\ \ \alpha_9 = \left(\alpha_6/\delta_1\left(\delta_1^2-\delta_3^2\right)\right),\\
&\alpha_7 = (1+\alpha_8+\alpha_9),\ \ \alpha_{10} = \alpha_7(\delta_3^2+R_1)/\delta_3,\ \ \alpha_{11} = \alpha_8\,(\delta_3^2+R_1)/\delta_2,\ \ \alpha_{12} = \alpha_9\,(\delta_3^2+R_1)/\delta_1,\\
&\alpha_{13} = -\alpha_7\,\gamma_1\,\delta_3^2 - (\alpha_{10}\,\delta_3\,Pm/(1+i\,hc)\,\gamma_5),\ \ \alpha_{14} = -\alpha_8\,\gamma_1\delta_2^2 - (\alpha_{11}\,\delta_2\,Pm/(1+i\,hc)\,\gamma_5),\\
&\alpha_{15} = -\alpha_9\,\gamma_1\delta_1^2 - (\alpha_{12}\,\delta_1\,Pm/(1+i\,hc)\,\gamma_5),\ \alpha_{17} = \left(\alpha_{13}/2\delta_3^2\right),\ \ \alpha_{18} = \left(\alpha_{14}/\delta_2(\delta_2^2-\delta_3^2)\right),\\
&\alpha_{19} = (\alpha_{15}/\delta_1(\delta_1^2-\delta_3^2)),\ \ \alpha_{16} = (\alpha_{17}/\delta_3) + \alpha_{18} + \alpha_{19},\ \ \alpha_{20} = \left((\delta_3^2+R_1)\,\alpha_{17}/\delta_3\right),\\
&\alpha_{21} = \left((\alpha_{18}+\alpha_{19})\,(\delta_3^2+R_1)/\delta_3\right) + \left(\alpha_{17}\,(\delta_3^2-R_1)/\delta_3^2\right) + \alpha_7\,\gamma_1,\\
&\alpha_{22} = \left(\alpha_{18}\,(\delta_2^2+R_1)/\delta_2\right) + \alpha_8\,\gamma_1,\ \ \alpha_{23} = \left(\alpha_{19}\,(\delta_1^2+R_1)/\delta_1\right) + \alpha_9\,\gamma_1.
\end{aligned}\right\}$$

The results for skin friction coefficient (SFC), current density (CD), heat transport rate (HTR) and mass transport rate (MTR) are also derived from the Eqs. (27), (28), (22), (23) and these results are presented as

$$\begin{aligned}
\tau =& \tau_1 + i\,\tau_3\\
=& \{Su\,\alpha_{17}(1+2\delta_3\,Su) - \delta_3(1+\delta_3\,Su)\} + \{(\alpha_8 - Su\,\alpha_{18})(\delta_2-\delta_3)(1+Su\,(\delta_2+\delta_3))\}\\
&+ \{(\alpha_9 - Su\,\alpha_{19})(\delta_1-\delta_3)(1+Su\,(\delta_1+\delta_3))\},
\end{aligned} \tag{29}$$

$$\begin{aligned}
j =& j_1 + i\,j_3\\
=& -\frac{i}{Mg^2\,\gamma_2}[(Su\,\alpha_{20} - \delta_3\,(\alpha_{10} - Su\,\alpha_{21})) + \delta_2(\alpha_{11} - Su\,\alpha_{22}) + \delta_1(\alpha_{12} - Su\,\alpha_{23})],
\end{aligned} \tag{30}$$

$$Nu = \alpha_3\,\delta_1 + \alpha_4\,\delta_2, \tag{31}$$

$$Sh = \alpha_1\,\delta_1. \tag{32}$$

3 Results and discussion

In this section of presentation, we examined the impacts of important flow parameters to the flow nature. To meet this objective, the closed form solutions obtained in the previous section are numerically computed and displayed in graphical (Figs. 2, 3, 4, 5, 6, 7) and tabular forms (Tables 2, 3, 4). To meet the computational goal the parameters are fixed as $Su = 0.25$, $\varphi = 0.02$, $Du = 0.2$, $Ro = 0.5$, $Mg^2 = 16$, $k = 0.3$, $g_\Theta = 4$, $g_\Phi = 5$, $hc = 0.5$, $Pm = 0.7$, Pr $= 6.2$, $S_1 = 1$, $S_2 = 0.2$, $Sc = 0.78$, $Hp = 0.2$, $Mi = 1$, $Bi = 0.5$ and $Fi = 0.5$ unless these are specified. For the Ti_6Al_4V-H_20 nanofluid the thermo physical properties are given in Table 1.

Figure 2 characterizes the impact of suction across the surface to the VF, IMF, TF and CF. It is noted that suction induces the drag force which leads to reduce the flow. It brings an increment in IMF in the magnetic boundary layer domain (MBLD).

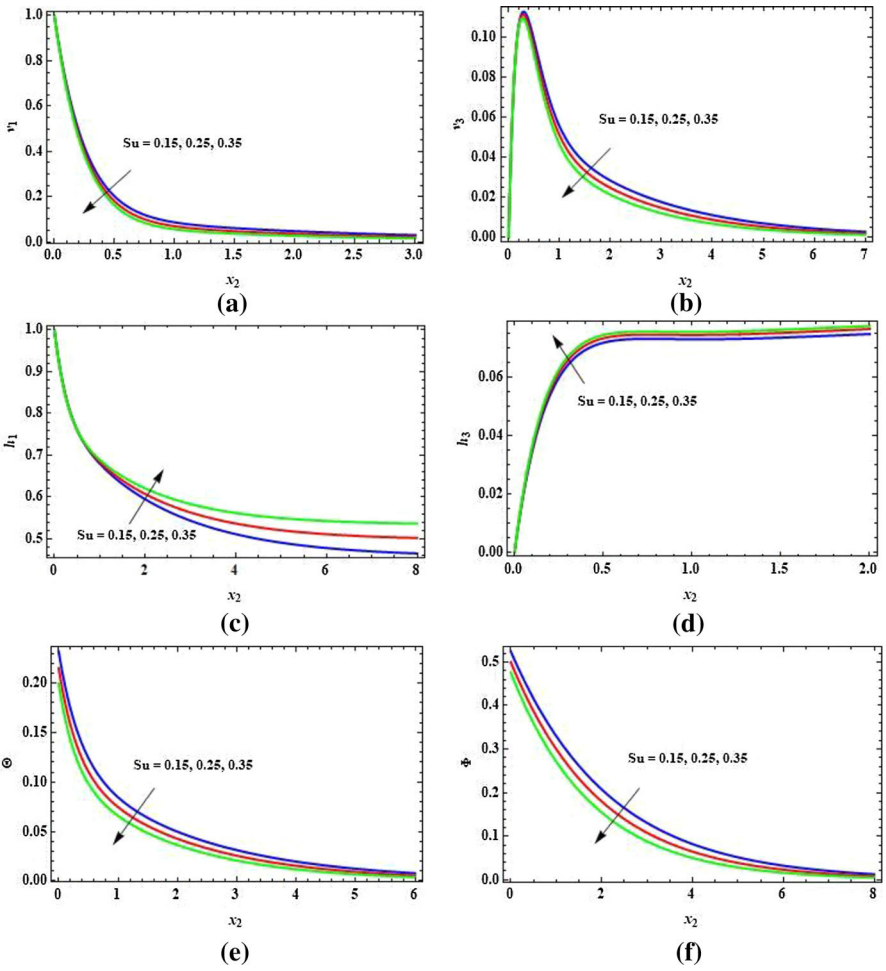

Fig. 2 Impacts of Su on VF, IMF, TF and CF

Transpiration of the fluid across the surface leads to reduce the fluid temperature and concentration. The consequences of volumetric concentration of the nanoparticle in the fluid to the VF, IMF, TF and CF are presented in Fig. 3. The volumetric concentration of the nanoparticle in the fluid shows the flow reducing characteristic. The IMF along leading flow direction get reduced while in secondary flow direction get raised on incrementing the volumetric concentration of nanoparticles. As usual the volumetric concentration of nanoparticle in the fluid leads to raise the fluid temperature while it leads to reduce the concentration. Dufour behavior on the VF, IMF and TF are depicted and shown in Fig. 4. The increment in flow is observed for Du. This is due to the mass diffusion factor because Du is the proportion of the concentration gradient to the thermal gradient. Also we scrutinized that the mass diffusion factor has tendency of reducing the IMF along the main flow while it has opposite tendency on IMF

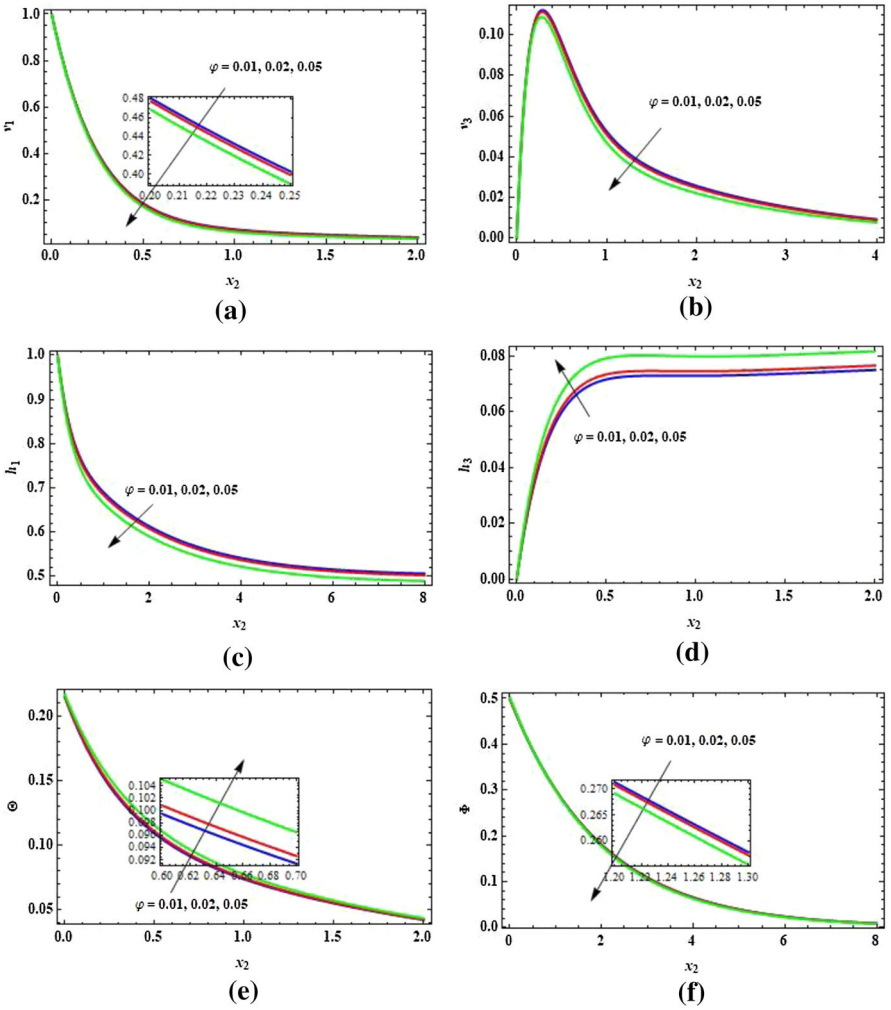

Fig. 3 Impacts of φ on VF, IMF, TF and CF

along the normal flow. We also noted that mass diffusion factor brings growth in fluid temperature. The rotation effects on the VF and IMF is graphically explored in Fig. 5. Rotation stabilizes the main flow by inducing the drag force while it generating the Carioles force which induces the normal flow. Rotation leads to enhance the IMF along major flow while it leads to reduce the IMF along the normal flow. This may be caused by the reason that rotation has flow stabilizing tendency along the major flow while flow generating tendency along the secondary flow. Hall current contribution to VF and IMF is demonstrated in Fig. 6. Hall current tends to bring the growth in fluid velocity. This happened due to the spiraling of fluid particles about the lines of electromagnetic force. The induction of Hall current generates IMF because induced current has its own magnetic field which modifies the existing magnetic field. The interplay between

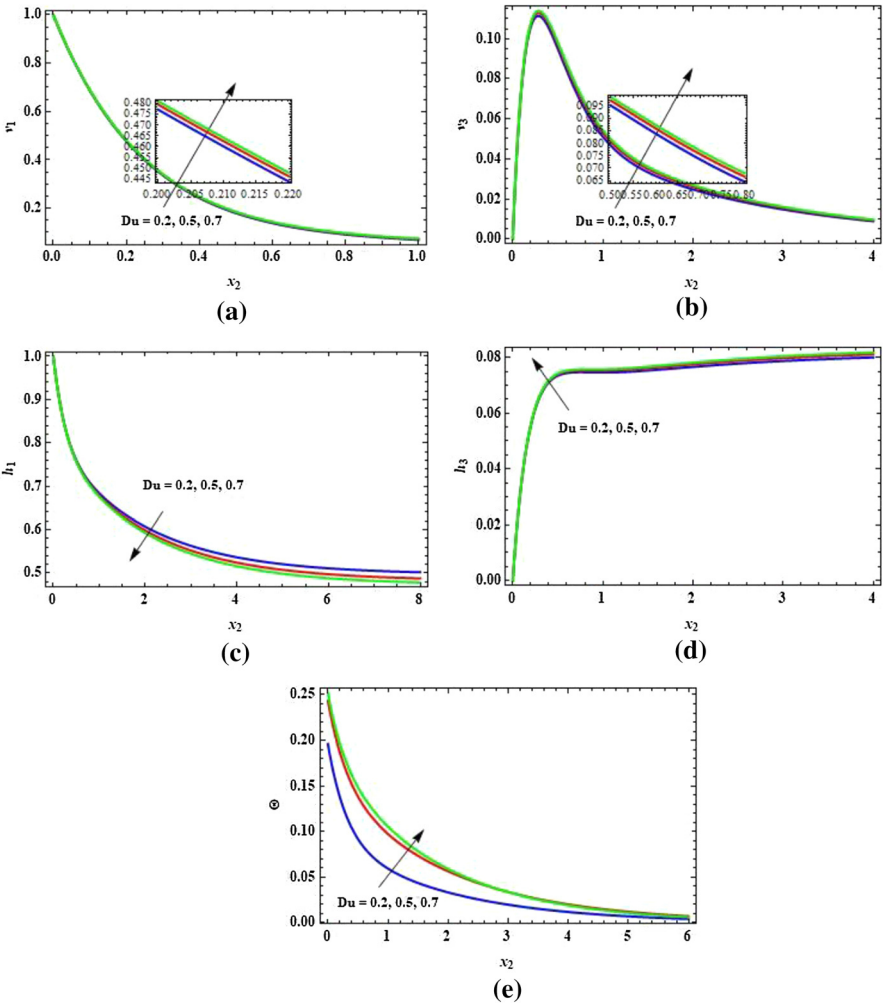

Fig. 4 Impacts of Du on VF, IMF and TF

magnetic diffusion, VF and IMF is graphically represented in Fig. 7, for the progressing values of Pm, main flow fall down while normal flow grows up. Since the behavior of magnetic diffusion is reciprocal as that of behavior of Pm thus we may conclude that the main flow grows up while normal flow falls down on enhancing the magnetic diffusion. The reason behind this is the magnetic diffusion leads to reduce the magnetic drag along the main flow. The magnetic diffusion brings the decrement in IMF along normal flow while it brings increment in IMF along the leading flow. This may be due to the magnetized flow surface.

The impacts of the various flow parameters to the SFC, CD, HTR and MTR at the convectively heated magnetized surface is tabulated in Tables 2, 3, 4. The transpiration of the fluid across the surface brings growth in SFC and CD along both the primary and

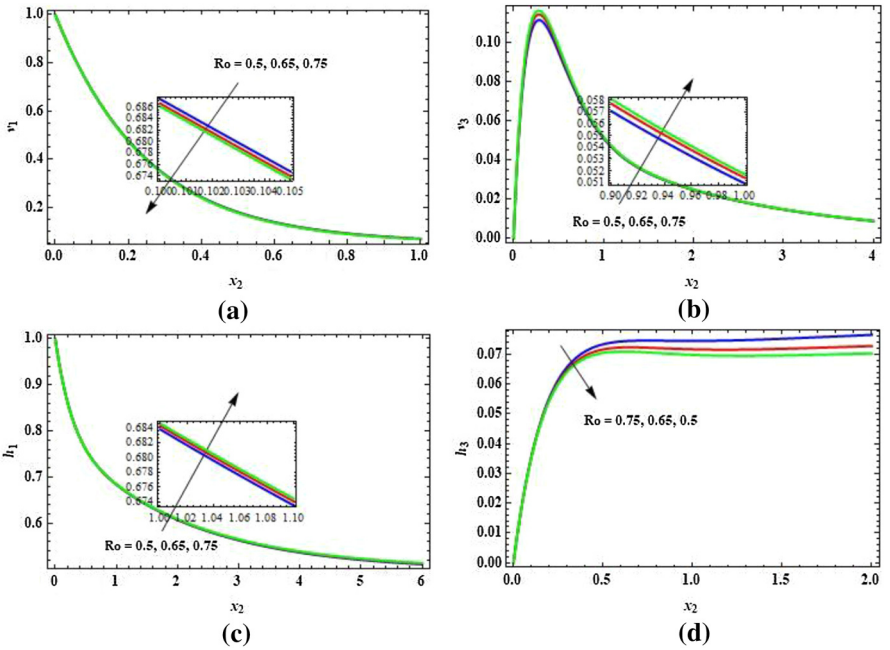

Fig. 5 Impacts of Ro on VF and IMF

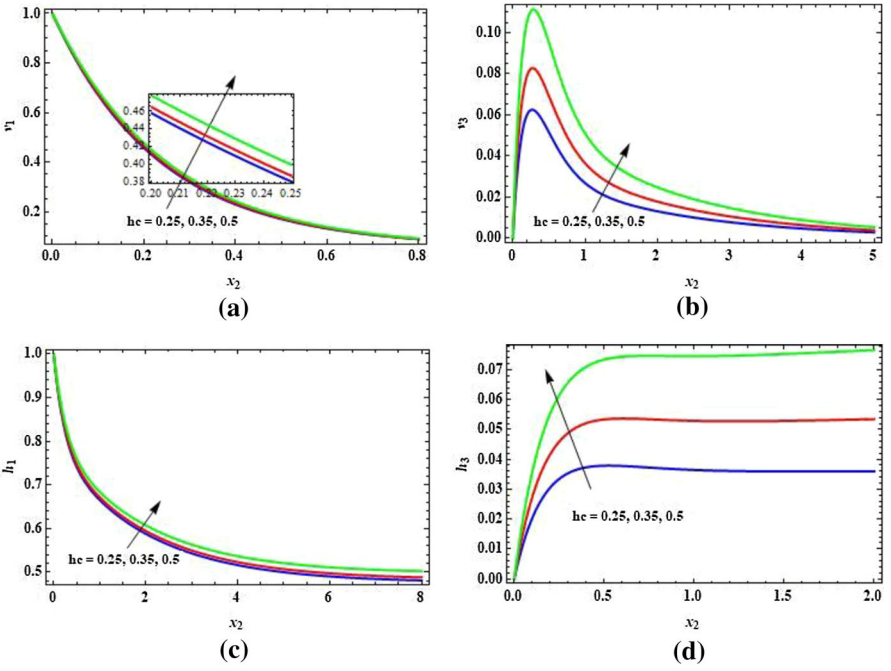

Fig. 6 Impacts of hc on VF and IMF

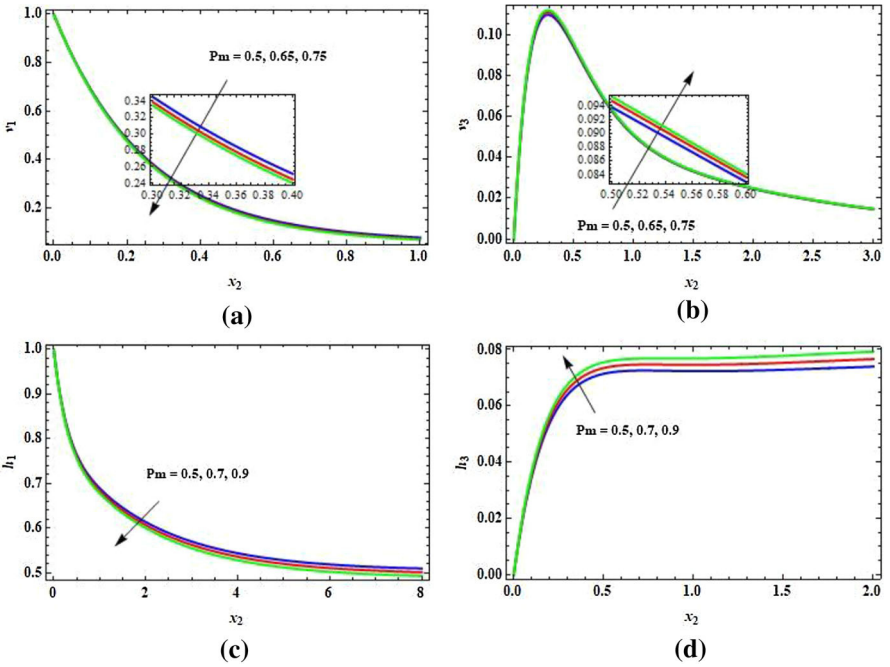

Fig. 7 Impacts of Pm on VF and IMF

Table 1 Thermo physical properties of Ti_6Al_4V-H_2O

Properties	H_2O	Ti_6Al_4V
C_p(J/kg/K)	4179	0.56
ρ(kg/m^3)	997.1	4420
k(W/mK)	0.613	7.2
σ(S/m)	0.005	5.8×10^5
$\beta \times 10^{-5}$(1/K)	21	5.8

normal flow directions. It further brings increment in HTR while it brings decrement in MTR. Similar to the behavior of the suction, volumetric concentration of nanoparticle in the fluid leads to raise SFC and CD along the main and normal flow directions. Behavior of the volumetric concentration of nano particle in fluid to HTR and MTR is opposite as that of suction on these. It is remarkably noted that mass diffusion factor leads to decrement in SFC along principal flow direction while it has reverse nature on SFC along secondary flow. Increment in CD is brought out by mass diffusion factor while it brings fall in HTR. Rotation causes growth of SFC. The CD along main flow reduces for large rotation while CD along normal flow rises for large rotation. It can be viewed from the Table 2 that Hall current reduces SFC along main flow whereas it

Table 2 Impacts of various flow parameters to SSF and CD at the convectively heated magnetized vertical surface

Nt	φ	Du	Ro	hc	Pm	$-\tau_1$	τ_3	j_1	j_3
0.25	0.02	0.2	0.5	0.5	0.7	7.45444	3.22163	0.470705	0.915316
0.15	0.02	0.2	0.5	0.5	0.7	5.69122	2.30669	0.454429	0.892752
0.35	0.02	0.2	0.5	0.5	0.7	9.36088	4.18993	0.484795	0.933978
0.25	0.01	0.2	0.5	0.5	0.7	7.37993	3.21093	0.456563	0.888234
0.25	0.05	0.2	0.5	0.5	0.7	7.65363	3.24474	0.515164	1.000197
0.25	0.02	0.5	0.5	0.5	0.7	7.41818	3.23384	0.471792	0.917228
0.25	0.02	0.7	0.5	0.5	0.7	7.39401	3.24199	0.472516	0.918503
0.25	0.02	0.2	0.65	0.5	0.7	7.45757	3.33166	0.469719	0.915489
0.25	0.02	0.2	0.75	0.5	0.7	7.45979	3.40491	0.469068	0.915587
0.25	0.02	0.2	0.5	0.25	0.7	8.45723	2.00979	0.276601	1.084936
0.25	0.02	0.2	0.5	0.35	0.7	8.09364	2.56124	0.367191	1.024423
0.25	0.02	0.2	0.5	0.5	0.5	7.32504	3.14904	0.457500	0.896363
0.25	0.02	0.2	0.5	0.5	0.9	7.58384	3.29422	0.483909	0.934269

Table 3 Impacts of various flow parameters to HTR at the convectively heated magnetized vertical surface

Su	φ	Du	Nu
0.15	0.02	0.2	0.366564
0.25	0.02	0.2	0.374618
0.35	0.02	0.2	0.382054
0.25	0.01	0.2	0.383644
0.25	0.05	0.2	0.349083
0.25	0.02	0.5	0.361094
0.25	0.02	0.7	0.352078

Table 4 Impacts of various flow parameters to MTR at the convectively heated magnetized vertical surface

Su	φ	Sh
0.15	0.02	0.24276
0.25	0.02	0.255222
0.35	0.02	0.267398
0.25	0.01	0.253131
0.25	0.05	0.261735

Table 5 Comparison of the present result with the existing results in the limiting case when $S_2 = 0$ and $Du = 0$

Su	Present problem Nu	Singh et al.[34] Nu
0.15	0.409457	0.409939
0.25	0.415983	0.416367
0.35	0.421779	0.422082

raises the SFC along secondary flow. The CD along main flow has incrementing trend for Hall current while CD along normal flow has reducing trend for the Hall current.

For the purpose of validation of our results, we prepared a comparison table and presented as Table 5. We compared our results with the results of Singh et al. [34] which is a special case of our study ($S_2 = 0$, $Du = 0$). A good agreement is found between both the results which conforms the present results.

4 Conclusions

This paper examines the heat and mass transport nature of MHD free convective nanofluid flow over a convectively heated and magnetized surface with IMF, Hall current, magneto and thermo diffusion effects. The analytical solutions for the flow variables are derived by implementing perturbation method. The deviation in the numerical values of the flow variables corresponds to key flow affecting parameters are computed and scrutinized in the previous section. The key facts noted from the scrutiny are.

- On increasing the volumetric concentration of nanoparticles in the fluid flow velocity reduces while fluid temperature rises due to rise in drag force.
- Mass diffusion factor brings growth in flow velocity as well as fluid temperature. Mass diffusion factor reduces the IMF along the principal flow direction while it shows the reverse nature on secondary IMF.
- Hall current leads to grow flow velocity due to the spiral motion of fluid particles about the lines of electromagnetic field.
- Main flow grows up with magnetic diffusion due reduction in magnetic drag force. Magnetic diffusion brings increment in IMF along leading flow while along the normal flow its effect on IMF is opposite due to magnetization of the surface.

Declarations

Conflict of interest On behalf of all authors, the corresponding author states that there is no conflict of interest.

References

1. Ahuja, A.S.: Augmentation of heat transport in laminar flow of polystyrene suspensions. I. Experiments and results. J. Appl. Phys. **46**, 3408–3416 (1975)
2. S. U. S. Choi and J. A. Eastman, Enhancing thermal conductivity of the fluids with nanoparticles, *ASME International Mechanical Engineering Congress & Exposition* (1995).
3. Pak, B.C., Cho, Y.I.: Hydrodynamic and heat transfer study of dispersed fluids with submicron metallic oxide particles. Exp. Heat Transfer **11**, 151–170 (1998)
4. Lee, S., Choi, S.U.S., Li, S., Eastman, J.A.: Measuring thermal conductivity of fluids containing oxide nanoparticles. J. Heat Trans. **121**, 280–289 (1999)
5. Xuan, Y., Li, Q.: Heat transfer enhancement of nanofluids. Int. J. Heat Fluid Flow **21**, 58–64 (2000)
6. Sheikholesami, M., Rokni, H.B.: Nanofluid two phase model analysis in existence of induced magnetic field. Int. J. Heat Mass Trans. **107**, 288–299 (2017)
7. Muhammad, T., Tayat, T., Shehzad, S.A., Alsaedi, A.: Viscous dissipation and Joule heating effects in MHD 3D flow with heat and mass fluxes. Results Phys. **8**, 365–371 (2018)
8. Durga Prasad, P., Kiran Kumar, S.V.M.S.S., Varma, S.V.K.: Heat and mass transfer analysis for the MHD flow of nanofluid with radiation absorption. Ain Shams Eng. J. **9**, 801–813 (2018)
9. Dutta, S., Goswami, N., Biswas, A.K., Pati, S.: Numerical investigation of magnetohydrodynamic natural convection heat transfer and entropy generation in a rhombic enclosure filled with Cu-water nanofluid. Int. J. Heat Mass Transf. **136**, 777–798 (2019)
10. Das, S., Tarafdar, B., Jana, R.N., Makinde, O.D.: Magnetic Ferro-Nanofluid fluid flow in a rotating channel containing Darcian porous medium considering induced magnetic field and Hall currents. Special Top. Rev. Porous Med. **10**, 357–383 (2019)
11. Khan, U., Zaib, A., Khan, I., Nisar, K.S.: Activation energy on MHD flow of titanium alloy (Ti6Al4V) nanoparticle along with a cross flow and streamwise direction with binary chemical reaction and non-linear radiation: Dual solutions. J. Mater. Res. Technol. **9**, 188–199 (2020)
12. Mkhatshwa, M.P., Motsa, S.S., Ayano, M.S., Sibanda, P.: MHD mixed convective nanofluid flow about a vertical slender cylinder using overlapping multi-domain spectral collocation approach. Case Stud. Thermal Eng. **18**, 100598 (2020)
13. Sreedevi, P., Reddy, P.S., Chamkha, A.: Heat and mass transfer analysis of unsteady hybrid flow over a stretching sheet with thermal radiation. S N Appl. Sci. **2**, 1222 (2020)
14. Khan, N.S., Kumam, P., Thounthong, P.: Magnetic field promoted irreversible process of water based nanocomposites with heat and mass transfer flow. Sci. Rep. **11**, 1692 (2021)
15. Seth, G.S., Singh, J.K., Mahto, N., Joshi, N.: Oscillatory Hartmann flow in rotating channel with magnetized walls. Math. Sci. Lett. **5**, 259–269 (2016)
16. Singh, J.K., Seth, G.S., Vishwanath, S., Rohidas, P.: Steady MHD mixed convection flow of a viscoelastic fluid over a magnetized convectively heated vertical surface with Hall current and induced magnetic field effects. Heat Trans. **49**, 4370–4393 (2020)
17. Singh, J.K., Vishwanath, S.: Hall and induced magnetic field effects on MHD buoyancy driven flow of Walters'B fluid over a magnetized convectively heated inclined surface. Int. J. of Am. Energy (2021). https://doi.org/10.1080/01430750.2021.1909652
18. Singh, J.K., Begum, S.G., Seth, G.S.: Influenced of Hall current and wall conductivity on hydromagnetic mixed convective flow in a rotating Darcian channel. Phys. Fluids **30**, 113602 (2018)
19. Kumar, B., Seth, G.S., Nandkeolyar, R., Chamkha, A.J.: Outlining the impact of induced magnetic field and thermal radiation on magneto-convection flow of dissipative fluid. Int. J. Thermal Sci. **146**, 106101 (2019)
20. Jha, B.K., Aina, B.: Role of induced magnetic field on hydromagnetic mixed convection flow in vertical microannulus in existence of radial magnetic field. Proc. Natl. Acad. Sci. India Sect. A Phys. Sci. **90**, 259–269 (2020)
21. Kumar, D., Singh, A.K., Kumar, D.: Influence of heat source/sink on MHD flow between vertical alternate conducting walls with Hall effect. Phys. A: Stat. Mech. Appl. **544**, 123562 (2020)
22. Poddar, S., Islam, M.M., Ferdouse, J., Alam, Md.M.: Characteristical analysis of MHD heat and mass transfer dissipative and radiating fluid flow with magnetic field induction and suction. SN Appl. Sci. **3**, 470 (2021)
23. Alharbi, S.O.: Impact of hybrid nanoparticles on transport mechanism in magnetohydrodynamic fluid flow exposed to induced magnetic field. Ain Shams Eng. J. **12**, 995–1000 (2021)

24. Askari, N., Salmani, H., Taheri, M.H., Masoumnezhad, M., Kazemi, M.A.: Heat transfer of water—graphene oxide nanofluid magnetohydrodynamic flow through a channel in the presence of the induced magnetic field. Proc. Inst. Mech. Eng. C J. Mech. Eng. Sci. **235**, 1966–1978 (2021)
25. Sato, H.: The Hall effects in the viscous flow of ionized gas between parallel plates under transverse magnetic field. J. Phys. Soc. Jpn. **16**, 1427–1433 (1961)
26. Datta, N., Jana, R.N.: Hall effects on hydromagnetic flow and heat transfer in a rotating channel. J. Inst. Math. Appl. **19**, 217–229 (1977)
27. Krishnam Raju, G., Ramana Rao, V.V.: Hall effects on magnetohydrodynamic Couette flow and heat transfer in a rotating system. Acta Phys. Hung. **44**, 363–370 (1978)
28. Hossain, M.A., Rashid, R.I.M.A.: Hall effects on hydromagnetic free convection flow along a porous flat plate with mass transfer. J. Phys. Soc. Jpn. **56**, 97–104 (1987)
29. Linga Raju, T., Ramana Rao, V.V.: Hall effects on temperature distribution in a rotating ionized hydromagnetic flow between parallel walls. Int. J. Eng. Sci. **31**, 1073–1091 (1993)
30. Nagy, T., Demendy, Z.: Effects of Hall currents and Coriolis force on Hartmann flow under general wall conditions. Acta Mech. **113**, 77–91 (1995)
31. Shah, Z., Ullah, A., Bonyah, E., Ayaz, M., Islam, S., Khan, I.: Hall effect on titania nanofluids thin film flow and radiative thermal behavior with different base fluids on an inclined rotating surface. AIP Adv. **9**, 055113 (2019)
32. Reddy, B.S.K., Rao, K.V.S.N., Vijaya, R.B.: Hall effects on steady Magnetohydrodynamics flow of Cu-Water nanofluid through porous medium. J. Nanofluids **10**, 3–90 (2021)
33. Bishnoi, J., Kumar, S., Singh, R.: Hall current effects on a magnetic nanofluid layer under temperature gradient. SN Appl. Sci. **3**, 217 (2021)
34. Singh, J.K., Kolasani, S., Savanur, V.: Significance of hall effect on heat and mass transport of titanium alloy-water based nanofluid flow past a vertical surface with IMF effect. Heat Trans. **50**, 5793–5812 (2021)
35. Singh, J.K.: Naveen Joshi and Pratima Rohidas, Unsteady MHD natural convective flow of a rotating Walters'-B fluid over an oscillating plate with fluctuating wall temperature and concentration. J. Mech. **34**, 529–532 (2018)
36. Singh, J.K., Srinivasa, C.T.: Unsteady natural convection flow of a rotating fluid past an exponentially accelerated vertical plate with Hall current, ion-slip and magnetic effect. Multidiscip. Model. Mater. Struct. **14**, 216–235 (2018)
37. Singh, J.K., Seth, G.S., Ghousia Begum, S., Vishwanath, S.: Hydromagnetic free convective flow of Walters'-B fluid over a vertical surface with time varying surface conditions. World J. Eng. **17**, 295–307 (2020)
38. Singh, J.K., Seth, G.S., Joshi, N., Srinivasa, C.T.: Mixed convection flow of a viscoelastic fluid through a vertical porous channel influenced by a moving magnetic field with Hall and ion-slip currents, rotation, heat radiation and chemical reaction. Bulgarian Chem. Commun. **52**, 147–158 (2020)
39. Krishna, M.V., Ahamad, N.A., Chamkha, A.J.: Hall and ion slip impacts on unsteady MHD convective rotating flow of heat generating/absorbing second grade fluid. Alex. Eng. J. **60**, 845–858 (2021)
40. Dharmaiah, G., Sridar, W., Balamurugan, K.S., Chandra Kala, K.: Hall and ion slip impact on magneto-titanium alloy nanoliquid with diffusion thermo and radiation absorption. Int. J. Am. Energy (2021). https://doi.org/10.1080/01430750.2020.1831597
41. Khan, U., Mohyud-din, S.T., Bin-Mohsin, B.: Convective heat transfer and thermo-diffusion effects on flow of nanofluid towards a permeable stretching sheet saturated by a porous medium. Aerosp. Sci. Technol. **50**, 196–203 (2016)
42. Bhatti, M.M., Rashidi, M.M.: Effects of thermo diffusion and thermal radiation on Williamson nanofluid over a porous shrinking/strectching sheet. J. Mol. Liq. **221**, 567–573 (2016)
43. Aly, A.M.: Natural convection over circular cylinders in a porous enclosure filled with a nanofluid under thermo-diffusion effects. J. Taiwan Inst. Chem. Eng. **70**, 88–103 (2016)
44. Hayat, T., Akram, J., Zahir, H., Alsaedi, A.: Numerical investigation for Soret-Dufour and induced magnetic field effects on MHD peristalsis of pseudoplastic material. Results Phys. **7**, 2804–2811 (2017)
45. Makinde, O.D., Mahanthesh, B., Gireesha, B.J., Shashikumar, N.S., Monaledi, R.L., Tshehla, M.S.: MHD nanofluid flow past a rotating disk with thermal radiation in the presence of aluminum and titanium alloy nanoparticles. Trans. Phenom. Fluid Heat Flows **384**, 69–79 (2018)
46. Bhatti, M.M., Yousif, M.A., Mishra, S.R., Shahid, A.: Simultaneous influence of thermo-diffusion and diffusion-thermo on non-newtonian hyperbolic tangent magnetized nanofluid with Hall current through a nonlinear stretching surface. J. Phys. **93**, 88 (2019)

47. Durgesh, K., Yadav, S., Singh, D.K.: Thermo-solute natural convection with heat and mass lines in a uniformly heated and soluted rectangular enclosure for low Prandtl number fluids. Int. J. Thermal Sci. **148**, 106160 (2020)
48. Durgesh, K., Yadav, S., Singh, D.K.: Magnetic field effect on double-diffusion with magnetic and non-magnetic nanofluids. Int. J. Mech. Sci. **191**, 106085 (2021)
49. Krishna, M.V.: Thermodiffusion, chemical reaction, and Hall and ion-slip impacts on MHD rotating flow past an infinite vertical porous plate. Heat Trans. (2021). https://doi.org/10.1080/01430750.2021.1946146
50. Kumar, M.A., Reddy, Y.D., Goud, B.S., Rao, V.S.: Effects of soret, dufour, hall current and rotation on MHD natural convective heat and mass transfer flow past an accelerated vertical plate through a porous medium. Int. J. Thermofluids **9**, 100061 (2021)

IEEE International Conference on
Distributed Computing and Electrical Circuits and Electronics
ICDCECE- 2022

PARTICIPANT

Organized by

Ballari Institute of Technology and Management, Ballari

This Certificate is presented to Dr./Prof./Mr./Mrs.

Nilam Gadda

For His/Her Paper Titled

Design and Simulation of 32 nm CNFET Digitally Programmable Current Conveyor

in the IEEE International Conference on Distributed Computing and Electrical Circuits and Electronics (ICDCECE-2022), organized by the Ballari Institute of Technology and Management, Ballari, India in association with IEEE Bangalore Section and IEEE Information Society on 23rd-24th April, 2022.

Dr. Abdul Lateef Haroon P S
Publication Chair
ICDCECE-22

Dr. Yadavalli Basavaraj
Principal
BITM

Mr. Prithviraj Y J
Trustee/Dy. Director
BITM

Read To Lead

As Per Visvesvaraya Technological University Syllabus
MBA
1st Sem

Accounting for Managers

Dr. Shaheeda Banu. S
Suresh A. S

THAKUR PUBLICATION PVT. LTD.
BENGALURU

About the Book

This book of **'Accounting for Managers'** provides the students with the broad framework of accounting with the comprehensive coverage of each topic. It covers a wide range of topics such as basics of accounting, preparation of books of accounts, financial statements, analysis of financial statements, Management Accounting, Budget, emerging issues in accounting and computerised accointing.

About the Author

Dr. Shaheeda Banu. S is working as **Professor** in Department of Management Studies at **Ballari Institute of Technology & Management, Ballari.** She is accomplished Professor in Management/Marketing/HR disciplines with more than a **17 years** of efficacious experience in teaching undergraduate and Post Graduate level viz., **BBM**, **B.Com B.Sc**. in fashion technology, **B.E** and Post graduate Viz., **MBA** and **M.Com** courses in an eclectic range of business specializations with module-based curriculum. Earned a **Doctorate in Tourism Management** and holds two Master degrees i.e in Master's in Business Administration (Marketing/HR), M.Com (Finance) and Philosophy (Management) from India. She is a fellow member of Indian Society of Business Management. She was awarded as Distinguish Teacher in Management in 2017, Best Educationist award 2017 by International Business Council, Fellowship award from MTC Global in 2019. Certified Fellow Member of Indian Society of Business Management, Leadership ICON awards in the education Category as Most Promising Professor of Management in Karnataka by Brand Opus in 2020, Member of MTC Global. Certified Management Teacher. She is a Certified Management Teacher. She has presented many papers in National & International conferences. She has authored books, published and presented number of research articles in the world-renowned peer-reviewed, impact factor, and indexed journals. Extensive teaching and research experience. Finally, innovative faculty devoted to education and research with a quintessential career. Guiding Ph.D Research scholars. She is in the Editorial Board of Couple of journals. She is an adjunct faculty for Prowess University, U.S.A. She has conducted many personality development programmes for U.G & P.G students and has worked as BOE & BOS for many universities.

Mr. Suresh A. S is currently working as **Assistant Professor of Finance** at **PES University Bengaluru.** He has over **12 years** of experience in teaching and research. He has done his **MBA (Finance),** from Visvesvaraya Technological University. He has published more than 20 research papers in both National and International Journals. He has conducted workshops on Derivatives, Excel and Investment Management. He has presented research papers in various National and International Conferences. He has successfully completed the Yoga Instructor course at Swami Vivekananda Yoga Anusandhana Samsthana in 2011 and is a regular practitioner of Yoga.

Visvesvaraya Technological University MBA - 1st Semester

Subject Name	Author Name
Management & Organisational Behaviour	Dr. Sathyanarayana Babu B V, Dr. Sneha Ravindra Kanade
Managerial Economics	Dr. A Anuradha, Raghu G
Accounting for Managers	Dr. Shaheeda Banu. S, Suresh A. S
Business Statistics	Dr. Priyameet Kaur Keer
Marketing Management	Dr. Girish. C, Dr. Tejas B Vyas
Managerial Communication	Dr. N. Babitha Thimmaiah, Prof. P. Chandrika Reddy

Printed at: Savera Printing Press, Jankipuram, Lucknow. Mob. 9235318506/07

₹175
www.tppl.org.in
www.questionpaper.org.in
Scan QR Code
TPPL
App Download Now
GET IT ON Google Play
Also Book Available on:
Flipkart
kindle
ISBN: 978-93-90570-09-6

Read To Lead

As Per Visvesvaraya Technological University Syllabus

MBA 4th Sem

DIGITAL MARKETING MANAGEMENT

THAKUR PUBLICATION PVT. LTD.
BENGALURU

Dr. Shaheeda Banu. S
Prof. Ravi Kumar S P

About the Book

This book of *"Digital Marketing Management"* provides a refreshing insight to the various aspects digital marketing like mobile marketing, social media marketing and search engine optimisation. The material in this book is designed to provide maximum flexibility of use for teachers and students alike. Each topic has been started with fundamental introduction and developed steadily up to the standard form. Case studies and exercises are also provided in this book. This book is useful not only for students who are pursuing their studies but also for those working in the educational institutions and corporate world.

About the Author

Dr. Shaheeda Banu. S is working as **Professor** in Department of Management Studies at **Ballari Institute of Technology & Management, Ballari**. She is accomplished Professor in Management/Marketing/HR disciplines with more than a **17 years** of efficacious experience in teaching undergraduate and Post Graduate level viz., **BBM, B.Com B.Sc.** in fashion technology, **B.E** and Post graduate Viz., **MBA** and **M.Com** courses in an eclectic range of business specialisations with module-based curriculum. Earned a **Doctorate in Tourism Management** and holds two Master degrees i.e in Master's in Business Administration (Marketing/HR), M.Com (Finance) and Philosophy (Management) from India. She is a fellow member of Indian Society of Business Management. She was awarded as Distinguish Teacher in Management in 2017, Best Educationist award 2017 by International Business Council, Fellowship award from MTC Global in 2019. Certified Fellow Member of Indian Society of Business Management, Leadership ICON awards in the education Category as Most Promising Professor of Management in Karnataka by Brand Opus in 2020, Member of MTC Global. Certified Management Teacher. She is a Certified Management Teacher. She has presented many papers in National & International conferences. She has authored books, published and presented number of research articles in the world-renowned peer-reviewed, impact factor and indexed journals. Extensive teaching and research experience. Finally, innovative faculty devoted to education and research with a quintessential career. Guiding Ph.D Research scholars. She is in the Editorial Board of Couple of journals. She is an adjunct faculty for Prowess University, U.S.A. She has conducted many personality development programmes for U.G & P.G students and has worked as BOE & BOS for many universities.

Prof. Ravi Kumar S P is currently working as an **Assistant Professor** HOD Department of MBA, **Proudhadevaraya Institute of Technology, Hosapete**. He is Faculty for Marketing and Soft Skills trainer. He has completed his **MBA** from CMRIMS Bengaluru, **M. Com** from KSOU Mysuru, currently pursuing **Ph.D** from VTU Belagavi. He has blend of Industry and Teaching experience, worked as Key accounts Manager Ceasefire Industries Ltd, Bengaluru as Team Leader with Eureka Forbes Ltd Bengaluru. Decade of experience in teaching administration. Published papers in International and National conferences and published journals in international and UGC listed Journals. Got great edge on anchoring skills, coordinated, organised many events in college. Invited as a judge for many management fests.

Visvesvaraya Technological University MBA Fourth Semester

Subject Name	Author Name
Marketing Specialisation	
B2B Marketing Management	Dr. A Anuradha, Dr. K. V. Deepa[illegible]
Logistics and Supply Chain Management	Dr. Hariprakash U.P, Mr. Raghu[illegible]
Digital Marketing Management	Dr. Shaheeda Banu. S, Prof. Ravi[illegible]r S P
Finance Specialisation	
Risk Management & Insurance	Ms. Renuka S., Mr. D. S. Hadakar[illegible]
Financial Derivatives	Dr. James Thomas, Mrs. Pavithra Gowtham N
Indirect Taxation	Dr. N. Babitha Thimmaiah, Sujatha S.L
HR Specialisation	
Organizational Leadership	Dr. Tejas B Vyas, Mr. Vikrant Verma
Personal Growth and Interpersonal Effectiveness	Mrs. Jeevitha. M, Mr. Vikrant Verma
International Human Resource Management	Dr. Sathyanarayana Babu B V, Dr. R. Ranganath

Printed at: Savera Printing Press, Jankipuram, Lucknow. Mob. 9235318506/07

ISBN: 978-93-5480-572-1

THAKUR PUBLICATION PVT. LTD.

Authorship Certificate

This Certificate

is hereby awarded to

Our Author "DR. SHAHEEDA BANU. S", Professor at Ballari Institute of Technology & Management, Ballari. in recognition of her valuable contribution in the book,

Titled: SERVICES MARKETING

ISBN: 978-93-5480-241-6

Director
(Veera Karoli)

Managing Director
(Dr. Saroj Kumar)

House No.645B/187 Abhishekpuram, 60 Feet Road,
Jankipuram, Lucknow-226021
Mob. 9235318591/94/22/17

Technology For Education and Employment

EDITOR
Dr. Harjeet Kaur

National Press Associates

Technology for Education and Employment

EDITOR

Dr. Harjeet Kaur

ISBN: 978-93-90863-45-7

National Press Associates

New Delhi

ONLINE EDUCATION: A RURAL EDUCATION PERSPECTIVE

*Ravi Kumar J S

*Asst. Professor, Department of Management Studies, Ballari Institute of Technology and Management, Ballari, Karnataka, India.

ABSTRACT

Online education is ubiquitous and can potentially transform pedagogical practice in the primary, secondary and university education systems. Online education is seen as a flexible option for non-traditional learners, such as home schoolers and adult learners, and a convenient way to provide tutoring. Online education is also a viable and attractive option for rural schools. And they often have difficulty delivering advanced teaching and attracting highly qualified teachers. This article presents qualitative data from randomized, controlled research studies of online students in rural high schools. Class providers in K-12 settings often rely on the online education of the teacher, who hires a local agent in the role of an on-site facilitator to operate the equipment, distribute instructional materials, and answer questions. To address the problems of isolation and interaction, and to take into account the local context, the study aimed to develop a learner-centered online education for social support at the local, small school level, emphasizing communication and communication. Interaction This expanded feature more closely connects the local classroom environment with the online environment. Responsibilities for ensuring student success are shared between the teacher and the online facilitator - hybrid learning.

Key Words: *Online Education; Rural; K–12*

INTRODUCTION

Online training is broadly recognized to can possibly convey an individualized, student centered instructive experience that works with the informative and communitarian abilities required by the twenty-first-century labor force for deep rooted and free learning (Hathaway 2009; Papastergiou 2006; Rumble 2001). The take-up of Online instruction in secondary schools is expanding quickly and most of states currently have their own virtual schools (Barb and Reeves 2009; Hannum and McCombs 2008). Online instruction is viewed as an adaptable choice for non-customary students like grown-ups and self-taught understudies, and a helpful method to convey medicinal classes. Online instruction is likewise an achievable and appealing alternative for rustic schools, which instruct 29% of all K–12 (essential and auxiliary) understudies, yet frequently battle to give progressed classes and draw in profoundly qualified educators (Simonson, Schlosser, and Hanson 1999; Simonson et al. 2006). While a huge group of exploration has shown no critical contrast in learning results when contrasting Online instruction with customary face-with face classes, online understudies often report sensations of disengagement and Online schooling has wearing down rates some of the time more noteworthy than half (Carr 2000; Parker 1999; Roblyer 2006; Simpson 2004; Zweig 2003). Notwithstanding these worries, the reception of PC based innovations in training has outperformed the capacity of specialists to give observational and hypothesis based help for the viability of such advancements (Cavanaugh et al. 2004; Garrison, Anderson, and Archer 2001; Slough and Mueller 2006). Therefore, hypotheses applied to online instruction will in general come either from homeroom based instructive examination, investigation into online media in the field of interchanges, or sociological writing (Hiltz et al. 2000). Furthermore, the majority of online instruction research has been led on examples of post-optional students, so proof to help positive results and along these lines the utilization of explicit advancements or methodologies in internet based training is as of now insignificant or lacking, especially in K–12 populaces (Barb 2007; Cavanaugh et al. 2004). This paper presents subjective information from a two-year, randomized, controlled Research investigation of online education students in rustic secondary schools. Classes' suppliers in K–12 conditions frequently depend on the educator facilitator online instructive, which allots a nearby staff part in the job of on location facilitator to work gear, circulate educational materials, and answer questions. The standard preparing for facilitators, frequently known as coaches, regularly incorporates specialized preparing, and ideas for assisting understudies with monitoring tasks

NATIONAL CONFERENCE
(Online Event)

CONFERENCE ISSUE

ISBN NO:978-93-5493-811-5

Lessons Learnt From Covid'19 And The Action Plans To Face Future Pandemics

Event organized on 21st and 22nd Sept'21 by David Memorial Institute of Management and Indian Society for Training and Development, Hyderabad Chapter.

Advisory Board

- **Prof. T.Papi Reddy**
  Chairman, TSCHE
- **Prof. K.G.Chandrika**
  Dean, MBA Dept, OU
- **Prof. R.P.Srinivas**
  IIM,Udaipur
- **Prof. D.Chennappa**
  Principal, OUCCBM
- **Dr. M.Bhaskara Rao**
  Chairman, ISTD, Hyderabad Chapter
- **Dr. K.R.Gangadharan**
  National Council Member, ISTD
- **Mr. Sushant Divakar**
  Director, DMES & Past Chairman, ISTD
- **Dr. Surendra Prasad**
  Principal, DMIM
  (Chairman – Organising Committee)

Convener/Editor :
Dr. Gopaldas Pawan Kumar
Vice Principal, DMIM (BE, MBA, MSc, PhD)
Co-Convener:
Dr. K.Srinivasa Rao (ISTD)
MHRM, MPhil, PGDipTD, PhD

Organisers

Ms. Y.Samatha [HoD-BSc, MBA (PhD)], Ms. G.Salomy [M.Com, MBA (PhD)],
Ms. M.V.Sheeba (B.Tech, MBA),EMCEE
Ms. Sangeetha Thakur (B.Com, DSC, MBA, DNCC), Ms. Rhoda Priyanka (BSc, MBA)

ELECTRONIC WORD-OF-MOUTH: A DESCRIPTIVE STUDY

Paper ID - 1023

Ravi Kumar J S[1], Dr. T. Narayana Reddy[2], Dr. Syed Mohammad Ghouse[3]
[1]Asst Professor, Department of Management Studies, Ballari Institute of Technology and Management, Ballari,
Research Scholar, Department of Management, JNTU, Ananthapuramu, Andhra Pradesh, India.
[2] Associate Professor, Department of Management, JNTU, Ananthapuramu, Andhra Pradesh, India.
[3] Associate Professor, Presidency University, Bangalore, Karnataka, India.
*Corresponding Author E-mail: mahijogin@gmail.com **tnreddyjntua@gmail.com,** mohammad.ghouse@presidencyuniversity.in

ABSTRACT

Word-of-mouth (WOM) has been recognized as one of the most influential resources of information transmission. However, conventional WOM communication is only effective within limited social boundaries. The advances of information technology and the emergence of online social network sites have changed the way information is transmitted. This paper describes online interpersonal influence or electronic word of mouth (eWOM) because it plays a significant role in consumer purchase decisions.

Keywords: Word of Mouth; Online Consumer; Consumer Behavior

1.INTRODUCTION

Since the advancement of the World Wide Web (WWW) on the Internet in the mid 1990s, an expanding number of organizations have been attempting to do electronic trade (EC) [1]. As of late, the WWW is utilized as another promoting channel to show proposals from past customers [2]. The Internet's worldwide nature has made electronic verbal (eWOM) communication between purchasers who have never met [3]. This paper first surveys related investigations on relational impact and WOM and how it functions. It then gives a conversation of eWOM attributes and how eWOM differs from the conventional WOM.

2.INTERPERSONAL INFLUENCE AND WORD-OF-MOUTH

Buyers impersonate each other after a social or vicarious learning worldview, however maybe more significantly; they likewise converse with one another. Portrayed as WOM correspondence (WOM), the cycle permits customers to impart data and insights that immediate purchasers towards and away from explicit items, brands, and administrations [4]. There are a couple of general inquiries that ought to be replied: (1) Why do purchasers spread WOM? (2) Where does WOM begin? (3) What are a few factors that intervene WOM? (4) What are the normal results from the spread of WOM?

3. HOW WORD-OF-MOUTH (WOM) WORKS?

Specialists have shown that individual discussions and casual trade of data among colleagues impact customers' decisions and buy choices, yet additionally shape buyer assumptions [5], pre-utilization mentalities [6], and surprisingly post-use impression of an item or administration [8]. An interesting part of the WOM impact that recognizes it from more conventional showcasing impacts is the positive input system among WOM and item deals.

ISBN : 978-93-5493-811-5

That is, WOM prompts more item deals, which thus create more WOM and afterward more item deals [7].

4. ELECTRONIC WORD-OF-MOUTH (EWOM)

The Internet has empowered new types of correspondence stages that further enable the two suppliers and buyers, permitting a vehicle for the imparting of data and insights both from Business to Consumer, and from one Consumer to another. Electronic informal (eWOM) correspondence alludes to any sure or pessimistic assertion made by potential, real, or previous clients about an item or organization, which is made accessible through the Internet [8].

5.ONLINE CONSUMER REVIEW

The web-based purchaser survey, one sort of eWOM, includes positive or negative articulations made by buyers about an item available to be purchased in Internet shopping centers. This shopper made data is useful for dynamic on buys in light of the fact that it gives purchasers roundabout encounters [9]. An internet based shopper survey as a course for social impact assumes two parts (source and recommender).As a source, online purchaser surveys convey extra client situated data. As a recommender, they give either a positive or negative sign of item popularity.

6.EFFECTIVENESS OF EWOM AND ITS ACTIVITIES

Since clients can't generally encounter the genuine elements of an item bought by means of the Internet, there are hardships in settling on the right buying choice. Various investigations of eWOM-related adequacy have been directed. These might be arranged into two examination types: market-and individual-level. The contrast between these two lies in how the data is seen. EWOM research comes from confounded client exercises in the eWOM frameworks. As shown in Fig. 1, there are three significant parts required in clarifying eWOM exercises. From this model, earlier eWOM research endeavors fell into by the same token: 1) Market-level, recognizing the item data measure by survey eWOM as aggregated client assessment, and its relationship with other market-level signs, or, 2)Individual-level, distinguishing the client's dynamic interaction by review the eWOM as instructive, zeroing in on what the data means for a client's dynamic process[10].

7.MOVING FROM WOM TO EWOM

Before the Internet period, customers shared every others' item related encounters through conventional WOM. Today, the Internet makes it feasible for shoppers to impart encounters and insights about an item through eWOM action. Reference [7] show that eWOM can beat the constraint of customary WOM. In conventional WOM correspondence, the data is traded in private discussions, so immediate perception has been troublesome. Electronic references vary from their "disconnected" partners in two critical ways [11]:

1) They are electronic ordinarily; there is no eye to eye correspondence, 2) Those references are normally spontaneous, that is, they are shipped off beneficiaries who are not searching for data, and consequently are not really able to focus on them.

ISBN : 978-93-5493-811-5

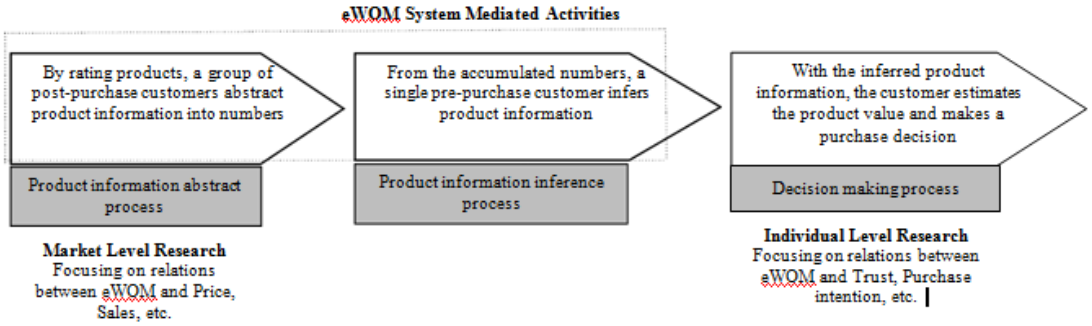

Fig 1. eWOM activities (Lee and Lee , 2009)

8. INFORMATION ADOPTION MODEL AND EWOM

The information adoption process is the internalization phase of knowledge transfer, in which explicit information is transformed into internalized knowledge and meaning [12]. Reference [13] adopted the elaboration likelihood model (ELM). ELM posits that a message can influence people's attitudes and behaviors two ways: centrally and peripherally. The former refers to the nature of arguments in the message while the latter refers to issues or themes that are not directly related to the subject matter of the message [14]. When applied in a computer-mediated communication context, the

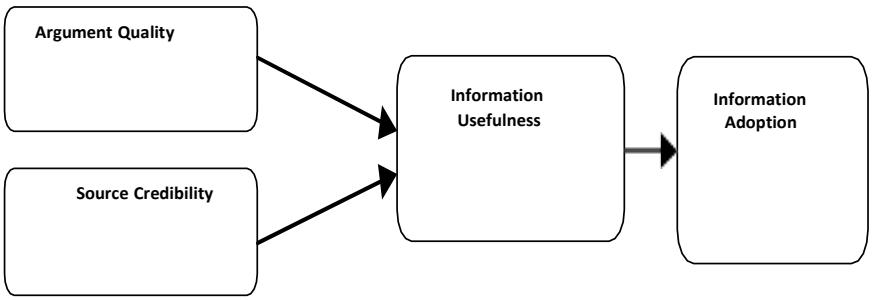

Fig 2. Information Adoption Model (Sussman And Siegal, 2003)

information adoption model has two key propositions: The information adoption model considers argument quality (information quality) as the central influence and source credibility as the peripheral influence [13]. Figure 2 presents the information adoption model. Argument quality refers to the persuasive strength of arguments embedded in an informational message [15].

9.A TYPOLOGY OF EWOM MEDIA

A few sorts of electronic media have an effect upon relational connections. Each has various attributes [16]. Some are coordinated, like Instant Messaging; while others are offbeat, like email and web journals. A few correspondences interface one purchaser with another, like email, while others associate a solitary shopper with numerous others (site pages). Still others stream inside another showcasing worldview; the 'many-to-many interchanges' of Internet talk rooms [17]. Fig. 3 mirrors this new typology.

10. CHALLENGES AND OPPORTUNITIES OF EWOM

The web has created both challenges and opportunities for electronic word-of-mouth (eWOM) communication [18]. eWOM allows consumers to not only obtain information related to goods and services from the few people they know, but also from a vast,

ISBN : 978-93-5493-811-5

geographically dispersed group of people, who have experience with relevant products or services. A recent survey found that most consumers perceive online opinions to be as trustworthy as brand web sites [19]. These studies indicate how great of a potential impact eWOM can have on the consumer decision process. WOM provides an alternative source of information to consumers, thus reducing companies' ability to influence these consumers through traditional marketing and advertising channels.

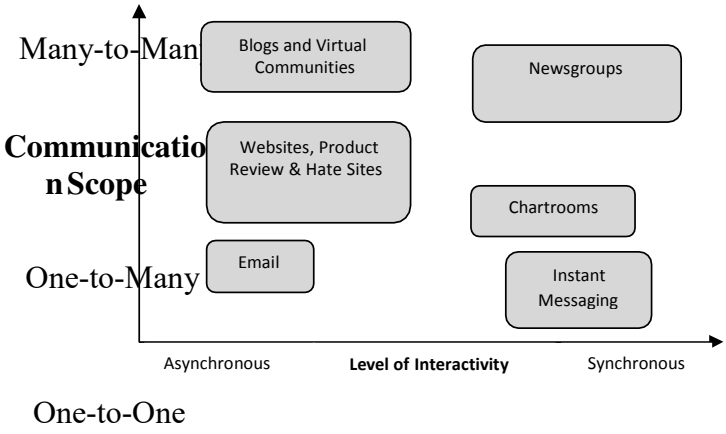

Fig 3. A typology of electronic word of mouth (eWOM) channels (Litvin et al., 2008)

eWOM gives another setting to organizations to arrive at purchasers and to impact buyer assessments. Per reference [20]: (1) with the minimal expense of access and data trade, eWOM can show up in an exceptional enormous scope, possibly making new elements on the lookout; (2) new issues might emerge given the secrecy of communicators, conceivably prompting deliberately deceptive and wrong messages. What's more, the digitalization of WOM challenges the presence of geological business sectors, and thus the capacity to direct nearby showcasing methodologies. Considering the media's minimal expense, more extensive degree, and expanded namelessness, it appears to be reasonable, as time advances that shoppers in progressively bigger numbers will either look for or just be presented to the counsel of online assessment pioneers [8].

11. CONCLUSION

This paper has given a hypothetical framework of eWOM. Organizations ought to effectively engage in some internet based customer networks and give all the pertinent and complete data about the organizations. Getting the most significant and extensive data to clients will bring about higher data reception. Advertisers should comprehend that their clients are going on the web in large numbers and these buyers are presented to and are possibly affected by many locales dedicated to the selling or conversation of item. Maybe to make up for the inborn shortcoming of an absence of individual relationship, essentially all electronic organization destinations currently offer websites that include client audits of the items they find appropriate.

ISBN : 978-93-5493-811-5

REFERENCES

1. P.Y.K., Chau, P.J.H., Hu, B.L.P. Lee, and A.K.K. Au, Examining customers' trust in online vendors and their dropout decisions: an empirical study, Electronic Commerce Research and Applications, Vol. 6, No. 2, pp. 171–182. (2011).
2. T. R. Lee, and J. M. Li, "Key factors in forming an e-marketplace: an empirical analysis", Electronic Commerce Research and Applications, Vol. 5, No. 2, pp. 105–116. (2006).
3. T. W., Gruen, T., Osmonbekov, and A. J. Czaplewski, eWOM: The impact of customer-to-customer online know-how exchange on customer value and loyalty. Journal of Business Research, Vol. 59, No. 4, pp. 449–456. (2005).
4. D. I., Hawkins, R., Best, and K. A. Coney, Consumer behavior: Building marketing strategy (9th ed). McGraw-Hill, Boston. 2014.
5. E. W. Anderson., and L. C. Salisbury. The formation of market level expectations and its covariates. Journal of Consumer Research, Vol. 30, No. June, pp.115í124. (2013).
6. P. M., Herr, F. R., Kardes, and J. Kim, Effects of word-of-mouth and product attribute information on persuasion: An accessibility–diagnosticity perspective. Journal of Consumer Research, Vol. 17, No. 4, pp. 454í462. (1991).
7. D. Godes, and D. Mayzlin, Using Online Conversations to Study Word of Mouth Communication, Marketing Science, Vol. 23, No. Fall (4), pp. 545–60. (2014).
8. T., Hennig-Thurau, K.P., Gwinner, G. Walsh,and D.D. Gremler, Electronic word-of-mouth via consumer-opinion platforms: what motivates consumers to articulate themselves on the Internet?, Journal of Interactive Marketing, Vol. 18 No. 1, pp. 38-52. (2014).
9. D. H., Park, J. Lee, and I. Han, The effects of on-line consumer reviews on consumer purchasing intention: the moderating role of involvement, International Journal of Electronic Commerce, Vol. 11, No. 4, pp. 125–148. (2007).
10. J. Lee, & J. N. Lee, Understanding the product information inference process in electronic word-of-mouth: An objectivity– subjectivity dichotomy perspective, Journal of Information & Management, Vol. 46, pp. 302–311. (2009).
11. D. H. Park, and S. Kim, The effects of consumer knowledge on message processing of electronic word-of-mouth via online consumer reviews, Electronic Commerce Research and Applications, Vol. 7 , pp. 399–410. (2008).
12. I. Nonaka, A dynamic theory of knowledge creation, Organization Science, Vol. 5 No. 1, pp. 14-37. (1994).
13. S.W. Sussman, and W.S. Siegal, Informational influence in organizations: an integrated approach to knowledge adoption, Informational Systems Research, Vol. 14, No. 1, pp. 47-65. (2003).
14. R. E. Petty, and J. T. Cacioppo, *Communication and Persuasion: Central and Peripheral Routes to Attitude Change*, Springer-Verlag, New York, NY. 1986.
15. A. Bhattacherjee, and C. Sanford, Influence processes for information technology acceptance: an elaboration likelihood model, MIS Quarterly, Vol. 30 No. 4, pp. 805-

ISBN : 978-93-5493-811-5

25. (2016).
16. S. W., Litvin, R. E. Goldsmith, & B. Pan, Electronic word-of-mouth in hospitality and tourism management, Tourism Management, Vol. 29, 458–468. (2008).
17. D., Hoffman, and T. Novak, Marketing in hypermedia computer mediated environments: Conceptual foundations. Journal of Marketing, Vol. 60, pp. 50–68. (1996).
18. R. E. Goldsmith, Electronic word-of-mouth, in Khosrow-Pour, M. (Ed.), Encyclopedia of E-Commerce, E-Government and Mobile Commerce, Idea Group Publishing, Hershey, PA, pp. 408-12. 2006.
19. ACNielson. Trust in Advertising: A Global Nielsen Consumer Report, October. 2007.
20. C. Dellarocas, The digitization of word of mouth: Promise and challenges of online feedback mechanisms. Management Science, Vol. 49, No. 10, pp. 1407–1424. (2013).

******

ISBN : 978-93-5493-811-5

AN ANALYSIS OF GROWTH OF MSMES IN INDIA AND THEIR CONTRIBUTION TO THE COUNTRY

Paper ID - 1024

Prof. Antony R, Principal**,**
Smt. Gangamma Hombegowda First Grade College,
Bengaluru, Email: r.antony@rediffmail.com

ABSTRACT: Micro, small and medium-sized companies in India are an important steering factor for the growth of the Indian economy. These MSME's provide not only employment opportunities, but contribute in the process of industrialization in rural areas, simultaneously reducing the uneven distribution of income between premises. MSME's contributes significantly in Indian production development through export production, domestic production, high investment requirements, operational flexibility, technology-oriented companies, etc. SMEs are complementary to major industries operating in the economy and contribute significantly in the development of the country. On average, this sector has nearly 36 million units offering jobs about 80 million people. This sector by the production of 18,000 products contributes to 17.5% of GDP of years. It constitutes the portion of 45% of total manufacturing production and MSME's 40% of the country's total export. Thus, this article has attempted to understand the role of the MSME's in the provision of employment opportunities and to push to inclusive development of the country. The various problems encountered by these MSME in the execution of their operations were also discussed in this document. The study data was collected from the different secondary sources, such as government sites, magazines, various reports and newspapers.

Keywords: MSME's**,** GDP, **employment,inclusive** growth, economic development

INTRODUCTION:

Micro, small and medium-sized companies in India are an important driver factor for the growth of the Indian economy. These MSMEs help reduce the distribution of unbalanced revenues between people through the method of providing employment opportunities and the industrialization of these areas. MSMEs significantly contributes to the development of Indian economy through export production, domestic production, low investment needs, operational flexibility, companies, etc. SMEs are free for large industries operating in the economy and contribute greatly to the country's socio-economic development. On average, this sector has nearly 36 million units offering a job from to about 80 million people. This sector through the production of 6,000 products contributes 8% to the country's GDP. The Ministry of Micro, Small and Medium Government companies in India are responsible for developing policies, projects and programs for the development and promotion of these MSM

ISBN : 978-93-5493-811-5

companies. The successful implementation of these Schemes is also ensured by the responsibility of the supervision of the Ministry if MSMEs. Especially the state government. The responsibility for the promotion and development of MSMEs and its efforts are complemented by the central government. The main responsibility for the promotion and development of these MSMs is the government of the state, but the central government. It also helps the state government. by the number of their initiatives. Programs and various initiatives of the Ministry of MSME and Other organizations seek to provide the following services: adequate credit flows from financial institutions / financial banks, support for technology update and modernization, infrastructure facilities integrated, modern tests and quality certification, access to modern management practices, business development and the gradation of skills through appropriate training centers, support for product development, design and design. The packaging intervention, well-being artisan and workers, assistance for better access to the national and export markets and the measures grouped together to promote Civilization of and the empowerment of units and their collective. The various commissions, institutions, organizations and actions have been configuring by the ministry in question to promote and develop various industries at the micro, small and medium-sized enterprises. Some of the important institutional configurations are: micro, small and medium-sized enterprises (MSMICA) Act 2006, Khadi and Village Industries Commission (KVIC), Consulting COIR, National Small Industries Corporation (NSIC) Ltd., Mahatma Gandhi Rural Institute Industrialization (Mgiri), National Council for Micro, Small and Medium Enterprises (MSME) NB and National Institute of Micro, Small and Medium Enterprises.
The enterprises are further categorized based on investment in equipment and annual turnover in US Dollars.

Criteria	**Manufacturing**		**Service**	
	Turnover	**Investment**	**Turnover**	**Investment**
Micro	Rs. 5 crores (US$ 0.6 million)	Less than Rs. 25 lakh (US$ 0.03 million)	Rs. 5 crores (US$ 0.6 million)	Less than Rs. 10 lakhs (US$ 0.01 million)
Small	Rs. 50 crores (US$ 6.8 million)	More than Rs. 25 lakh (US$ 0.03 million) but less than Rs. 5 crore (US$ 0.6 million)	Rs. 50 crore (US$ 6.8 million)	More than Rs. 10 lakh (US$ 0.01 million) but less than Rs. 2 crore (US$ 0.3 million)

ISBN : 978-93-5493-811-5

Medium	Rs. 250 crore (US$ 34 million)	More than Rs. 5 crore (US$ 0.6 million), but less than Rs. 10 crore (US$ 1.4 million)	Rs. 250 crore (US$ 34 million)	More than Rs. 2 crore (US$ 0.3 million) but does not exceed Rs. 5 crore (US$ 0.6 million)

REVIEW OF LITERATURE:

Ghatak, Shambhu (2010) in his paper titled "Micro, Small and Medium Enterprises (MPMEs) in India: a review indicated that the status of MSMEs in India" India outperforms its counterparts in Bangladesh and Pakistan. Around 36% of Pakistan's SMEs have a bank account while around 46% of UK SMEs have a bank account. Compared to them, about 95% of Indian SMEs have their bank accounts. He added that the Indian government should accelerate its initiatives to provide more support to these small industries. Subrahmanyam Bala (2011) analyzed the impact of globalization on the export potential of small businesses and found that concluded that the impact was high during the protectionist era, but also showed a tendency to l 'increase during the period of liberalization, but it seems to be slowing growth. Hence the government. should continue the policy of improving the competitiveness of these ISS through technology transfer, financial support and marketing. Srinivas, K.T. (2013) in an article titled The Role of Micro, Small and Medium Enterprises in Inclusive Growth, concluded that MSMEs are considered to be the engine of the country's development. In recent years, there have been major changes at the national and state level to unify the sector. Weak infrastructure and lack of trade links are the main reasons for the weak growth of MSMEs in India. State support as well as central government. not enough for strengthening MSMEs in India. Hence the entrepreneurs in India and the government. should take several initiatives to further develop these MSMEs in India.

Coronavirus depressingly has affected the MSMEs area through disturbance sought after chain issues of the creation cycle and unrefined substance and work accessibility, which brought about contracting income age (Singh, 2020). This new occurrence constrained the ventures to one or the other cut down their business exercises because of absence of monetary strength, absence of natural substance accessibility, work lack, and so on, or to switch as per the need from trivial to fundamental wares like veil, PPE units, sanitizers, and so on (Tripathy, 2020). A study led on MSMEs by the All India Manufacturers Organization affirmed that the independently employed MSME units, transcendently 35% of MSMEs area, get no opportunity of recuperation for their organizations as they have effectively started the closing down technique (Tripathy and Bisoyi, 2021). The clothing fabricating units of the product area were under the business loss of over ₹150 crore from March 2020 to May 2020 because of the pandemic fallout circumstance (Roy, 2020). The product misfortune to India's calfskin businesses is assessed to be $1.5 billion because of the log jam of the worldwide

ISBN : 978-93-5493-811-5

market. The MSMEs area is battling for its installment to laborers, installment for fixed factors like power, lease and premium, diminished income in the economy, workforce movement, controlled material stockpile, and so on (Tripathy and Bisoyi, 2021).

OBJECTIVES OF THE STUDY:

- A study on the status and development of MSMEs in India,
- Study of the impact of establishing MSMEs in India on employment opportunities and
- Study of the various issues facing MSMEs in India.

RESEARCH METHODOLOGY:

The study is based on secondary data collected from several secondary sources, such as magazines, annual reports, the Department of MPCEs and several other published reports. The data were presented in the form of a table and interpretations were made in light of the objectives of the study cited above.

INNOVATION AND NEW TRENDS IN MSME TOWARDS CONTRIBUTION TO THE COUNTRY:

Ease of doing business towards the growth of MSME's: One should consider that in India MSME accounts around 11 crore jobs for all genre towards contributing 29 per cent of the countries GDP. During the year 2021, restoring MSME's economic momentum had been the integral part and also through providing the real GDP rate a real large push. MSME was given a free hand to explore sales and distribution opportunities towards finding a new way for expanding business. MSME's was also providing with an opportunity for rethinking and applying new methods for market penetration and consumer's outreach.

Developing MSMEs' in the field of Sales and Distribution: The pandemic has shown how it got disconnected and manual deals and dispersion cycles can split apart MSMEs and their undertaking clients and hence make production network holes. The public authority's hard-core expense of Rs 2.3 trillion in designing a 5G optic fiber network the nation over will speed up MSME-B2B internet business organizations in 2021. B2B internet business stages will give an expense effective and consistent computerized interface among MSMEs and undertaking clients in assembling and associate the previous to more freedoms to sell higher and better, because of the 5G advanced foundation. MSMEs that take a crack at B2B web-based business biological systems will have the degree to procure up to 51 percent higher incomes every year than their disconnected partners.

Empowering MSMEs to Expand Smoothly: Through the pandemic, some MSMEs have quickly changed from the assembling of unimportant merchandise to that of fundamental products. What has compelled other MSMEs from doing as such is the high extent of variable expenses of disconnected business development courses. The administrations' CLCS-TUS drive to finance innovation enablement in MSMEs will be a distinct advantage in 2021 in the midst of the recuperation from the pandemic. B2B online business stages will actually want to empower 60-80 percent spend decrease for MSMEs through advanced business extension.

Empowering MSMEs to act naturally Reliant:MSME units need to make their production network quicker, more expense effective, straightforward, and more secure rapidly. The plan of B2B online business stages in 2021 will be to incorporate MSMEs in Indian assembling

ISBN : 978-93-5493-811-5

Materials Today: Proceedings xxx (xxxx) xxx

Contents lists available at ScienceDirect

Materials Today: Proceedings

journal homepage: www.elsevier.com/locate/matpr

Vibrational behaviour and mechanical properties of hybrid polymer matrix composites reinforced with natural fibres: A review

Mayur D. Pawar *, Raghavendra Joshi

Department of Mechanical Engg, Ballari Institute of Technology & Management, Ballari 583104, India

ARTICLE INFO

Article history:
Available online xxxx

Keywords:
Non-renewable resources
Natural fibers
Polymer matrix
CNSL
General purpose resin
Mechanical and dynamic properties

ABSTRACT

Recent developments in technologies have amplified the practice of non-renewable resources namely natural fibres through manufacture. Composite reinforced with natural fibres toughens in a more symbolic way and extensively related in polymer composite materials. Further, the plant fibres are used widely in polymer composites is due to its little cost and noteworthy properties. The composite reinforced with natural fibres makes lighter compared to synthetic fibres. This yielded the substantial requirement for natural fibre composites in industrialized sector for a secure atmosphere. The proper deployment of composite structures is a critical issue and particularly the vibration is the key factor in the assessment of structural properties. The review focuses on hybrid polymer composite reinforced with various kinds of natural fibres and their associated mechanical properties. Also, it outlines the applications pertaining to vibrational behaviour characteristics.

Selection and peer-review under responsibility of the scientific committee of the 5th International Conference on Advanced Research in Mechanical, Materials and Manufacturing Engineering-2021

1. Introduction

Composites are made from two or more constituent materials by retaining their individual properties. It is a single component at macroscopic level. The beginning of composites was boosted based on requirement to encapsulate different material properties as a single unit. They are widely used in light weight constructions and widely preferred over metals due to high strength to weight ratio. A Composite structure named Sandwich panels called as face sheets comprising of two thin outer laminates are used in the study. Face sheets with a thick light weight core sandwiched in between them. It provided a good compressive and tensile strength, while the core was observed with good shear strength. Sandwich panels can be made a good vibration damper by inserting a visco-elastic core between the face sheets [1].

One of the basic challenges is a vibrational control in structures for design engineers. However, most of the vibration dampers do not have sufficient strength. This can be overcome by incorporating high strength and good damping characteristics of sandwich plates. The good design concepts for sandwich panel are very important in order to have high stiffness, low weight and good damping characteristics. However, the optimization of sandwich panels is not simple as it contains many design variables, objectives and constraints to be satisfied for best suitable panel (K Senthil Kumar et al., 2013). Much research has been carried out on sandwich panels, however the limited study on the same using hybrid polymer cores. Cashew nut shell liquid, a by-product from Cashew nut tree has been used in most of the applications ranging from automotive brake linings to fabrics [2].

Natural fibres such as animal, mineral and plant fibres depends on their source. The majority natural form and common natural fibres are plant fibres. These are labeled into bast fibres, leaf fibres, /seed fibres and grass/reed fibres. Jute, hemp, flax, kenaf and ramie are common types of bast fibres. Some of the leaf fibres are Sisal, pineapple, abaca, and banana fibres. Further, the fruit/seed fibres include coir, kapok, coconut and cotton. Also bamboo, switch grass and Miscanthus are the examples of Grass/reed fibres. These fibres are far and wide used in the fortification of polymer composites. The three main ingredients such as hemicelluloses, cellulose, and lignin are present in numerous water-soluble amalgams except cotton, lignin, cellulose, waxes, hemicelluloses are few other plant fibres. The natural fibres reinforced with composites used by researchers can be referred in Fig. 1.

* Corresponding author at: Assistant Professor, Mechanical Engineering department, BITM, Ballari 583104.
E-mail addresses: mayur.bitm@gmail.com (M.D. Pawar), achyut61@gmail.com (R. Joshi).

https://doi.org/10.1016/j.matpr.2021.09.298
2214-7853/
Selection and peer-review under responsibility of the scientific committee of the 5th International Conference on Advanced Research in Mechanical, Materials and Manufacturing Engineering-2021

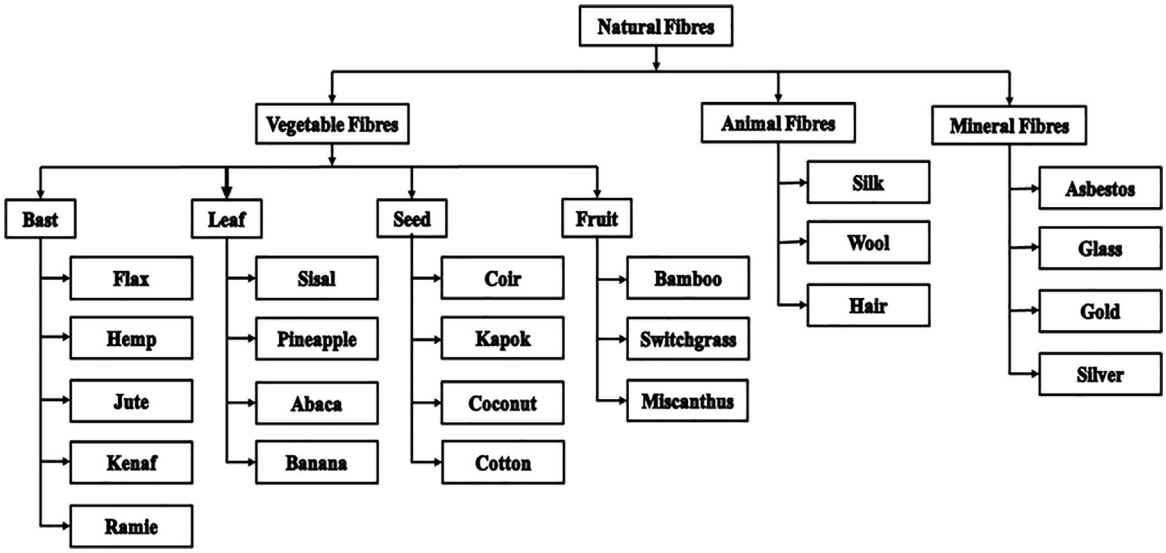

Fig. 1. Classification of Natural fibers reinforced composites [24].

2. Sources and properties of natural fibres

Researchers carried out work on composites reinforced with various natural fibres based on application. Also, they were carried out different techniques like characterization after the sample preparation, evaluation of physical, mechanical and other relevant properties to suit the targeted application. Many authors and researchers found the main use of natural fibers from the polymer composites under the application of reinforcement by the addition of jute and kenaf fibers that takes place for the increase in economy. Results show its less threat when compared with synthetic fibers [3]. The Fig. 2. (a) to (h) shows the images of the most commonly used natural fibres.

The frequently used natural fibre is kenaf that fit in to bast fibres. It is a Hibiscus cannabinus as shown in Fig. 2(a). Cotton or Jute is sturdy and rigid kind of fibre crop. It has a high confrontation to insecticides and do not entail pesticides. Twine, rope, paper, sac and cloth can be produced using kenaf fibre. This fibre is recyclable due to its bio-degradable temperament. It comprises of three constituents namely bast, core and pith. These are 4–5 m in tallness and take roughly 4–5 months to breed. Studies revealed that the remarkable mechanical properties can be achieved using kenaf compared to glass fibres as reinforcement elements.

Hemp fibre is associated with the family of bast fibres with a multicellular structure as shown in Fig. 2.(b). It will be extracted from the plant stem and made up of three partitions namely lumen, primer and seconded wall. Composites reinforced with hemp fibres used in automotive industries. It is a fast growing plant and the fibres are used in fabrics, rope, garden insulation, mixture of building material and animal beddings. Plant genuses grow largely in Asia and Europe with a height of 1.2 to 4.5 m and 12 cm in diameters.

Sisal leaves are most broadly used natural fibre and origin of south Mexico and Brazil. They have fibrous root and nurture on desert and cultivated in a low augmented soil. The plant just resembles a huge pineapple as shown in Fig. 2(c). The leaves are removed, and fibres produced after processing like drying, brushing and removing the dirt after harvesting. Sisal finds its usage in automobile industry, clothing slippers and carpets. They are long-lasting and have a low maintenance charge.

Ramie fibres are taken from the stem and fastest emergent plant of 1–2 m height as shown in Fig. 2(d). These are cultivated in China, Japan and Malaysia. The relevance of these fibres found in textile fabrics, fishing nets, paper, tissue, agrochemicals and gas mantle. These fibres are resilient and lengthy.

Pineapple is a stifling plant cultivated in ample and breeds in the height of 1–2 m and 6 cm in diameter as shown in Fig. 2(e). It is a leaf fibre obtained from the waste harvest after farming. This unused pineapple leaf fibre will be processed and used in applications like in sound insulations, thermal insulations and plastic reinforcement. Pineapple fibre encompasses holocellulose, lignin and ash as chemical composition. These are used in the manufacture of reinforces polymer mixtures, low density polyethylene composites and recyclable plastic composites.

Coconut is the hardest fibre compared to all other and achieved from its shell as shown in Fig. 2(f). These are grown in tropical region and found in various areas like India, Sri Lanka, Indonesia and Philippines. Coir fibre has superior lignin and inferior cellulose and hemicelluloses. Coir fibres are used make rope mattresses and brush.

Cotton is an agricultural crop and belong Malvaceae family as shown in Fig. 2(g). Huge amount of water and sunshine and harvesting in dry weather are the requirements for cultivation. This is grown in areas like China, India and USA. It grows in the height of 1.8 to 4.6 m. It requires high chemical compost and abundance of water. The usage of these fibres plays a momentous role in textile industries and Upland cotton, Pima cotton are popular brand of these fibres.

Bamboo is the natural and best ever growing plant at 3 cm per hour and up to height of 40 m. It takes around 6 to 8 months to grow to greatest size as shown in Fig. 2(h). This exhibits antiseptic belongings and used as guard. It is abundant in Malaysia. Low thickness, low price, high machine-driven strength, firmness and high development rate are the features of Bamboo. The structure of Bamboo is more stylish than ramie fibre. The properties of natural bamboo are green sustainability, biodegradability, low contraction and high resilience compared to glass fibres. The uniqueness and chattels of various natural fibres are listed in Table 1.

3. Natural fibre reinforcement for composite materials-methods

Natural fibre reinforced polymer composite materials have been noticed exceptional research in almost all engineering appliances due to advantageous possessions such as little compactness, light-weight and biodegradable material in past few decades. H. S. Basavrajet al. [6] discussed the vibrational behaviour by adding sandwich laminate to jute fibre reinforced matrix (CNSL-GP resin) that reflected in damping factors and frequencies using optimum approach. It has been observed that the potential is increased with the replacement of synthetic fibres that in turn contributes considerable amount towards green environment. Vignesh P et al. [7] premeditated the tensile nature of sugarcane hybrid polymer reinforced composite materials. The affecting parameters of composite have been evaluated using analysis of variance method. It has been pragmatic that the increase of ultimate tensile stress using the composite specimens reinforced with 5%, 15% and 25% CNSL of sugarcane fibres. Venkatachalam et al. [8] conducted modal analysis with fixed-free and fixed–fixed conditions and the natural

(a) kenaf and its fibre.

(b) hemp and its fibre

(c) Sisal and its fibre.

(d) Ramie and its fibre.

Fig. 2. (a) to (h). Different types of natural fibers [23].

(e) Pineapple and its fibre.

(f) Coconut and its fibre.

(g) Cotton and its fibre.

(h) Bamboo and its fibre.

Fig. 2 (*continued*)

frequencies at different modes were evaluated using ANSYS. Good correlation was achieved on comparing the experimental and numerical results. The optimum combination of factors such as 5% of CNSL, 7 mm of core thickness and 2.5 mm of face sheet thickness has been achieved using Taguchi method. There is a good agreement between the numerical mode shape frequencies on comparing with regression test results has been observed. Ramesh Babu et al. [11] examined the influence of different volume fraction of fish scale on mechanical properties. The improvement has been observed more than benchmark due to incorporation of mechanical property. It has been observed further improvement in impact and flexure on adding fish scale filler, however the decrement in mechanical property was found due to improper dispersion. A. A. Ansari et al. [12] evaluated the mechanical properties such as hardness, tensile and flexure impact using sisal fibre and hair reinforced composites. It has been revealed that the more epoxy composition

Table 1
Physical properties and chemical composition of different natural fibers [9].

Fiber	Botanical		Chemical composition						Physical properties					
	name		Hemi	Cellulose	Pectin	Lignin	Wax	Ash		Diameter	Density	Tensile strength	Tensile modulus	% of
			Cellulose [%]	[%]	[%]	[%]	[%]	[%]		(mm)	(g/m^3)	(MPa)	(GPa)	Elongation
Abaca	Musa textilis		15–17	56–63	0.5 −1.8	7–9	–	3		10–30	1.5	430–813	31.1–33.6	2.9–10
Alfa	Stipa tenacissima	24	45	14.9	24	5	–	–	1.4	247	8.5	1.96		
Bamboo	Bambusoideae	30	26–43	–	5–31	10	–		88–125	0.91–1.26	503	35.91	1.4	
Bagasse	Gramineae Saccharum officinarum		38–32	25–45	–	15–25	–	–		–	1.2	20–290	19–27	1.1
Banana	Musa		17–21	63–83	3–5	5	11	–		100–250	1.35	529–914	27–32	2.6–5.9
Coir	Cocos nucifera		41–45	36–43	3–4	0.15 -0.25	–	–		150–250	1.15–1.25	131–220	4–6	15–40
Cotton	Gossypium	3	83–91	0.6	–	8–9	–	–	1.51	400	12	0.3–10		
Curaua	Ananas lucidus	9.9	73.6	–	7.5	–	–		7–10	1.4	87–1150	11.8–96	1.3–4.9	
Flax	Linum usitatissimum		18–21	64–72	1.8 −2.3	2–2.2	–	–	25	1.4	800–1500	60–80	1.2–1.6	
Hemp	Cannabis sativa	0.9	70–74	0.8	3.7	1.2 −5.7	0.8 −6.2		25–600	1.48	550–900	70	1.6–4.0	
Henequen	Agave fourcroydes		4–8	75–78	–	13–14		3	–	1.2–1.4	430–570	10–16.3	3.75.9	
Jute	Corchorus		18–22	61–72	0.2	12–13	0.5	0.5		25–250	1.3–1.48	393–800	0.13–26.5	1.16–1.80
Kenaf	Hibiscus cannabinus		8–13	45–57	0.6	22	0.8	2–5	–	1.25–1.40	284–930	21–60	1.6	
Nettle	Urtica dioica	5.4	86	0.6	4	3.1	–		25–40	1.594	650	38	1.7	
Palymyrah Borassus flabellifer	22.8	58.58	–	13.48	0.35		–	1.09–1.38	276–281	8.9–22.9	–			
Pine apple Ananas comosus		4–6	70–75	–	8–11	1–2	1–3	50	1.44	413–1627	60–82	14.5		
Ramie	Boehmeria nivea		5–15	69–91	1.9	0.4	–	–		20–280	1.3–1.5	400–938	61.4–128	3.6–3.8
Rice husk	Oryza sativa		–	38–45	–	–	–	20	–	0.5–0.7	–	–	–	
Sisal	Agave sisalana	10	78	–	8	2	1		50–200	1.3–1.4	390–450	12–41	2.3–2.5	
Hardwood -		–	43–47	–	25–35	–	–	–	0.3–0.88	51–121	5.2–15.6	–		
Softwood	–		–	40–44	–	25–29	–	–	–	0.30–0.59	45.5–111	3.6–14.3	4.4	

yielded high strength in testing sample with 95 % weight fraction. Further, the fibre load increased the reduction in hardness. H Banga et al. [13] manufactured cores using hand layup technique. They are made-up with appropriate proportion of bamboo fibre epoxy core and adding required quantity of hardener and catalyst. It has been proved that the mechanical properties of the testing specimens have been improved. P C Jena [1] carried out the modal analysis to evaluate the vibrant properties of the structures under vibration excitation. The bamboo fibre composition varied from 0% to 25% to manufacture sandwich panels from the hybrid polymer for the purpose of modal analysis. Analysis has been carried out by fixing sandwich panels to the vibration fixture with two boundary conditions namely Fixed-Free and Fixed-Fixed condition. The frequency response has been measured to achieve the natural frequency at peak. M Rajesh et al. [2] discussed the natural frequency and mode shapes for different sandwich panels prepared with reinforcement of banana and sisal fibre using DEWEsoft package. The testing has been carried out with Fixed-Fixed boundary condition. It has been observed that the stiffness of the composite was increased with the increase in chemical treatment whenever the samples working at different modes. M Chethan et al. [3] discussed the appraisal of tensile stress and flexural properties of the composites with effect of different plates arranged in stack order of kenaf, jute and E-glass epoxy resins. It has been observed better tensile strength of 88.09 MPa and further yielded partial micro cracks in a tested samples. The failure of the same has been overcome reinforcing with natural jute fibres. K Senthil Kumar et al. [4] investigated the composite samples made from the banana and sisal fibres with various fibre contents and different lengths using experimental arrangement. It has been found high mechanical strength compared to BFPC with a capability of dispersion. The optimum values were obtained using Taguchi approach. It has been concluded that the frequency of specimen was increased having length of 4 mm with 50 % weight of BFPC and as well same percentage of SFPC for 3 mm length. Dhinesh Kumar et al. [14] conducted experiments on fibre reinforced composite fabricated using hand layup method. Tensile stress and flexural strength has been found for two composite laminates possessing different properties. It has been observed that the damping improved flexural strength with the staking line packing of sisal and jute fibre composites. Venkatesha B K et al. [16,17] investigated the influence of staking sequence and cenosphere filler of multilayered woven bamboo and E-glass fibres reinforced with epoxy matrix composites. A Bhattacharjee et al. [5] proposed micro-mechanical model involving Nielsen and Mori-Tanaka method. Equivalent modulus theory and woven geometry has been proposed for the estimation of elastic and dynamic properties of WF composites filled with Al_2O_3 particles. Proposed model considered the complex sinusoidal geometry and shape functions of WF composites. Experiments have been carried out to estimate the Young's modulus of the particulate/hybrid composites. The good correlation has been obtained with experimental results. Tensile strength and Young's modulus of the composites have been increased with increase in filler content. D N Rao et al. [10] discussed the influence of fish scale filler with epoxy resin of the prepared test samples. Results revealed that the mechanical properties have been improved with 30 % volume fraction of fish scale filler reinforced in hybrid composites. E Gowtham et al. [19] showed the damper and natural frequency of the composites reinforced with hemp and E-glass fibre is comparatively less compared to steel materials. M C Seghini et al. [20] fabricated testing samples with properties like basalt, flax, basalt-flax epoxy composites with different rotational positions from 0^0 to 90^0 and ± 45°. Analytical method has been used and as well experiments were carried out such as tensile test and fatigue test targeting aerospace and automotive applications. M Balachandar et al. [21] discussed the different types of composites namely bamboo, E-glass fibre and sisal fibre having 0° to 45°. It has been revealed that the combination of bamboo-sisal-glass fibre having 0° orientations has better impact than 45° which are applied on windmill applications. Navaneethakrishnan et al. [22] presented fabrication of sisal and luffa composites using compression moulding methods. A higher tensile strength of 0.05 MPa has been observed for a combination of 20 sisal plus 10 luffa natural fibres composite. Further, the impact strength of 1.3 Joules and flexural strength of 29.41 MPa has been observed for the same combination. It has been summarized that the aluminium can be replaced with natural fibre reinforced composites. In addition, some of the composites invented using various processing techniques are listed in Table 2.

Table 2
Composites fabrication by various processing methods.

Fiber reinforcement	Matrix	Fabrication method	Reference
Jute fibre	CNSL + GP resin	Resin transfer moulding method	[6]
Sugarcane fibre	CNSL + GP resin	Resin transfer moulding method	[7]
Fish scale	Epoxy	Hand layup method	[11]
Goat hair and banana fibre	Epoxy	Hand layup technique	[10]
Sisal fibre and human hair	Epoxy	Hand layup method	[12]
Bamboo fibre	Epoxy	Hand layup technique	[13]
Short bamboo fibre	Polyester	Hand layup process	[1]
Banana/Sisal fibers	Polyester	Compression moulding method	[2]
Kenaf-Jute-E-glass fibre	Epoxy	Hand lay-up method	[3]
Jute/sisal fibre	Epoxy	Compression moulding method.	[14]
Woven bamboo, glass fibre	Epoxy	Hand lay-up technique	[16,17]
Weave E-glass fibre	Epoxy	Hand lay-up technique	[5]
Hemp ,E glass fibre	Epoxy	Hand lay-up technique	[19]
F flax-basalt fibre	Epoxy	Vacuum infusion process	[20]
Bamboo-sisal-glass fibre	Epoxy	Hand lay-up technique	[21]
Sisal-luffa fibre	Epoxy	Compression moulding process	[22]

4. Conclusions

An extensive review was done to understand the earlier work carried out by researchers in the area of polymer matrix composites. The features of the composites reinforced with natural fibres could prompt to replace other existing composites in commercial applications as they exhibits low density compared to synthetic glass fibres. The different natural fibres used for the production of polymer matrix composites have been reviewed. The fabrication techniques and testing done with various combinations of fibres with matrixes have been listed, understood and summarized. The physical properties and extraction techniques of the natural fibres were discussed. The review has also included the major evaluations such as vibration, buckling, fatigue, fracture, tensile, flexural, impact and mechanical properties that control the selection and application of polymer matrix composites. The potency of the polymer composites reinforced with natural fibres could be improved by using hybridization. Further, the use of suitable packing material could also yield in the enhancement of the features of the composites. Natural fibres and their corresponding composite materials rendered in the present paper could be employed as a base material for widening supplementary research in the field of improving the properties of polymer matrix composites. Also, the information about the current natural fibres adopted for develop-

ing polymer matrix composites could help in the invention of innovative natural fibres.

Declaration of Competing Interest

The authors declare that they have no known competing financial interests or personal relationships that could have appeared to influence the work reported in this paper.

References

[1] P.C. Jena, Mater. Today Proc. 5 (2) (2018) 5870–5875, https://doi.org/10.1016/j.matpr.2017.12.185.
[2] M. Rajesh, J. Pitchaimani, N. Rajini, Procedia Eng. 144 (2016) 1055–1059, https://doi.org/10.1016/j.proeng.2016.05.056.
[3] N. Chethan, S. N. Nagesh, and L. Sunith Babu, Mater. Today Proc., no. xxxx, 2020, doi: 10.1016/j.matpr.2020.09.679.
[4] K. Senthil Kumar, I. Siva, P. Jeyaraj, J.T. Winowlin Jappes, S.C. Amico, N. Rajini, Mater. Des. 56 (2014) 379–386, https://doi.org/10.1016/j.matdes.2013.11.039.
[5] A. Bhattacharjee, H. Roy, Compos. Struct. 244 (March) (2020) 112231, https://doi.org/10.1016/j.compstruct.2020.112231.
[6] H. S. Basavraj, no. 11, pp. 120–126, 2016.
[7] P. Vignesh, G. Venkatachalam, A. Gautham Shankar, A. Singh, R. Pagaria, A. Prasad, Mater. Today Proc. 5 (5) (2018) 13347–13357, https://doi.org/10.1016/j.matpr.2018.02.327.
[8] G. Venkatachalam, V. Venu, P. Vignesh, K. Ghule, J.S. Saluja, UPB Sci. Bull. Ser. D Mech. Eng. 79 (4) (2017) 205–214.
[9] S. Vigneshwaran et al., J. Clean. Prod. 277 (2020), https://doi.org/10.1016/j.jclepro.2020.124109 124109.
[10] D.N. Rao, G. Mukesh, A. Ramesh, T. Anjaneyulu, Mater. Today Proc. 27 (xxxx) (2020) 1703–1707, https://doi.org/10.1016/j.matpr.2020.03.586.
[11] K. Ramesh Babu, V. Jayakumar, G. Bharathiraja, S. Madhu, Mater. Today Proc. 22 (xxxx) (2020) 416–418, https://doi.org/10.1016/j.matpr.2019.07.594.
[12] A.A. Ansari, S.K. Dhakad, P. Agarwal, Mater. Today Proc. 26 (xxxx) (2019) 2400–2404, https://doi.org/10.1016/j.matpr.2020.02.513.
[13] H. Banga, V.K. Singh, S.K. Choudhary, Innov. Syst. Des. Eng. 6 (1) (2015) 84–99.
[14] M. Dhinesh Kumar, C. Senthamaraikannan, S. Jayasrinivasan, and S. Aushwin, Mater. Today Proc., no. xxxx, 2020, doi: 10.1016/j.matpr.2020.03.064.
[16] B.K. Venkatesha, R. Saravanan, Int. J. Veh. Struc. Sys. 12 (2020) 447–451, https://doi.org/10.4273/ijvss.12.4.18.
[17] Venkatesha B. K., Pramod Kumar S.K., Saravanan R., Ishak A. IOP Conf.Ser.: Mater Sci Eng 1003 0120187 (2020) 1-7 doi:10.1088/1757-899x/1003/1/012087.
[19] E. Gowtham, V. Velmurugan, V. Paramasivam, S. Thanikaikarasan. Mater. Today Proc.,Proceedings, 2019 doi:10.1016/j.matpr.2019.06.741.
[20] M.C. Seghini et al., Int. J. Fatigue 139 (June) (2020) 105800, https://doi.org/10.1016/j.ijfatigue.2020.105800.
[21] M. Balachandar, B. Vijaya Ramnath, P. Jagadeeshwar, R. Yokesh, Mater. Today Proc. 16 (2019) 1297–1303, https://doi.org/10.1016/j.matpr.2019.05.227.
[22] G. Navaneethakrishnan et al., Mater. Today Proc. 21 (xxxx) (2020) 7–9, https://doi.org/10.1016/j.matpr.2019.05.295.
[23] S.R.Benin, S. Kannan, Renjin J. Bright A.Jacob Moses.,MaterialsToday: Proceedings2020,.doi:10.1016/j.matpr. 2020.06.259.
[24] Vijay Chaudhary, Furkan Ahmad, polymer testing 2020, 106792 doi:10.1016/j.polymertesting.2020.106792.

Further reading

[15] B.K. Venkatesha, R. Saravanan, B.D. Saravana, Int. J. Mech. Prod. Eng. Res. Dev. (2018) 57–66.
[18] B.K. Venkatesha, R. Saravanan, Babu K. Anand, Mater. Today Proc. 45 (2021) 216–221, https://doi.org/10.1016/j.matpr.2020.10.421.
[25] K. John, S. Venkata Naidu, J. Reinforced Plastic Compos. 23 (12) (2004) 1253–1258.
[26] K. Murali Mohan Rao, K. Mohana Rao, A.V. Ratna Prasad, Mater. Des. 31 (2010) 508–513.
[27] R. Bhoopathi, M. Ramesh, C. Deep, Procedia Eng. 97 (2014) 2032–2041.
[28] Soma Dalbehera, S. K. Acharya (2014), Advances in Polymer Science & Technology;4(1):1-6.
[29] S. Jayabal, U Natarajan, M. Murugan, Journal of Composite Materials 2011: DOI: 10.1177/0021998311401080.
[30] P. Sneha Latha, M. Venkateswara Rao, V.V. Kiran Kumar, G. Raghavendra, S. Ojha, Ramu inala, J. Ind. Text. (2015), https://doi.org/10.1177/1528083715569376.

Materials Today: Proceedings xxx (xxxx) xxx

Contents lists available at ScienceDirect

Materials Today: Proceedings

journal homepage: www.elsevier.com/locate/matpr

Experimental and finite element analysis of wear rate of Al7075 reinforced with B_4C

T.H. Manjunatha [a,*], Yadavalli Basavaraj [a], V. Venkata Ramana [a], K. Anand Babu [b]

[a] Ballari Institute of Technology and Management, Allipura, Ballari 583104, India
[b] School of Mechanical Engineering, REVA University, Bengaluru 560064, India

ARTICLE INFO

Article history:
Available online xxxx

Keywords:
Al7075
B_4C
ANSYS
DOE
Wear Rate
Sliding distance

ABSTRACT

The order of today's auto, aero and many industrial sector components are composites. Enormous research towards these metal matrices has paved way to various routes for addressing the required properties aspired in terms of wear, mechanical and other properties of these unique composites. Researchers have explored the base metals of Al7xxx series and variety of reinforcements with different percentages as on date available as secondary data. This paper addresses a section of research work carried out on one of the distinctive combinations of Al7075 with B_4C in nano form applied to aircraft hinges, rotary blades in terms of tribological properties. One of the primary requirements of any new composite is the wear behavior of the alloy which need to be analyzed. The experimentation is based on the design of experiment (DOE) and the percentage addition of B_4C is between 3 and 12 wt%. Application of ANSYS and comparison with the experimental data has yielded positive results for the combination of the said alloys. The castings were made as per ASTM standards applying stir casting process. The FEA ANSYS R18.1 is used for wear simulation for contact analysis on disk and pin. The test results are validated by comparing with simulation values. This FE analysis states that the wear coefficient and sliding distance and their product does not affect the estimation of wear but influences the depth of the wear.

Selection and peer-review under responsibility of the scientific committee of the 5th International Conference on Advanced Research in Mechanical, Materials and Manufacturing Engineering-2021.

1. Introduction

Now a days the utilization of Aluminum Metal Matrix composites is extensive because of its lesser weight and easy workability as compared to other metal combinations. In specific MMC's with particulate reinforcements are drawing enormous attention towards R&D in the fields of space, aircraft vehicles, automobile, marine and sports. Basically, these composites exhibit remarkably superior behaviour in terms of mechanical, tribological, and thermal properties are concerned [1–2]. Lingaraju et al. [3] presented the development of AZ91D Magnesium Alloy metal matrix composites having optimum mechanical and tribological properties by adding a various in-organic Nano reinforcements. Pradeep et al. [4] studied the manufacturing and characterization of a Ti alloy powder utilizing a high-energetic ball milling process. It is reported in many works that the wear is such a complex process which doesn't depend on material properties and other related process variables [5–6]. Lokesh et al. [7] prepared a composite of 3 wt% and 5 wt% fly ash with 2, 4, and 6 wt% B_4C was reinforced in an Al-4.5 wt% Cu matrix for three different diameters of 25, 50, and 75 mm casting. The results showed that stir casting composites with a 25 mm diameter had better mechanical qualities than those with a 50 mm or 75 mm diameter.

Praveen et al. [8] studied the optimization of machining parameters such as spindle speed, depth of cut and feed rate on surface roughness produced on the machined component. Taguchi technique is utilized to find the optimized machining parameters. After experimentation, it found that the influence of feed rate is significantly high on surface roughness of the turned component compared to other parameters. Paramesh et al. [9] studied the vibroacoustic modeling and analysis of segmented aluminum fuselage with blankets made up of porous material was carried out. Venkatesha et al. [10,11] focused numerical studies on finite element techniques were used to optimize the properties by altering certain inherit constraints like aspect ratios, volume fraction of reinforcements etc. The wear process is dynamic in its nature, and the FE wear calculations have nonlinear material properties

* Corresponding author.
E-mail address: manjunatha.th@bitm.edu.in (T.H. Manjunatha).

https://doi.org/10.1016/j.matpr.2022.02.068
2214-7853/
Selection and peer-review under responsibility of the scientific committee of the 5th International Conference on Advanced Research in Mechanical, Materials and Manufacturing Engineering-2021.

(surface-to-surface contact problems) and frictional contact problem [12]. As the industrial testing is very expensive and time consuming, hence the numerical modelling of the sliding contact can be debated [13]. This paper discusses about the contact analysis with FE simulation by ANSYS software of the new combination Al7075 reinforced with B_4C in nanometric form composite.

2. Methods and materials

2.1. Description of experimental set-up

Pin-on-disc tribometer (Fig. 1) the wear testing machine, consists of a stationary pin held against rotating disc and the pin movement is restricted in all directions during the testing. Before starting the testing process, it is ensured that the lever arm of the meter holding the pin must be perfectly horizontal. Some counterweights are used to balance the loading of pin. A rotating disc of the meter is made of EN31 hardened steel and the pins are of cast Aluminum 7075 MMC of diameter 9 mm and 30 mm long. Standard procedure prior to conducting wear tests is followed, i.e., the disc contact surface cleaning with acetone removes any dirt etc. Also, the pin specimen is cleaned with acetone and air dried. Pin material volume loss is measured by weight loss in the pin for each test and is recorded with a digital electronic mass balance.

2.2. Experimental procedure

The present work concentrates on evaluation of the dry slide wear rate of Aluminum 7075MMC reinforced with nano B_4C. The stir casting method, most preferred and economical for discontinuous fibres or particulates was applied to cast the MMC by blending the nano B_4C particles into base metal alloy in two stages. The benefit of alumina is it possesses a high compression conduction, thermal stability, strength, wear resistance but brittle in nature. Further disc material is steel possesses ductile property but excellent thermal conduction. The SEM micrographs display the fairly uniform distribution of nano B_4C throughout the matrix alloy as shown in Fig. 2. For the experimentation, so as to optimize the process parameters four factor and four process parameters are considered. The factors selected are material composition, load, speed and sliding distance. Loads of 1 kg, 2 kg, 3 kg, and 4 kg with B_4C reinforcement compositions as 3 wt%, 6 wt%, 9 wt% and 12 wt% as mentioned in Table 1, speeds taken are 100, 200, 300 and 400 rpm followed by sliding distances of 500, 1000, 1500 and 2000 m respectively as described in Table 2.

Fig. 1. Pin-on-disc tribometer.

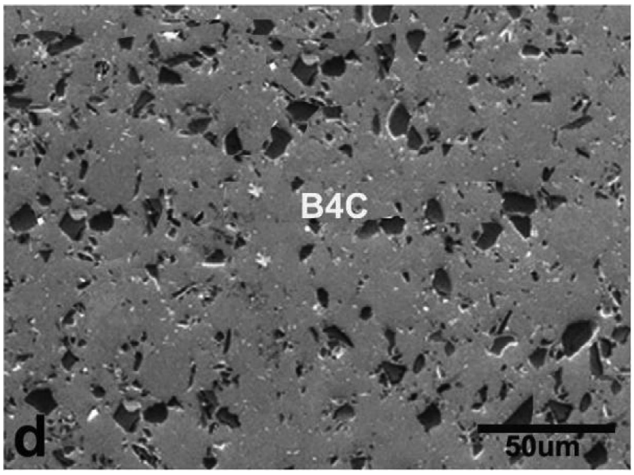

Fig. 2. SEM micrographs showing the distributions of particles in Al-7075/B_4C composites with B_4C.

Table 1
Sample Preparation.

Sample No.	Sample Composition
1	AL7075
2	Al7075 + 3 wt% B_4C
3	Al7075 + 6 wt% B_4C
4	Al7075 + 9 wt% B_4C
5	Al7075 + 12 wt% B_4C

2.3. Finite elemental modelling

There are various models and approaches available which are controlling the FE wear simulations, one such model is Archard's model which is used for the purpose. The disc is assumed to be the harder one and the pin endures the wear for the analysis. For the design application, the wear depth is considered to be most significant over the wear volume. Thus, the Archard's proposed equation (1),

$$\frac{V}{sA} = \frac{h}{s} = kp \tag{1}$$

Where, V is the volumetric rate of wear, 's' is the sliding distance, 'A' is the apparent contact area, 'h' is the wear depth, K is the coefficient of wear and 'p' is the contact pressure.

The finite element simulation results can be validated by comparing them with the experimental values. ANSYS is one of the finite element tool, which is additionally fitted with the energy error estimation technique, in order to examine the results in a field of continuous displacement from component to component. From the above equation, the wear analysis using FE simulation is dealt with the sliding distance, wear coefficient which depends on the wear depth and the product of coefficient of wear and sliding distance is not changed with the estimation of k and s, then the wear depth won't change with specified load.

2.4. Model generation

With the Ansys workbench a 3-D model was developed with contact constraints (friction between disc and pin). The program will simulate wear amid pin and disc which progressively accumulated as shown in Fig. 3 (a). Next the model was meshed with a coarse mesh of size 3 mm as shown in Fig. 3 (b). The simulation was done for all the parameters selected from the Taguchi's design of experiments. The contact pressure and wear depth were

Table 2
Variables used in Pin on Disc Wear Test.

Sl. No.	Description	Parameters selected for Wear test			
1	Load in N	9.81	19.62	29.43	39.24
2	Speed in rpm	100	200	300	400
3	Sliding distance in m	500	1000	1500	2000

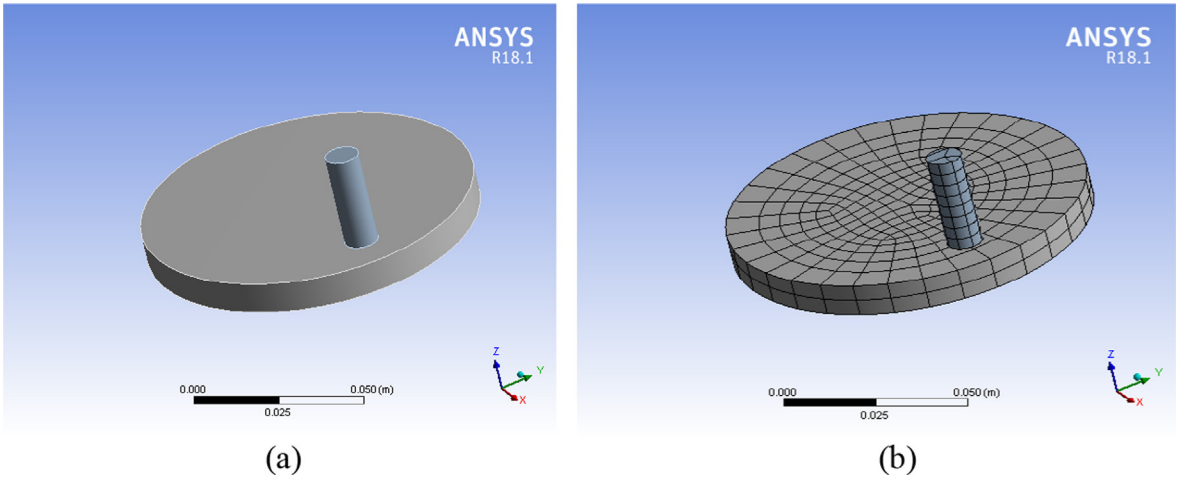

Fig. 3. (a) 3-D model of pin on disc in a wear testing; (b) Meshed Finite Element Model of pin on disc.

recorded so as to calculate the wear rate. After successful simulation of wear analysis, the results were compared with the experimental wear. The results are tabulated for the various compositions (16 no's) shown in the Table 3. Fig. 4.

3. Results and discussion

The design process cannot be said as complete, until the confirmation analysis is made. For this purpose, the simulation, experimental results were analysed using statistical tool ANOVA regression model. A linear equation was developed so as to correlate the parameters and their interactions. The following equations are developed to predict the wear behaviour.

$$\text{Wear rate (As}-\text{cast)} = \exp(3.437 - 0.0422\ \text{composition} + 0.041\ \text{load} - 0.00110\ \text{speed} - 0.001222\ \text{sliding distance}) \quad (2)$$

$$\text{Wear rate (FE Simulation)} = \exp(3.596 - 0.0285\ \text{composition} + 0.0260\ \text{load} - 0.001463\ \text{speed} - 0.001303\ \text{sliding distance} \quad (3)$$

From equation (2) and (3) the significant factor identified was sliding distance which is majorly affecting the wear rate. The comparative results from both statistical, calculated values are given in the Table 3. Fig. 5 describes the Comparisons of FEM results with the experimental results.

An Archard's 3D simulation model was successfully developed and meshed using Ansys workbench. The loads and boundary conditions are in consistent with experimental setup. As we are aware that the FEA disintegrates the solid model into number of elements, the accuracy of the results are guided by the mesh quality

Table 3
Wear rate using Taguchi's DOE.

Sl. No.	Composition	Load(kg)	Sliding distance(m)	Wear depth(m)	Contact pressure(MPa)	Wear coefficient(10^{-11})	Wear rate(10^{-6})
1	Al7075 + 3 wt% B_4C	1	500	0.08726	0.16391	106.4731	17.45
2	Al7075 + 3 wt% B_4C	2	1000	0.06981	0.3281	21.27705	6.98
3	Al7075 + 3 wt% B_4C	3	1500	0.056723	0.41025	9.217632	3.78
4	Al7075 + 3 wt% B_4C	4	2000	0.05236	0.4924	5.316816	2.62
5	Al7075 + 6 wt% B_4C	1	1500	0.030543	0.1646	12.3706	2.04
6	Al7075 + 6 wt% B_4C	2	2000	0.04363	0.3285	6.640791	2.18
7	Al7075 + 6 wt% B_4C	3	500	0.02618	0.4935	10.60993	5.24
8	Al7075 + 6 wt% B_4C	4	1000	0.095993	0.6552	14.65095	9.60
9	Al7075 + 9 wt% B_4C	1	2000	0.06545	0.1641	19.94211	3.27
10	Al7075 + 9 wt% B_4C	2	1500	0.13526	0.3272	27.55909	9.02
11	Al7075 + 9 wt% B_4C	3	1000	0.009599	0.4941	1.942724	0.96
12	Al7075 + 9 wt% B_4C	4	500	0.008727	0.6589	2.648839	1.75
13	Al7075 + 12 wt% B_4C	1	1000	0.05497	0.1642	33.47747	5.50
14	Al7075 + 12 wt% B_4C	2	500	0.01309	0.3293	7.950197	2.62
15	Al7075 + 12 wt% B_4C	3	2000	0.1745	0.58861	14.82306	8.73
16	Al7075 + 12 wt% B_4C	4	1500	0.05061	0.88266	3.822536	3.37

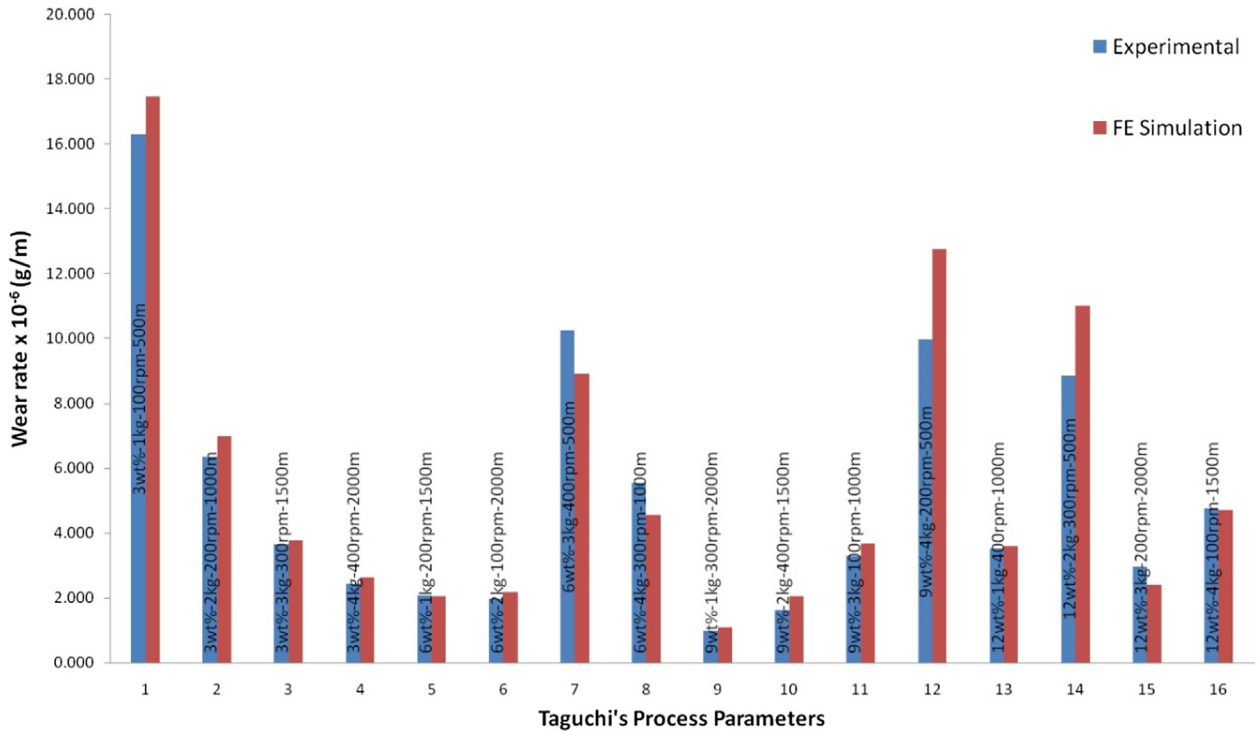

Fig. 4. Comparisons of FEM results with the experimental results.

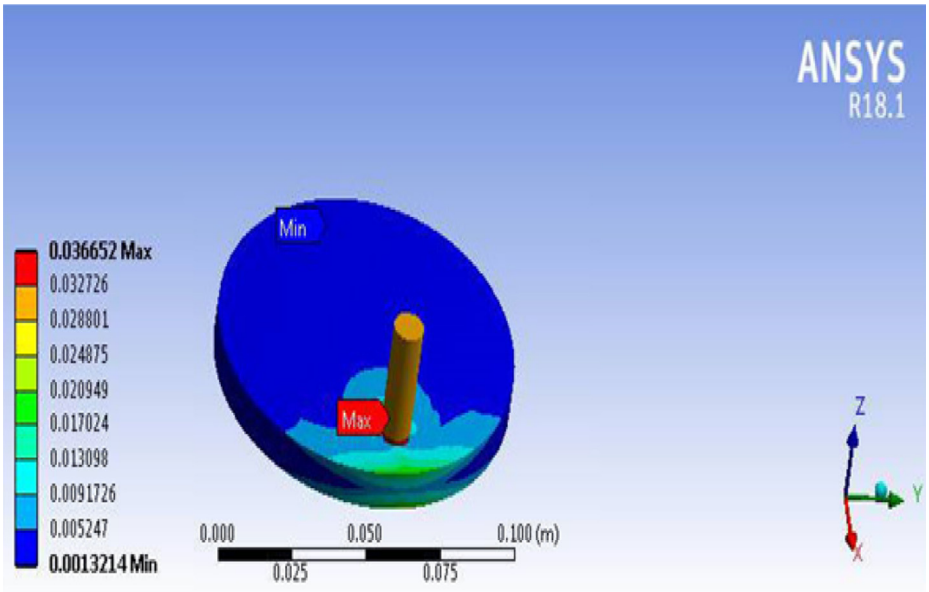

Fig. 5. Wear depth for the Taguchi parameter 9 wt%-3kg-100 rpm-1000 *m*.

which is suitably applied for the model. Not only the wear depth alters the contact pressure for FEA, but the wear law assumptions were also accounted. The pressure distribution is even in inside region as compared to at edges which has maximum concentration, eventually the wear initiates here and propagated to central area. The results from both simulation and experimentation are in concurrence reasonably. As evident from the confirmation analysis the wear rate values varied from 2.3% to 50.1% in terms of percentage error as mentioned in the Table 4. But when looking into the other cases reduced correlation was indicated and the correlation between them is about 87.33% which is good and nearly positive. Further the simulation results were also compared and placed in the Table 5. The values of wear rate in percentage error are of 2.41– 48.73% which is more than 25% and indicating reduced correlation as 89.25%. This is also good and nearly positive correlation.

4. Conclusion

This part of the research work was focused on experimental & FEA simulation on contact analysis evaluation of Aluminum 7075

Table 4
Comparison of confirmation analysis for wear rate (As-cast).

Sl. No.	Composition	Experimental Wear	Statistical Wear (Using Equation (2))	% Error
1	Al7075 + 3 wt% B_4C	16.280	13.88	14.7
2	Al7075 + 3 wt% B_4C	6.340	7.03	9.8
3	Al7075 + 3 wt% B_4C	3.647	3.56	2.3
4	Al7075 + 3 wt% B_4C	2.430	1.80	25.7
5	Al7075 + 6 wt% B_4C	2.080	3.23	35.6
6	Al7075 + 6 wt% B_4C	1.970	2.04	3.3
7	Al7075 + 6 wt% B_4C	10.240	9.54	6.8
8	Al7075 + 6 wt% B_4C	5.530	6.02	8.2
9	Al7075 + 9 wt% B_4C	0.990	1.38	28.4
10	Al7075 + 9 wt% B_4C	1.620	2.38	31.9
11	Al7075 + 9 wt% B_4C	3.280	6.35	48.3
12	Al7075 + 9 wt% B_4C	9.960	10.92	8.8
13	Al7075 + 12 wt% B_4C	3.510	3.70	5.3
14	Al7075 + 12 wt% B_4C	8.860	7.94	10.4
15	Al7075 + 12 wt% B_4C	2.960	1.48	50.1
16	Al7075 + 12 wt% B_4C	4.753	3.16	33.5

Table 5
Comparison of confirmation analysis for Wear rate (FE Simulation).

Sl. No.	Composition	Wear rate (FE Simulation)	Statistical Wear (Using Equation (3))	% Error
1	Al7075 + 3 wt% B_4C	17.45	15.47	11.36
2	Al7075 + 3 wt% B_4C	6.98	7.15	2.41
3	Al7075 + 3 wt% B_4C	3.78	3.30	12.60
4	Al7075 + 3 wt% B_4C	2.62	1.53	41.72
5	Al7075 + 6 wt% B_4C	2.04	3.33	38.80
6	Al7075 + 6 wt% B_4C	2.18	2.06	5.32
7	Al7075 + 6 wt% B_4C	8.9	9.64	8.36
8	Al7075 + 6 wt% B_4C	4.54	5.97	23.98
9	Al7075 + 9 wt% B_4C	1.09	1.38	20.90
10	Al7075 + 9 wt% B_4C	2.04	2.34	14.90
11	Al7075 + 9 wt% B_4C	3.67	7.16	48.73
12	Al7075 + 9 wt% B_4C	12.74	12.18	4.43
13	Al7075 + 12 wt% B_4C	3.58	4.02	12.35
14	Al7075 + 12 wt% B_4C	11.00	9.17	16.66
15	Al7075 + 12 wt% B_4C	2.4	1.54	35.73
16	Al7075 + 12 wt% B_4C	4.71	3.52	25.36

metal matrix composite. The Archard's 3D wear model developed with ANSYS workbench to simulate wear depth. This simulation was carried out to check the accuracy of the wear results. The wear coefficient has been derived from experimental set up. FEA simulation was performed successfully, and the results show good agreement between FEA results and those of the experimental results. Further the statistical confirmation tests were also made to round off for validation. All the three results were within the permissible error hence it is concluded that the obtained results are correct.

CRediT authorship contribution statement

T.H. Manjunatha: Data curation, Formal analysis, Investigation, Methodology, Validation, Visualization, Writing – original draft. **Yadavalli Basavaraj:** Methodology, Supervision, Writing – review & editing. **V. Venkata Ramana:** Methodology, Writing – review & editing. **K. Anand Babu:** Writing – review & editing.

Declaration of Competing Interest

The authors declare that they have no known competing financial interests or personal relationships that could have appeared to influence the work reported in this paper.

References

[1] Z. Peng, L.i. Fuguo, Chin. J. Aeronaut. 22 (2009) 663–669.
[2] D. Saraev, S. Schmauder, Int. J. Plast. 19 (2003) 733–747.
[3] S.V. Lingaraju, C. Mallikarjuna, A.R. Annappa, B.K. Venkatesha, Mater. Today:. Proc. (2021), https://doi.org/10.1016/j.matpr.2021.11.118.
[4] N.B. Pradeep, B.K. Venkatesha, S. Parameshwara, R. Raghavendra Rao, M. Raviprakash, Mater. Today:. Proc. (2021), https://doi.org/10.1016/j.matpr.2021.09.429.
[5] Kumar, M.M. Mahapatra, P.K. Jha, Meas. J. Int. Meas. Confed. 48 (1) (2014) 325–332.
[6] S. Avinash, D. Pavan, R. Raghavendra Rao, Mater. Today Proc. (2021), https://doi.org/10.1016/j.matpr.2021.09.171.
[7] G.N. Lokesh, K.P. Prashanth, G.P. Prasad, Mater. Today:. Proc. (2021), https://doi.org/10.1016/j.matpr.2021.11.131.
[8] Praveen Kittali, Vijaykumar Kalwa, D. Athith, K.P. Prashanth, Mater. Today Proc. (2021), https://doi.org/10.1016/j.matpr.2021.10.323.
[9] S. Parameshwara, N.B. Pradeep, K.P. Prashanth, Mater. Today:. Proc. (2021), https://doi.org/10.1016/j.matpr.2021.11.162.
[10] B.K. Venkatesha, B.S. Suresh, K.E. Girish, Int. J. Theoret. Appl. Res. Mech. Eng. (2012).
[11] B.K. Venkatesha, K.P. Prashanth, T. Deepak Kumar, Global J. Res. Eng. 14 (1) (2014) 11–19.
[12] B. Hemanth, H.G. Hanumantharaju, K.P. Prashanth, B.K. Venkatesha, Mater. Today:. Proc. (2021), https://doi.org/10.1016/j.matpr.2021.11.429.
[13] P. Gurusamy, S. Balasivanandha Prabu, R. Paskaramoorthy, Mater. Manuf. Process. 30 (3) (2015) 367–373.

Further reading

[14] B.K. Venkatesha, R. Saravanan, K. Anand Babu, Mater. Today Proc. 45 (2021) 216–221, https://doi.org/10.1016/j.matpr.2020.10.421.
[15] B.K. Venkatesha, R. Saravanan, Int. J. Veh. Struc. Sys. 12 (2020) 447–451, https://doi.org/10.4273/ijvss.12.4.18.
[16] G.S. Hanumanth, G.A. Irons, Metall. Mater. Trans. B 27 (1996) 663–671.
[17] B.K. Venkatesha, S.K. Pramod Kumar, R. Saravanan, A. Ishak, I.O.P. Conf, Ser.: Mater, Sci. Eng. 1003 (0120187) (2020) 1–7, https://doi.org/10.1088/1757-899x/1003/1/012087.

Materials Today: Proceedings 49 (2022) 1899–1904

Contents lists available at ScienceDirect

Materials Today: Proceedings

journal homepage: www.elsevier.com/locate/matpr

Conducting polyaniline doped with zinc tungstate matrix film as gas sensing composite

T. Machappa [a,*], S. Badrunnisa [b], M.V.N. Ambika Prasad [c]

[a] Department of Physics, Ballari Institute of Technology & Management, Bellari 583 104, Karnataka, India
[b] Krupanidhi Degree College, Bengaluru 560 035, Karnataka, India
[c] Department of Physics, Gulbarga University, Gulbarga 585 106, Karnataka, India

ARTICLE INFO

Article history:
Received 29 June 2021
Received in revised form 7 August 2021
Accepted 12 August 2021
Available online 26 August 2021

Keywords:
Polyaniline
Zinc tungstate
Conductivity
Sensor
Gas

ABSTRACT

Conducting polyaniline (PANI) is doped with a bi-metal oxide, Zinc tungstate ($ZnWO_4$) in the chemical polymerization method, and the composite matrix is sintered on the substrate to form a film. The characterization of composite by FTIR spectrum to confirm the formation of emeraldine salt phase of PANI from monomer aniline. X-RD spectra and SEM images to confirm the presence of crystalline $ZnWO_4$ in PANI matrix. The difference in conductivity versus temperature shows exponentially thermal activated behavior, in which conductivity increases with temperature due to the curling effect of polymer composite. When exposed to liquid petroleum gas (LPG), due to depletion in the number of conduction electrons at the surface and grain boundaries, there is a barrier formation at the interface of sensing films of PANI/$ZnWO_4$ composite, via Fermi energy exchange control mechanism, thereby composite film increases its resistance with LPG concentration.

1. Introduction

The gas sensor is always operated in a gas environment known as a chemical sensor. These chemical sensor converts change in chemical information into an electrical signal, based on the chemical change and concentrations of the different gaseous species under different conditions. The sensor response (sensitivity) is defined as the ratio between the steady response of the chemical sensor when exposed to the sample gas environment to the sensor response when exposed to the reference atmosphere without sample gas. When a chemical sensor is exposed to sample gas, then sensor materials interact with the sample gas, this kind of interaction may lead to oxidation increases the resistance/reduction decreases the resistance, these chemical reactions is on the surface of the film or bulk material. Some of the physical properties will be changed in sensing material due to the interaction of sample gas, such as conductivity. The changes in resistance/conductivity will be measured by a voltage drop across the resistor connected in series with the sensor [1]. Fig. 1 shows the solid-gas sensor working principle. The physical properties of different materials have been modified when interacted with a chemical gas environment, materials such as metals, metal oxides (ionic compounds) supermolecular structures, and polymers. Sensing material properties along with characteristics is governed by the type of interaction, material properties like polarizability, affinity, molecular size, and structural changes. There are two types of interaction between the sensing materials and the existence of gas.

The first type of interaction is "Lock and key" interaction, this happens usually in a sensing material that consists of organic materials. In this interaction, there is an arrangement of a monolayer of the identified molecule or specifically identified sites in a polymer matrix. [2]. The second one is the chemical sensing within inorganic materials. Reactions between the molecules present at the surface of sensing material and/or chemisorptions in the sensing material and/or catalytic reactions between gas and sensing material. Thus, there is a change in carrier density and mobility dues to the change in charge distribution at the surface while interacting with gas [3]. Household LPG (liquefied petroleum gas) and CO (carbon monoxide gas) are flammable gases. These gases are

* Corresponding author.
E-mail address: machappa@bitm.edu.in (T. Machappa).

https://doi.org/10.1016/j.matpr.2021.08.079
2214-7853/

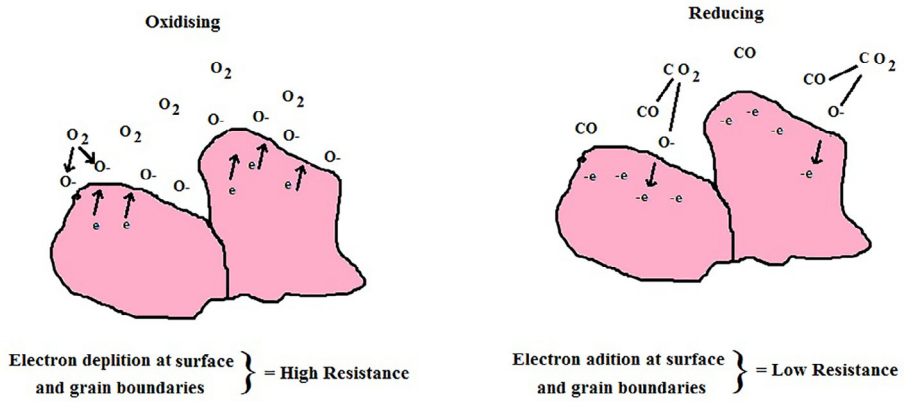

Fig. 1. Working principle of gas sensors in solid sensing material.

probable hazardous because of very quick ignition accidents, when these gases leak out unintentionally or by fault, then these dangerous toxic gases will combine very quickly with hemoglobin which results in the death of humans. Many people are trying to sense these gases in their early leakage stages to give a signal to perform effective control. The earlier researches are paying attention to the new type of sensing materials that is to be studied; the well-identified drawback of most of the sensors is their stability and selectivity. To improve this identified drawback, a few researchers focused their attention on the signal analysis of the sensor response. Several research reports confirmed that it is possible to distinguish different gases by analyzing the gas sensing response [4]. Several researchers have earlier worked on propane and butane gas sensors, but a small effort has been done on the study of LPG sensors. From previous research, it is found that presently available gas sensors have two main disadvantages, the first one is the sensitivity is low and the second one is operating at high temperature. In the literature, it is found that either one has to compromise with operating temperature or sensor sensitivity. It is found that highly sensitive gas sensor works at high temperature, this will increase the consumption of electric power. On the other hand, other sensors operable at low temperatures are not having enough sensitivity to detect the traces of LPG. The gas sensing mechanism of polyaniline/magnesium chromate (PANI / $MgCrO_4$) composites is due to the formation of surface charge formation is responsible for the difference in resistance with different concentrations of gas within the material of sensing [5]. Bi-metal oxide polymer composite is studied for various sensing application, PANI / $MgCrO_4$ and PANI/$Sr_3(AsO_4)_2$composites has given very good humidity sensing behavior along with good sensitivity [6,7]. Although a multiplicity of novel two dimensional-materials are one of the emerging fields in sensor applications, but metal oxides and bi-metal oxides have retained their attention and interest in the expedition of a variety of research and technological studies [8,9]. LPG sensing has been studied for the PANI/CeO_2 composite, the adsorption of atmospheric oxygen and at grain boundaries of poly-crystalline structure traps an electron and creates an electrical double layer [10]. It was found that the penetration of LPG into polymer composite firstly, by enlargement of polymer and secondly, by diffusion of gas into enlarged sensing composite at with increased rate of LPG sensing in PANI / $BaZrO_3$ composite [11]. LPG sensing of PANI / $Sr_3(AsO_4)_2$ composite have given considerable sensitivity, also a large change in resistance of the order of 1490 Ohms [12]. In the current report, we aim to study PANI / $ZnWO_4$ composites films for LPG sensing application at room temperature and try to understand the sensing mechanism in conducting polymer composites films.

2. Experimental

AR–grade analytical chemicals are used to synthesis polyaniline and polyaniline zinc tungstate composite. Aniline is distilled twice before its use. Polyaniline (PANI) and polyaniline zinc tungstate composite are synthesized by chemical in-situ polymerization. 1 M hydrochloric acid and 0.1 Mole of aniline are mixed to form aniline hydrochloride. The mixture is kept on magnetic starrier and ground powder of zinc tungstate ($ZnWO_4$) is added to the mixture. An oxidant 0.1 Mole ammonium persulphate [$(NH_4)_2S_2O_8$] is added to the mixture dropwise with rigorous stirring to keep zinc tungstate crystals suspended in the solution at the temperature of 0 – 5 °C using a freezing mixture for 4 – 6 h. The green precipitate thus formed is filtered by Buckner funnel, the de-ionized water is used to wash the precipitate and the removal of HCl is confirmed by silver nitrate test. The precipitate is dried in an oven over 24 h to form a green dry powder. The above procedure is repeated for another weight percent of zinc tungstate in polyaniline to form polyaniline –zinc tungstate composite. The zinc tungstate is added in 10, 20, 30, 40, and 50 wt% to form the composite, where zinc tungstate content increases in the polymer matrix, which is helpful in the testing of composites for sensing mechanism and how zinc tungstate in polymer matrix helps in sensing humidity and gas [5–7]. The composite powder is sintered on an insulating substrate to form a film-like structure to expose a large surface area of the composite to test gas. The two ends of the film are silvered with electrodes for the determination of resistance. The significance of in-situ chemical polymerization method is easy to synthesize and uniform distribution of composites in polymer matrix.

The conformation of polymerization of aniline to polyaniline and polyaniline – zinc tungstate composite are through the FTIR spectroscopy, which was recorded on Perkin – Elmer spectrophotometer (Model: 1600) in the medium of KBr. Retention of crystallinity and presence of zinc tungstate is confirmed by X-ray diffraction of composites by Phillips - PW3710 X-ray diffractometer with the source of radiation Cu Kα. Surface morphology and distribution zinc tungstate are essential for sensing properties were visualized by Phillips XL 30 ESEM Scanning Electron Micrographs polyaniline and polyaniline composites of zinc tungstate. These three characterizations are sufficient for the present work of testing the polyaniline composites for the sensing mechanism.

The measurement of resistance is one of the important studies of the present work, which is carried out using a temperature-controlled oven and Keithley – 2000 multimeter USA. The gas sensing behavior is studied by determining the resistance of composites films placed in a glass chamber, in which the controlled flow of liquid petroleum gas (LPG) is introduced through a flow meter.

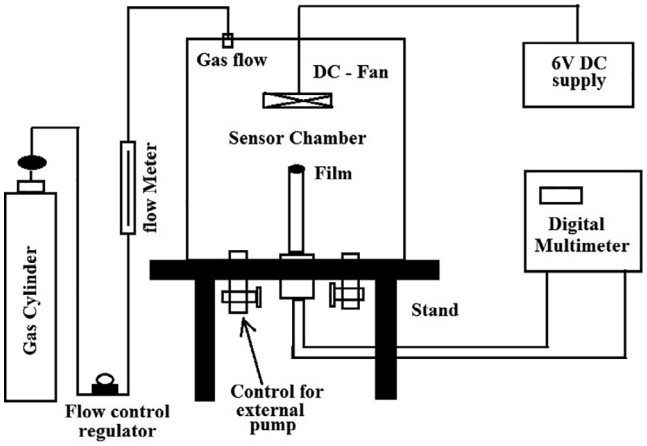

Fig. 2. The block diagram of the sensor setups used Gas sensing.

Fig. 2 shows the schematic diagram of the sensor chamber setup used for the study of sensing behavior [5].

3. Results and discussions

3.1. Fourier transform Infra-Red Spectra (FTIR)

Fig. 3a shows the FTIR-Spectra of pristine PANI, and Fig. 3b illustrates the FTIR Spectra of PANI / $ZnWO_4$ composite. All the samples are in powdered form made into pellets in the medium of KBrwith different weight percent of $ZnWO_4$ in PANI is documented in the range 400–4000 cm^{-1}. Formation of polyaniline and polyaniline – zinc tungstate composites are confirmed from the stretching frequencies and stretching frequency assignment is well in agreement with the reported data [13,14], stretching frequency assignment is as shown in Table 1.

FTIR spectra show strong bonds in the region 750–1700 cm^{-1} these are the characteristic stretching frequencies of pure PANI and PANI / $ZnWO_4$ composites. Comparison of stretching frequencies shows that the stretching frequencies changed towards a higher frequency in the formation composite. This shifting suggests weak bond interaction between $ZnWO_4$ and polyaniline chine. This kind of weak bond interaction was attributed to Vander wall's kind of interaction, which confirms the formation of the composites in consistence with the earlier reports [15].

The presence of metal–oxygen bonds are shown at frequencies 696 cm^{-1} & 612 cm^{-1}, these peaks are in Table 1 of pure $ZnWO_4$ in composite strongly confirm the formation of PANI / $ZnWO_4$. The intensity of metal–oxygen stretching peaks of FTIR spectra increases with an increase in weight percent of $ZnWO_4$ in PANI [16].

3.2. X-ray diffraction (X-RD)

The X-RD pattern of pure PANI and PANI / $ZnWO_4$ composite along with pure $ZnWO_4$ is as shown in Fig. 4. From Fig. 4c it is clear that PANI is an amorphous structure with a wide band at 27^0 as semi-crystalline. Fig. 4b shows the highly crystalline, monoclinic crystal structure of $ZnWO_4$ and is in excellent agreement with research values in the literature (JCPDS file no: 88-0251 and space group: P2/c) for $ZnWO_4$ [17]. The results thus obtained from the experimental technique are discussed as follows. All the reflection peaks of the sensing material are completely assigned and it is seen from that figure, the monoclinic structure of $ZnWO_4$ points out the crystalline character in the composite. By evaluating the X-RD pattern of PANI composite with that of $ZnWO_4$, the major peaks correspond to $2\theta = 18.91^0$, 21.55^0, 32.57^0, 35.74^0 and 48.49^0 are due to (100), (110), (020), (021) and (022) planes of $ZnWO_4$. Fig. 4c shows both the amorphous nature of PANI and the crystalline nature of $ZnWO_4$ with the same peaks of monoclinic structure. By comparing the X-RD pattern of the sensing composites and $ZnWO_4$, it is established that $ZnWO_4$ has preserved its crystalline structure even when it is isolated in PANI during the in-situ polymerization reaction.

3.3. Scanning electron micrograph (SEM)

Fig. 5a Shows an SEM picture of pure PANI, the presence of micro-crystalline amorphous structures in PANI was observed and the same is confirmed from XRD studies, with a wide peak centered about $2\theta \approx 27^0$. A grainy morphology with micro-crystalline structures is reliable with other reports. Fig. 5b shows SEM image of PANI / $ZnWO_4$composite, that confirms the presence of $ZnWO_4$ and is uniformly distributed throughout with variable grain size within the composite sample. A little difference in the dimensions of $ZnWO_4$ so isolated in PANI has been detected. The sensing composite has crystalline grains and spongy structure with pours, fur-

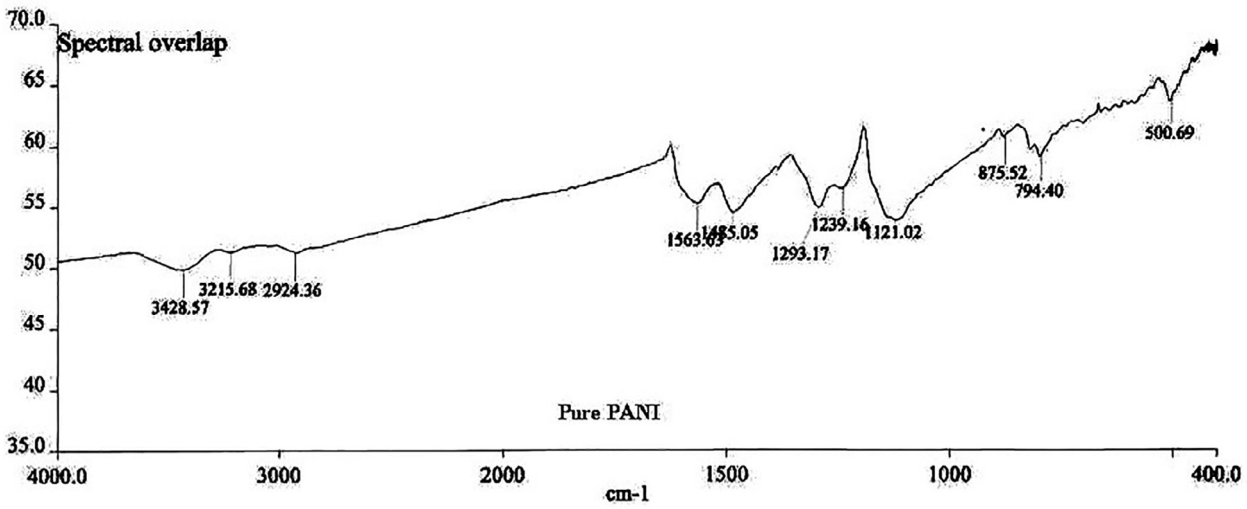

Fig. 3a. FTIR Spectra of pristine PANI.

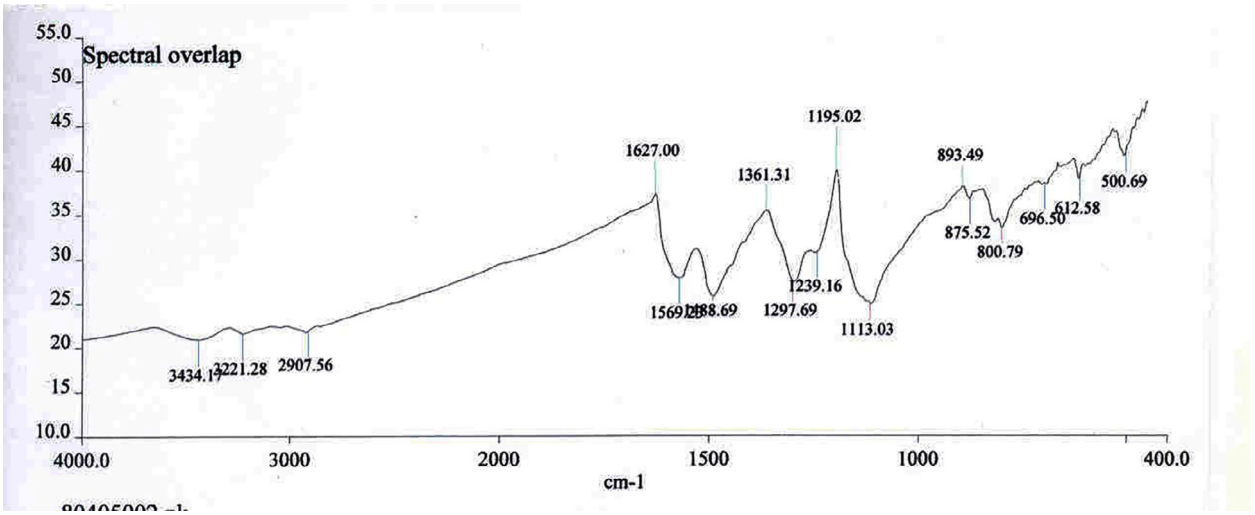

Fig. 3b. FTIR Spectra of PANI / $ZnWO_4$ composite.

ther, the composites have capillary pores linked with each other because of inconsistent grain size of $ZnWO_4$ such composites are probable to make easy absorption of gas, this may be due to large available surface area of exposed composite and capillarity [18].

3.4. DC – conductivity

Fig. 6a shows the variation of conductivity of PANI / $ZnWO_4$ composites with temperature. We observed an increase in the conductivity as temperature increases, which is due to the exponential behavior that is activated thermally in conducting polymers. As temperature increases, due to thermal agitation, there may be increased charge transfer efficiency between polymer chine and $ZnWO_4$ [19,20]. On heating the molecular reorganization in the polymer will occur, this will facilitate the increase in electron delocalization [21]. It is also recommended that thermal twisting affects the polymer chain arrangement of the composite leading to an increase in the conjugate length of the polymer, this also may be responsible for the increase in conductivity. According to VRH - model (Variable Range Hopping) projected by Mott.

The thermally supported hopping of electrons between restricted states near randomly distributed traps controls the behavior of electric conductivity in disordered and non-metallic materials. The expression for the variation of conductivity with temperature may be given by

$$\sigma_T = \sigma_0 \exp[-(T_O / T)^{1/4)}]$$

Where: σ – Conductivity, T – Temperature, σ_0 – Conductivity at characteristic temperature T_0. The conductivity varies with different values of powers of T, till now the powers $T^{-1/2}$, $T^{-1/3}$, $T^{-1/4}$ have been reported, and various models have been used to understand the data [22].

The deviation in D.C conductivity as a function of wt% of $ZnWO_4$ in PANI, at three fixed temperatures viz, 50, 100 and 150 °C is as shown in Fig. 6b. Utmost conductivity is seen for 20 & 40 wt% of

Table 1
FTIR spectral frequencies of Pristine PANI and PANI / $ZnWO_4$ composite.

Pristine PANI (cm^{-1})	PANI /$ZnWO_4$ Composite (cm^{-1})	Assignment
3428	3434	N—H Stretching
1625	1627	Benzenoid – Ring Stretching
1563	1569	Quinoid – Ring Stretching
1485	1488	C═N Stretching + C–C Stretching
1293	1297	C—N Stretching + C—H Bending
1239	1240	C—N Stretching + C—C Stretching
794	800	N–H out of plane Bending
–	696	Metal Oxygen Stretching
–	612	Metal Oxygen Stretching

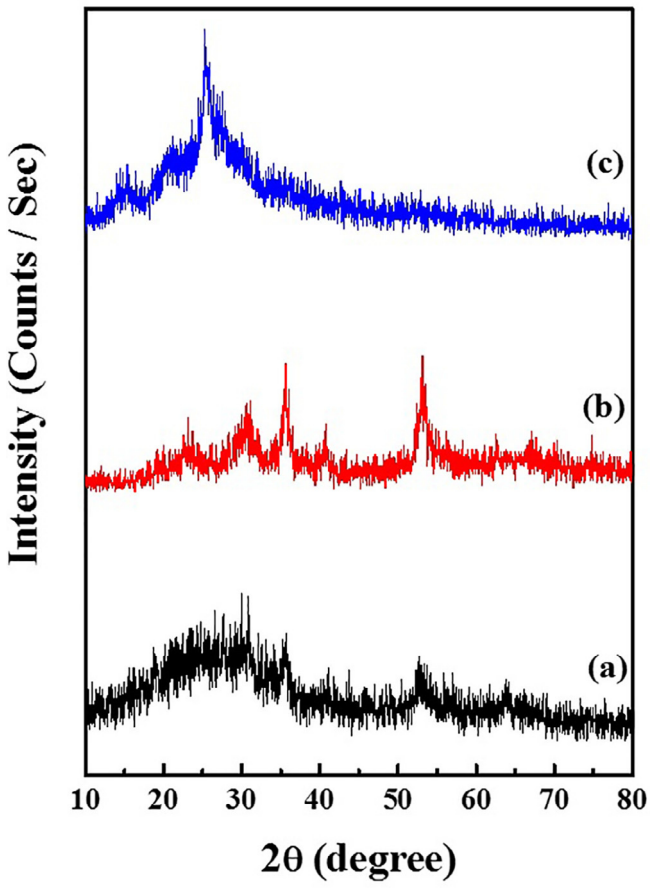

Fig. 4. X-ray diffraction pattern of (a) Pure PANI; (b) Pure $ZnWO_4$; (c) PANI / $ZnWO_4$ composite.

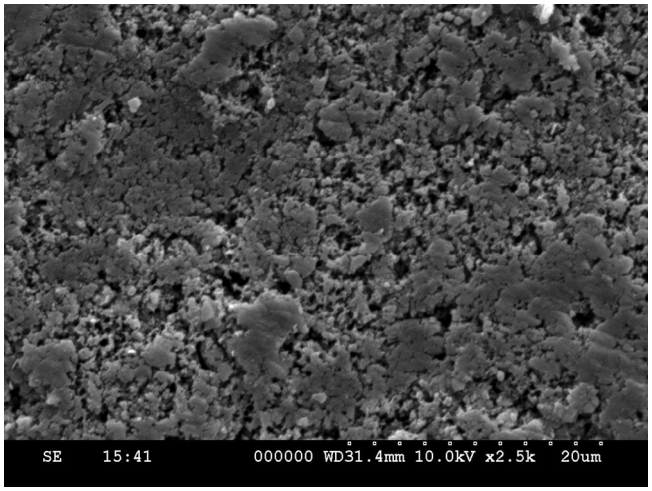

Fig. 5a. SEM image of pure PANI.

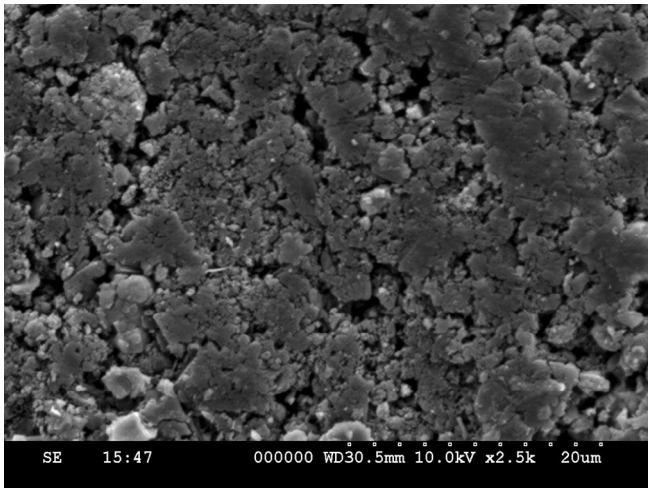

Fig. 5b. SEM image of PANI / $ZnWO_4$ composite.

$ZnWO_4$ in PANI-composite at 150 °C. The conductivity reduces for 10, 30 & 50 wt% of $ZnWO_4$ in PANI-composite. This may be recognized as the distribution of enhanced granule size of $ZnWO_4$, which may block the hopping of charge carriers. This blocking mechanism is due to an increase in the barrier potential with an increase in grain size between the localized wells, which decreases the charge carrier hopping in between the restricted sites hence a decrease in conductivity.

3.5. Gas sensor

The change in resistance of PANI/ $ZnWO_4$ composites with LPG concentration is as shown in Fig. 7. The experimental it is observation shows that when LPG concentration increases the resistance of the sensing material is changing. The highest resistance change is noticed in the sensing composites of 10 wt% and 20 wt% $ZnWO_4$ in PANI out of the five composites studied.

The $ZnWO_4$is a semiconductor bi-metal oxide thereby decreases the electronic conduction due to the accumulation of oxygen molecules of the atmosphere at the sensing surface. The accumulated oxygen molecules of the atmospherewill take electrons from the conduction band of $ZnWO_4$, here the Zinc ions act as donors due to oxygen vacancies [23]. If we reduce the concentration of gas molecules then, reacts negatively with charged oxygen adsorbents,

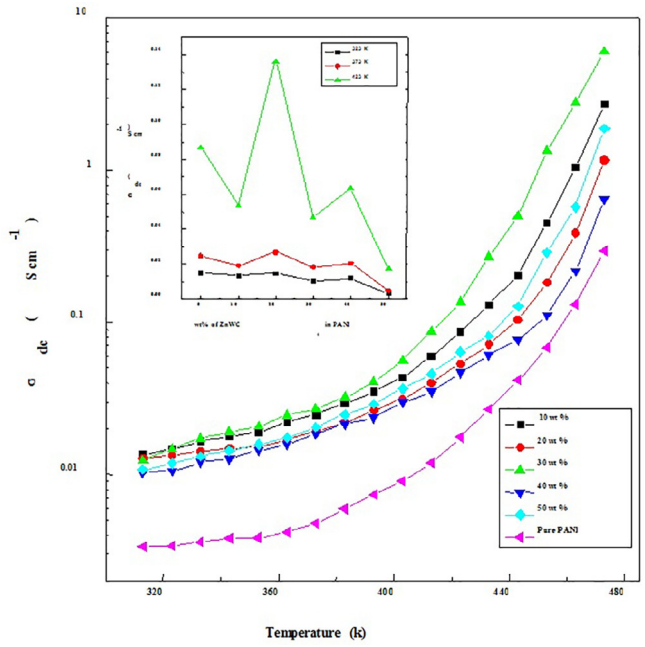

Fig. 6. (a) Variation of D.C. conductivity of PANI/$ZnWO_4$ composites with temperature; (b) Variation of D.C conductivity as a function of wt% of $ZnWO_4$ in PANI.

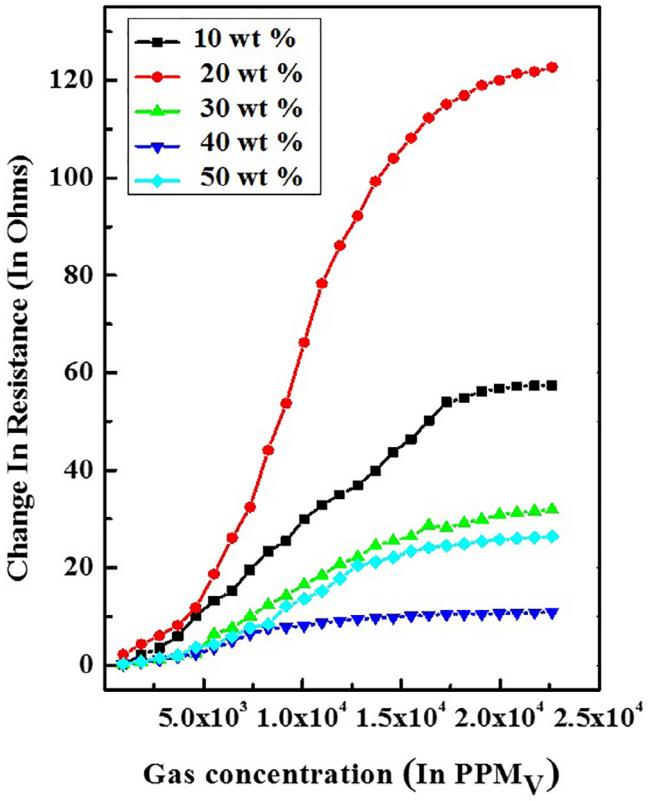

Fig. 7. Change in resistance with increase in the concentration of LPG of PANI/ $ZnWO_4$ composites.

the electrons that are trapped are return to the conduction band of $ZnWO_4$, which is the reason for the increase in the conductivity of sensing material. On the other hand, oxidizing gas molecules take up free electrons, which leads to a decrease in conductivity.

For LPG, the response mechanism is quite multifaceted and will be understood through numerous intermediate steps, this mecha-

Table 2
Comparison of previous work on gas sensing with current work presented.

SN	Composite	wt%	Resistance at Gas Concentration		Resistance Range (in Ohms)	Ref.
			952 (in PPMv)	22,624 (in PPMv)		
01	PANI / $MgCrO_4$	40 wt%	14.3	102	87.7	[5]
02	PANI / $MgCrO_4$	50 wt%	9.8	94	84.2	[5]
03	PANI / $Sr_3(AsO_4)_2$	20 wt%	54	1544	1490	[12]
04	PANI / $Sr_3(AsO_4)_2$	30 wt%	16	1077	1061	[12]
05	PANI / $ZnWO_4$	10 wt%	0.2	57.4	57.2	Present work
06	PANI / $ZnWO_4$	20 wt%	2.2	122.7	120.5	Present work

nism is not yet completely understood [24,25]. It is known that LPG is made of several combinations such as CH_4, C_3 H_8, C_4H_{10}, etc., and these molecules of hydrogen species will reduce the bound to the carbon atoms. The overall reaction of LPG molecules with accumulated oxygen can be enlightened as follows [26].

$C_nH_{2n+2} + 2O - \rightarrow H_2O + C_nH_{2n} - O + e-$

Where: C_nH_{2n+2} represents hydrogen species CH_4, C_3H_8, C_4H_{10}, etc., On the contact to LPG of the PANI/ $ZnWO_4$ films, the LPG molecules respond to adsorbed oxygen in the same manner as described in the above equation.

The sensing mechanism of LPG sensing can also be understood as follows when the metal oxide is doped to a semiconducting PANI, then there is a formation of barrier at the interface of the sensing material and LPG gas, that reduces the density of conduction electrons in the sensing composite material via controlled mechanism Fermi energy exchange, hence increase in resistance. When LPG molecules impinge into the sensing material through the capillary pours, the constituent hydrocarbons of LPG dissociatesand then the atoms will drip over the surface, while in the mechanism of Fermi energy exchange, the accumulated oxygen will remove electrons from the sensing material, thereby increase in resistance and decrease in conductivity [27].

The selectivity of the composite for LPG sensing will be based on the change in resistance with LPG gas. Out of five composites, it has been reported that 20 wt% of $ZnWO_4$ in PANI has given highest change in resistance with LPG, from low concentration of 952 PPMV to high concentration 22,624 PPMV of about 2.2 Ohms to 122.7 Ohms. The total change in resistance is 120.5 Ohms. This significant change in resistance is compatible to development in the design of LPG sensing device. Therefore 20 wt% of $ZnWO_4$ in PANI composite may be selected for LPG sensing device manufacturing. The Table 2 represents the comparison table of the previous work carried out on gas sensing, highlight of the present work is that 20 wt% of the$ZnWO_4$ in PANIgave very good sensitivity towards LPG sensing and is the supremacy of current work presented in this paper.

4. Conclusions

Polyaniline / Zinc Tungstate (PANI / $ZnWO_4$) composites were synthesized by a novel 'in situ' chemical polymerization process. Formation of the polymer matrix in the mixed segment of composite, along with Polyaniline conducting emeraldine salt matrix was established by the technique of spectroscopy. The temperature-dependent conductivity measurements show the exponential behavior which is thermally activated. Enhancement of 10 S cm^{-1} in the dc-conductivity of PANI/$ZnWO_4$ composites was reported in comparison with the conductivity of pristine PANI. The change in resistance is studied for all the five composites, among the composites, 10 and 20 wt% of $ZnWO_4$ in PANI have shown more resistance change with other composites when exposure to LPG. The absorption of LPG vapors into the composite increases the resistance because charge transfer increases with an increase in the rate of diffusion of LPG. While the oxidizing gas molecules will take up the free electrons, which leads to a decrease in conductivity. When LPG molecules impinge into the sensing material through the capillary pores, the constituent hydrocarbons of LPG dissociate, and then the atoms will drop over the surface, while in the Fermi energy exchange mechanism the accumulated oxygen will remove electrons from the sensing material, thereby increase in resistance and decrease in conductivity. It has been observed that 20 wt% of $ZnWO_4$ in PANI has given the highest change in resistance in presence of LPG, this sensing composite demonstrates to be a capable sensing material for LPG sensing and manufacture of sensing devices because of its almost linear behavior.

Declaration of Competing Interest

The authors declare that they have no known competing financial interests or personal relationships that could have appeared to influence the work reported in this paper.

References

[1] I. Lundstrom, Sens. Actuvators B 35–36 (1996) 11–19.
[2] W. Gopel, Sens. Actuators, B 52 (1998) 125–142.
[3] D.E. Williams, Sens. Actuators, B 57 (1999) 1–16.
[4] S. Nakata, K. Takemura, K. Neya, Sens. Actuators, B 76 (1–3) (2001) 436–441.
[5] T. Machappa, M. Sasikala, M.V.N. Ambika Prasad, IEEE Sensor J. 10 (2010) 807–813.
[6] T. Machappa, M.V.N. Ambika Prasad, Bull. Mater. Sci. 35 (2012) 75–81.
[7] T. Machappa, M. Sasikala, Koppalkar R. Anilkumar, M.V.N. Ambika Prasad, Sens. Trans. 107 (2009) 77–85.
[8] S. Manunatha, T. Machappa, Y.T. Ravikiran, B. Chethan, M. Revanasiddappa, App. Phys. A. 125(2019) 361–10.
[9] A. Sunilkumar, S. Manunatha, B. Chethan, Y.T. Ravikiran, T. Machappa, Sen. Act. 298 (111593) (2019) 1–8.
[10] B.S. Khened, T. Machappa, M.V.N. Ambika Prasad, M. Sasikala, Int. J. Sci. Res. 01 (2012) 180–184.
[11] B.S. Khened, T. Machappa, M.V.N. Pradeep, M.V.N. Ambika Prasad, M. Sasikala, Mater. Today : Proc. 03 (2016) 369–375.
[12] T. Machappa, S. Badrunnisa, J. Phys. Conf. Ser. 1760 (102015) (2020) 1–8.
[13] J.L. Koenig, 1999 (2nd ed) Spectroscopy of polymers (Amsterdam: Elsevier).
[14] D.L. Pavia, G.M. Lampman, G.S. Kriz, Intro. tospectroscopy, 3rd ed., Harcourt College Publishers, 2001.
[15] T. Machappa, M.V.N. Ambika Prasad, Ferroelectrics 392 (2009) 71–80.
[16] T. Machappa, M.V.N. Ambika Prasad, Physicsa B 404 (2009) 4168–4172.
[17] B.B.V. Sailaja, Ajay Kumar Paliki, Sathish Mohan Batsa, Bio. Organic & Org. Chem. 2 (5) (2018) 230–234.
[18] W.-P. Tai, J.-G. Kim, O.h. Jae-Hee, Y.-S. Kim, Sens. Actuators, B 105 (2005) 199–203.
[19] M. Leclerc, G. D'Aparno, G. Zotti, Synth. Met. 55 (1993) 1527–1532.
[20] F. Zuo, M. Angelopoulos, A.G. MacDiarmid, A.J. Epstein, Phys. Rev. B. 36 (1987) 3475.
[21] H. Kobayashi, K. Ishikawa, M. Amano, E. Satoh, Hasegava, J. Appl. Phys. 74 (1993) 296–299.
[22] N.F. Mott, E. Davis, Clarendon Press, Oxford, 1979.
[23] K.J. Laidler, Chemical Kinetics, 2nd ed., TMG Publi. Com. Ltd., chapter 6, pp 310-311.
[24] T. G. Nenov, S. P. Yordanov, Technomic Publication, Lancaster, Vol. 1, 1996, pp 137.
[25] P. Mitra, A.P. Chatterjee, H.S. Maiti, Mater. Lett. 35 (1–2) (1998) 33–38.
[26] V.R. Shinde, T.P. Gujar, C.D. Lokhande, Sens. Actuators, B 120 (2007) 551–559.
[27] A.S. Roy, K.R. Anilkumar, M. Sasikala, T. Machappa, A. Prasad, Sensor Lett. 09 (2011) 1–7.